Spring 10-31-1984

Mathematical simulation of proteins separation in a packed bed

Jing James Huang
New Jersey Institute of Technology

Copyright Warning & Restrictions

The copyright law of the United States (Title 17, United States Code) governs the making of photocopies or other reproductions of copyrighted material.

Under certain conditions specified in the law, libraries and archives are authorized to furnish a photocopy or other reproduction. One of these specified conditions is that the photocopy or reproduction is not to be "used for any purpose other than private study, scholarship, or research." If a, user makes a request for, or later uses, a photocopy or reproduction for purposes in excess of "fair use" that user may be liable for copyright infringement,

This institution reserves the right to refuse to accept a copying order if, in its judgment, fulfillment of the order would involve violation of copyright law.

Please Note: The author retains the copyright while the New Jersey Institute of Technology reserves the right to distribute this thesis or dissertation

Printing note: If you do not wish to print this page, then select "Pages from: first page # to: last page #" on the print dialog screen

MATHEMATICAL SIMULATION OF PROTEINS SEPARATION IN A PACKED BED

BY

JING JAMES HUANG

Dissertation submitted to the Faculty of the Graduate School of the New Jersey Institute of Technology in partial fulfillment of the requirements for the degree of Doctor of Engineering Science
1984

APPROVAL SHEET

Title of Thesis:

MATHEMATICAL SIMULATION OF
PROTEINS SEPARATION IN A PACKED BED

Name of Candidate:

JING JAMES HUANG

Doctor of Engineering Science, 1984

Thesis and Abstract Approved:

Dr. Ching-Rong Huang Professor & Assistant Chairman for Graduate Studies Department of Chemical Engineering	Date
	Date
	Date

VITA

Name: Jing James Huang

Degree and date to be conferred: D.Eng.Sc., 1984

Collegiate institutions attended	Dates	Degree	Date of Degree
New Jersey Institute of Technology	1980	D.Eng.Sc.	Oct., 1984
Chung Yuan University	1975	M.S.	June, 1978
Chung Yuan University	1971	B.S.	June, 1975

Major: Chemical Engineering

Minor: Mathematics

Publications:

"Natural Convection Heat Transfer in Vertical Cylindric Enclosures," Proceedings of the National Science Council of R.O.C., Vol. 2, No. 4, pp 424-430, 1978

"Continuous Multiaffinity Separation of Proteins: Cyclic Processes," AICHE Symposium Series, Vol. 78, No. 219, pp 39-45, 1982

"Parametric Pumping--A Unique Separation Science," Journal of Parenteral Science & Technology, Jan./Feb., 1983

ABSTRACT

Title of Dissertation:

MATHEMATICAL SIMULATION OF
PROTEINS SEPARATION IN A PACKED BED

Jing James Huang
Doctor of Engineering Science, 1984

Dissertation directed by:

Dr. Ching-Rong Huang
Professor & Assistant Chairman
Department of Chemical Engineering & Chemistry

The generalized adsorption models are developed to simulate the unsteady state mass transfer behavior in a packed column. Based on the nature of adsorbent particles, the adsorption models may be classified into two categories: (1) the surface adsorption model, (2) the pore diffusion model. In the first model, it is assumed that the internal diffusion is negligible, and the adsorption rate is determined by external diffusion and surface adsorption. In the second model, the effect of internal diffusion is considered as significant as that of external diffusion. For both models, the effect of axial dispersion in fluid phase is emphasized.

A total of four different kinds of adsorption models are solved analytically- two in each category.

In the modelling of adsorption process with axial dispersion (dispersion model), the boundary conditions provided in published literatures are inadequate to describe the real situations. In this study, a novel and rigorous approach using the mass conservation law is employed to set up the proper boundary conditions. Two different sets of boundary conditions are used for the dispersion model; one set is specified by the continuity equation of adsorbate at the inlet of the column (at z=0), and the other set is characterized by the total material balance of adsorbate over the entire column. The analytic solutions are presented as dimensionless effluent concentration (C_A/C_{Ao}) versus effluent volume or elapsed time in terms of the variations of system parameters. These results provide quantitative information for the design and scale-up of packed bed operations. Moreover, the proposed adsorption models are verified experimentally with the system of hemoglobin- albumin- CM sepharose- DEAE sepharose. The theoretical predictions of concentration variations are shown to be a good representation of experimental data.

DEDICATION

To my beloved parents,

Mr. and Mrs. J.C. Huang

ACKNOWLEDGEMENTS

The author is especially grateful to Professor Ching-Rong Huang for his guidance, encouragement, and assistance during the course of this research.

The author also wish to acknowledge his gratitude to the other committee members for their interest and useful suggestions. Special appreciations are extended to Dr. J.F. Chao, Dr. W.D. Pan, Mr. S.R. Khan, and Mr. T.K. Yu for their valuable comments and suggestions in preparing this manuscript.

Finally, the author would like to express his sincere gratitude to his wife, Yan-Whau, for her understanding, patience, and inspiration.

TABLE OF CONTENTS

LIST OF TABLES

LIST OF FIGURES

CHAPTER I

INTRODUCTION

Separation processes are of unique and fundamental importance to the chemical process industries. The importance of separation as a chemical engineering unit operation lies in the fact that the main objective of most chemical processes is to produce a product with a higher degree of purity, and this purpose could only be achieved by isolating the impurities from the products. Therefore, separation may be defined as an operation which isolates specific ingredients from the mixture usually without a chemical reaction taking place. In most separation processes, the concentration or composition of mixture(solution) changes due to the mass transfer of specific chemical species onto adsorbent and back into solvent, which are also known as mass transfer operations.

There are many chemical engineering processes that utilize the unsteady state mass transfer operation in a packed bed. The most common examples include the adsorption column, the ion exchange column, and the chromatographic column. The adsorption process could best be represented by a typical packed bed operation. Usually, the equipment of adsorption

process consists of a column packed with solid particles that have adsorbing characteristics. A fluid mixture is then passed through the column and mass transfer occurs between the fluid phase and the solid phase. Since the solid remains stationary and the composition of solid phase changes with time, the packed bed operation is an unsteady state mass transfer process. The packed bed adsorption process has the advantages of simple and convenient operation, and the cost for its applications is relatively low compared to other continuous processes (22,40). The range of conventional applications of packed bed operation has been found in such diverse fields as the purification of gases, the recovery of valuable solvent from a waste effluent, the concentration of valuable solutes from liquid solutions, the purification of water, and the waste water treatment.

The principles of packed bed adsorption operation have also been adapted to cyclic separation processes such as parametric pumping operation, cycling zone adsorption, and the simulated moving bed operation. The basic ideas of parametric pumping operation were first introduced by Wilhelm and his coworkers (37,38). The operation of parametric pumping involves the reciprociating flow of a fluid mixture to be separated through a fixed bed as shown in Fig. 1. One or more of the fluid components can be physically or chemically adsorbed onto solid(adsorbent). The coupling of flow reversal with a change of a thermodynamic intensive

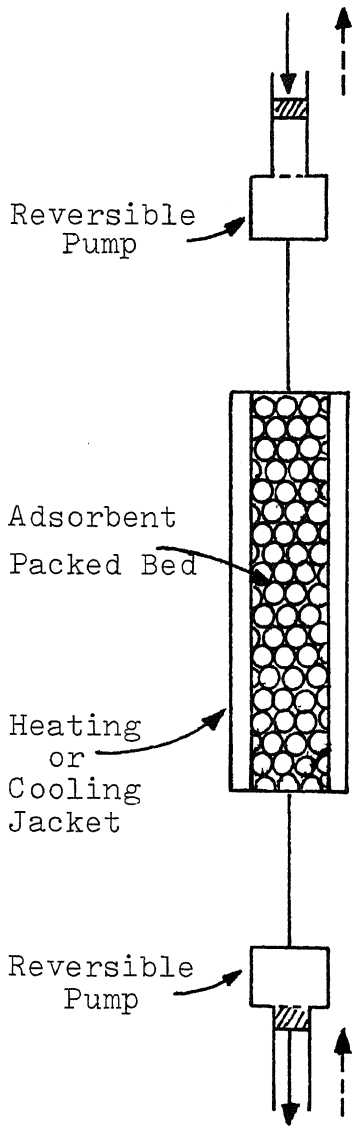

Figure 1. Operation scheme for parametric pumping or cyling zone adsorption

variables(i.e. temperature, pressure, electric field, ionic strength, pH, or affinity) will induce the separation. The parametric pumping operation was initially developed to separate the organic compounds. Now, it is applied to separate biochemicals (7- 12). The cycling zone adsorption was first developed by Pigford and his coworkers (27). This process is very similar to the parametric pumping operation except that it utilizes the unidirectional fluid flow. As in parametric pumping, the separation of cycling zone adsorption is caused by a peroidic alternation of the process control variables in the column. Theoretical analyses of cycling zone adsorption by Pigford et.al. indicated that the separation attainable with N zones in series is the same as that attainable after N cycles in parametric pumping. The most important difference between parametric pumping operation and cycling zone adsorption is that the continuous feed input and product withdrawal in the later process, and low cost of design and operation in former process. The process of simulated moving bed represents a method of separating the species by selective adsorption from the liquid solution in a fixed bed of adsorbents. This process is generally used to simulate a countercurrent flow of liquid and solid phases without actual movement of solids as shown in Figure 2 (5). In this process, the bed is divided into several zones(adsorption, desorption, regeneration, etc.) by the position of external streams. By continuously shift-

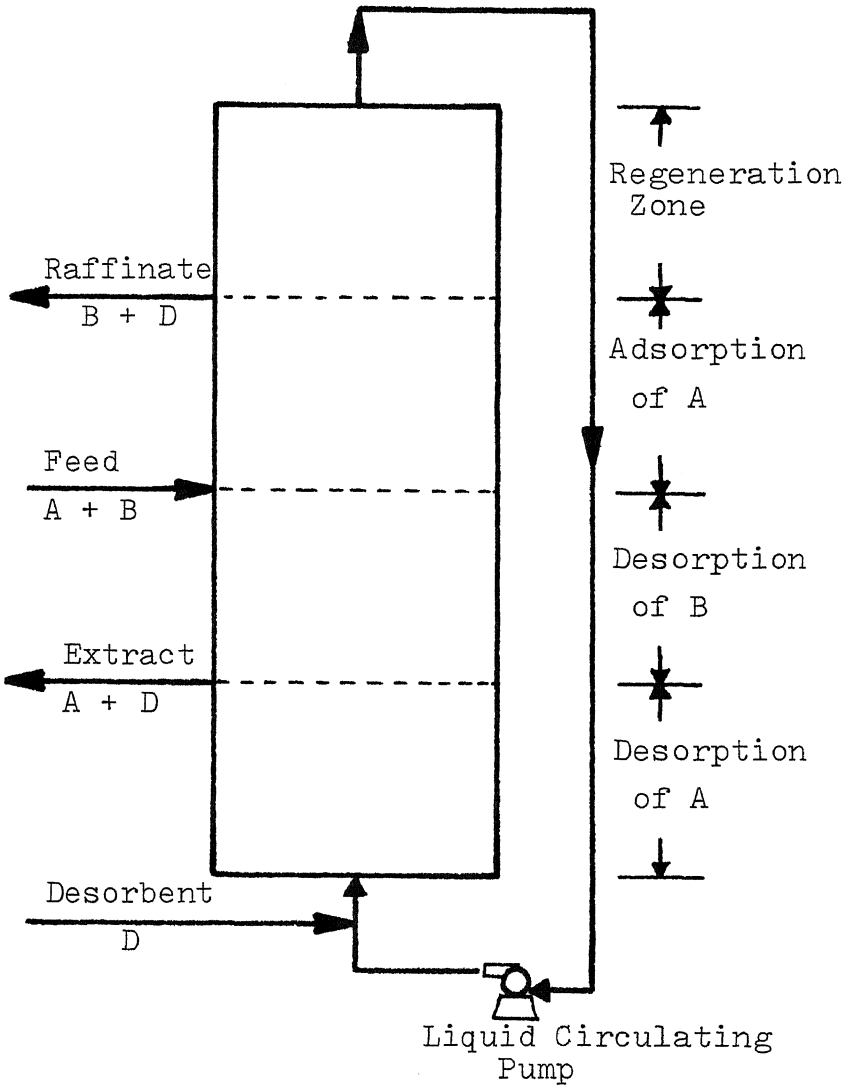

Figure 2. Schematic diagram of simulated moving bed operation

ing the position of external streams, the separation process can be practiced in each zone. The simulated moving bed operation has been commericalized by the company named Universal Oil Product(UOP) (2, 3, 31) for recovering paraxylene from hydrocarbon mixtures, extracting normal paraffins from kerosene, and separating the fructose from corn syrup. In recent years, the principles of chromatographic separation have been extended to modern liquid chromatography (4,35) for the separation of proteins, enzymes, and other biochemicals.

The engineering design of fixed bed adsorption system is closely tied to the column dynamics. The studies of column performance of a packed bed adsorption involve particularly the breakthrough curve of effluent concentration, or the variation in effluent concentration with respect to time or the volume of effluent. Figure 3 (40) shows the transient movement of the adsorption wave and its corresponding changes in effluent concentration(breakthrough curve). Consider the case in Figure 3, a binary fluid mixture containing a strong adsorbate with concentration C_o is introduced into the upper end of the packed bed where the bed is initially free of adsorbate. As the solution continues to flow down, the adsorption zone moves downward as a wave, at a rate which is much slower than the linear velocity of the fluid through the bed. In the begining,

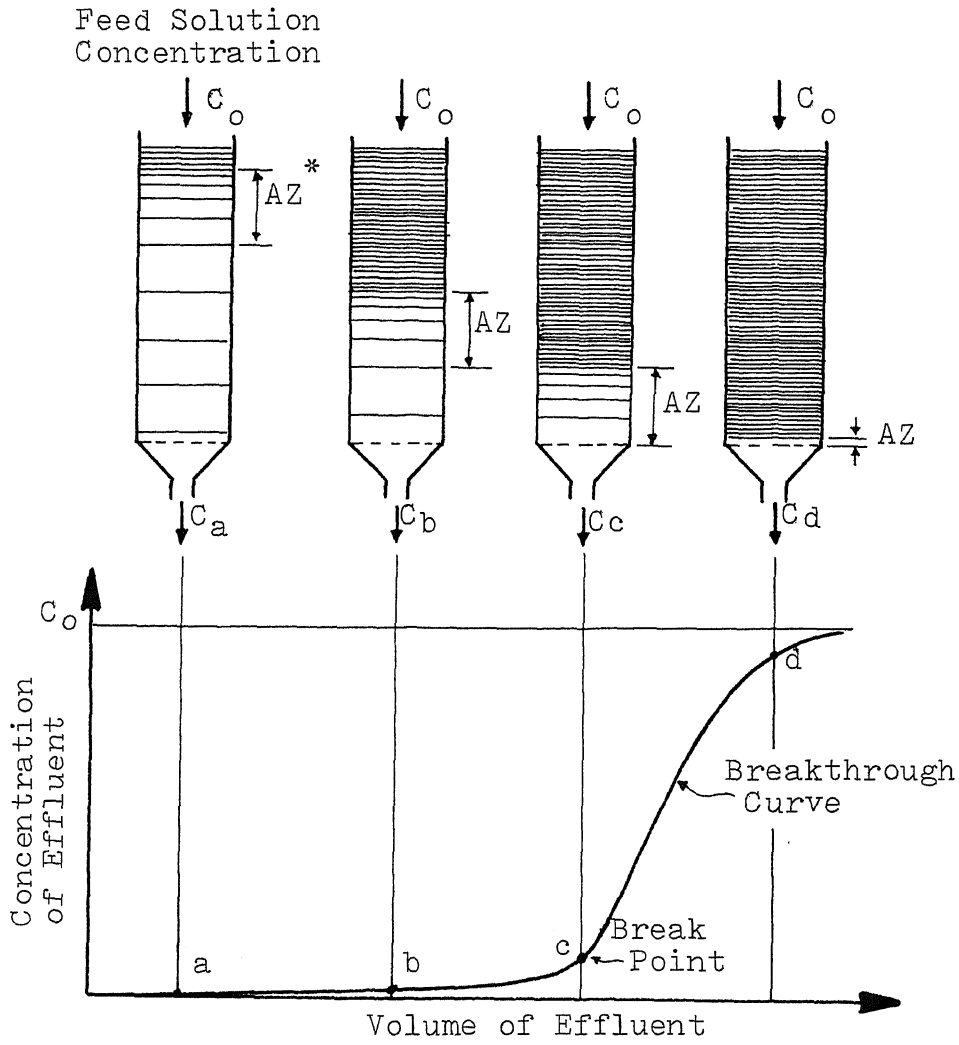

* AZ = Adsorption Zone

Figure 3. The adsorption wave and its corresponding breakthrough curve

the uppermost layer of solid adsorbs most adsorbate, so that the effluent from the bottom of bed is free of adsorbate, as shown in point a. At point b in the Figure 3, roughly half of the bed is saturated with adsorbate but the effluent concentration of adsorbate is still substantially zero. At point c, the lower portion of the adsorption zone just hits the bottom of the bed, the concentration of effluent rises to some value. At this point, the system is said to have reached the break point. From Figure 3, it can be seen that the effluent concentration at point d has nearly reached the initial value C_0. This point d is sometimes called as exhaustion point; it means that the bed is full of adsorbate, and it must be regenerated to restore its adsorptive capacity and to recover the adsorbed materials. To design and operate a packed bed adsorption process, dynamic data in the form of breakthrough curves are usually needed. In order to avoid excessive laboratory work and pilot plant facilities to obtain such data, adsorption models are used to predict component breakthrough curves based on the available equilibrium relationship and mass transfer data.

A number of models have been developed to simulate the adsorption and ion exchange separations in a packed bed. These models are usually based on the assumption that the rate of adsorption is controlled by one or a combination of the following mechanisms: (a) the external resistance due

to the diffusion of adsorbate molecules through the stagnant film surrounding the solid particle, (b) the internal diffusion of adsorbate molecules through the porous network of solid particles, (c) the rate of adsorption onto the surface of the adsorbent, (d) the axial dispersion of adsorbate molecules in fluid phase. Referring to the adsorption process described above, the adsorption models may broadly be classified into two types based upon the nature of adsorbent particles: (1) the surface adsorption model, and (2) the pore diffusion model. In the models of first kind, the size of pores inside solid particles is assumed extremely small than that of adsorbate molecules, so that the internal diffusion phenomena is disregarded. In the second type of models, all mechanisms controlling the adsorption process are taken into account.

Early in 1947, Hougen and Marshall (19) presented a mathematical model to simulate an isothermal packed bed operation. They neglected the effect of axial dispersion in the fluid phase. In that proposed model, Hougen and Marshall assumed that the equilibrium relationship between liquid phase and solid phase is linear, and the adsorption process is controlled by external diffusion and surface adsorption. Similar work has been done by Lapidus and Amundson (23) to investigate the effect of axial dispersion both in equilibrium case and non-equilibrium case. Chao and Hoelscher (6)

studied the simultaneous axial dispersion and surface adsorption process in a packed bed, the method of moments was proposed to correlate experimental results instead of obtaining an analytic solution. Zwiebel et. al. (41,42,43) investigated the external diffusion transport mechanism and attributed the difference between adsorption and desorption to the nonlinearity of adsorption. Bird et. al. (1) and Mickley et. al. (26) presented the surface adsorption model as a case study by neglecting the axial dispersion term, and obtained an analytic solution in integral form. The same case was also investigated by Tien and Thodos (39) by assuming the equilibrium isotherm in the form of $C_S^*=k_1+k_2C_A^*$ where C_S^* and C_A^* are the equilibrium concentration of solid phase and liquid phase respectively. An analytic solution in series form was obtained.

For modelling the adsorption process, the significance of mass transfer in the pores of adsorbent particles may be neglected in the case of very fine adsorbents such as those found in most of chromatographic columns. However, fine particles are not widely used in industrial applications, and a comprehensive mathematical model is then needed to include the internal diffusion phenomena. Due to the mathematical complexities, most of the researcher neglected the effect of axial dispersion. This assumption could only be valid if the fluid velocity is kept high relative to dispersion.

The adsorption process that is controlled by simultaneous external and internal diffusions was first considered by Rosen (32). By assuming a linear equilibrium isotherm, unit imposed surface concentration on solid phase, and negligible axial dispersion; Rosen obtained an analytic solution in the form of a complicated infinite integral. In order to evaluate that integral, Rosen furnished an approximation method(32), and in addition carried out the integration by numerical method (33). Rosen's solution has been applied by Colwell et. al. (13,14) to determine the relative significance of diffusion resistances in liquid-phase adsorption process. Kasten et. al. (20) made an independent study of the same mechanism as that of Rosen, and obtained an analytic solution including the effect of axial dispersion. Deisler and Wilhelm (15) studied all of the adsorption mechanisms by use of steady state frequency response of a cosine concentration input. They claimed that the axial dispersion does have a significant effect on adsorption process. In serial studies of a packed bed adsorption operation, Masamune and Smith (24,25) developed a general method to analyze their experimental data. From the results, they found that the internal surface adsorption is a very rapid process and the internal diffusion determines the overall adsorption rate. Furthermore, they presented an analytic solution in integral form for the case of adsorption process controlled by simultaneous external and internal diffusions. Schneider and Smith (34) applied the

method of moments to determine the equilibrium constant, the adsorption rate constant, and internal diffusivities for light hydrocarbons. Later, they used these constants to predict breakthrough curves. Recently, the pore diffusion model has been resolved analytically by Rasmuson et. al. (29,30), and also been treated numerically by Raghaven and Ruthven (28).

In view of the work done by previous researchers, the adsorption models of packed bed operation range in complexity from that described by simplified equation of continuity to that describing a detailed and complex situation where in all the kinetic effects are taken into consideration. Most of the investigators worked on the simplified models, while some workers (15,23,28-30) dealt with the complex models.

Although various attempts have been made to extend the simplified model to the complex model, there still are some drawbacks in setting up the boundary conditions to fit the specific system. The most important drawbacks as seen by previous studies in solving the complex model surface from the fact that the selection of boundary condition can not be accepted as adequate to describe the real situation. In this study, a novel and rigorous approach by using the mass conservation law is employed to set up the proper boundary conditions. The objective of this work is to develop generalized mathematical models from different

considerations, then utilizes these models to predict the unsteady state mass transfer behavior in a packed bed.

The basic equations for designing a packed bed operation are derived in chapter II and chapter III. These equations consist of (i) the continuity equation describing the mass conservation of adsorbate in fluid phase, (ii) the rate equation of adsorption process upon solid phase, and (iii) the equilibrium relationship to link the fluid phase and the solid phase. Although the continuity equation is general, the exact form of rate equation for adsorption process depends deeply on the nature of adsorbent. Chapter II deals with the surface adsorption model, where the significance of diffusion in the solid phase is assumed negligible ($D_s = 0$), and the rate equation for adsorption process is expressed in terms of the rate of mass transfer of adsorbate from the bulk flow of fluid across the stagnant film that around the surface of solid particles. Chapter III presents the pore diffusion model in which the resistance in solid phase is assumed as significant as that in fluid phase, and the rate equation for adsorption process is expressed as a second order partial differential equation. In both chapter II & III, two different cases are examined separately based on the consideration of axial dispersion in fluid phase. For the equilibrium isotherm, only the linear equilibrium relationship is adopted due to the mathematical restrictions.

Since most adsorption operations are conducted under the circumstance of very dilute feed concentration, hence the assumption of linear equilibrium between the fluid phase and the solid phase is reasonable. In chapter IV, the calculated breakthrough curves are presented as dimensionless effluent concentration versus time or effluent volume in terms of the variation of system parameters. Besides, the proposed adsorption models are experimentally verified by the system of hemoglobin- albumin- CM sepharose(R^-)- DEAE sepharose(R^+). Finally, some conclusions and recommendations are drawn in chapter V.

CHAPTER II

SURFACE ADSORPTION MODEL

The study of adsorption and regeneration of adsorbents in packed beds is of practical interest in process design. Theories have been developed to explain the adsorption phenomena, and a number of mathematical models have been proposed. For a given fixed bed operation where the packed materials are composed of very fine particles, the process can be simulated by the surface adsorption model. The surface adsorption model is a compact model. This model is assumed that the rate of adsorption is determined by the sequential couplings of fluid film resistance and surface adsorption, where the internal solid diffusion is negligible.

In this chapter, two different cases of surface adsorption model are examined individely. One case considers the effect of axial dispersion in the fluid phase, the other does not. Generally, in higher fluid velocity system, such as gas chromatography, the effect of axial dispersion may be negligible as compared to the contribution of convective flow of fluid through the column. But under some situation, when the fluid velocity is low, the effect of axial dispersion may be

superimposed upon the convective flow and affect the performance of the adsorption process.

The adsorption process which involves the mass transfer between fluid phase and solid phase is usually complex. In order to simplify the analytic treatment of a packed bed operation, the following assumptions are usually made in the mathematical modelling:

1. The physical properties of fluid phase and solid phase are constant.
2. There is plug flow across the bed, so that the concentration of adsorbate in mobile phase is independent of the radial position at any cross section of the bed.
3. The adsorption process is assumed under the condition of isothermal and isobaric.
4. The adsorbent particles are perfectly spherical and maintain uniform porosity across the bed.
5. A linear equilibrium relationship between the fluid phase and the solid phase is assumed.
6. The rate of mass transfer can be approximated by a linear driving force expression.

A. Simple Model (neglecting axial dispersion)

Consider a packed bed operation as shown in Figure 1, in which the column is filled with divided spherical adsorbents (with radius r_o), and pure solvent occupying the interparticle volume initially. At time zero, a fluid mixture containing an active component A (adsorbate A) at concentration C_{Ao} is introduced into one end of the column, say z=0. It is required to find the concentration of adsorbate in the fluid phase and on the solid phase at any time and at any position.

In order to describe the system in a simpler way, one may think of the fluid phase and the solid phase as continuous and existing side by side as shown in Figure 4a. If one examines an element of length Δz and cross sectional area S of a column (Figure 4b), the material balance of the adsorbate A in the fluid phase and on the solid phase can be derived as follows: The rate at which the adsorbate enters the element at z by convective flow is

$$(v S C_A)_z$$

and the rate at which it leaves the element $S\Delta z$ can be given by the same expression evaluated at $z+\Delta z$, where v is the superficial velocity of flow and C_A is the local concentration of adsorbate A. If the rate at which adsorbate transfer from the fluid phase to the surface of

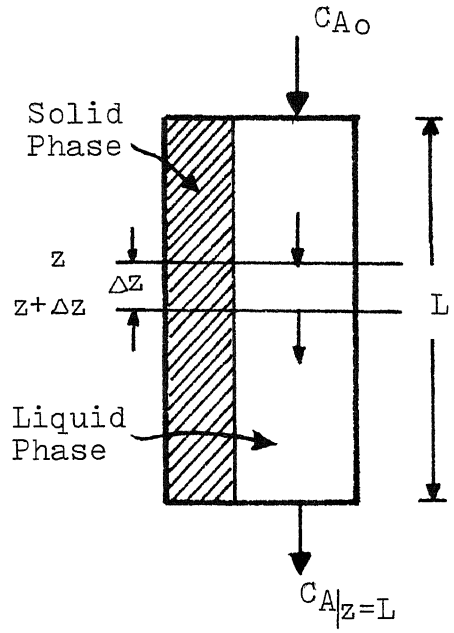

(a)

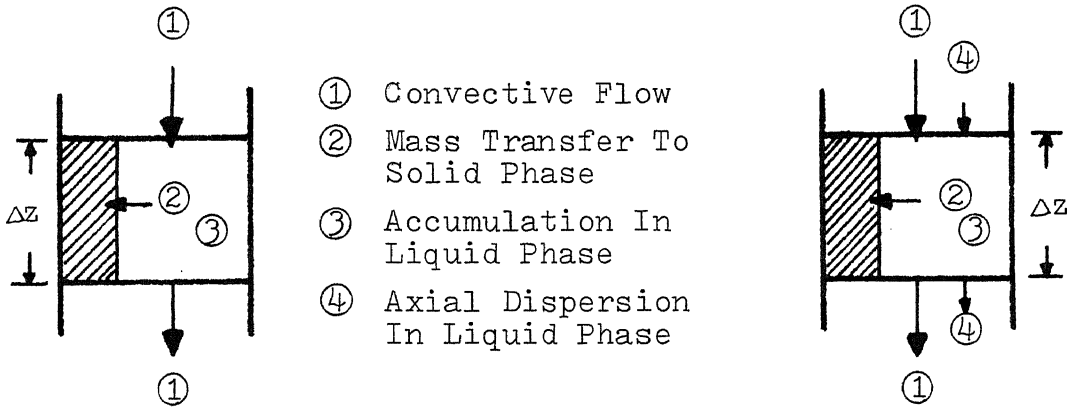

(b) (c)

Figure 4. Schematic diagram of a packed bed operation
(a) a packed bed unit
(b) material balance for simple model
(c) material balance for dispersion model

an adsorbent particle is

$$- 4 \pi r_o^2 K_L (C_A - C_A^*)$$

where C_A^* is the adsorbate concentration at interface, and K_L is the effective mass transfer coefficient in the fluid phase. Then the total mass transfer rate at which adsorbate transfer to all solid particles in element $S\Delta z$ is

$$- \left[\frac{S\Delta z(1-\epsilon)}{\frac{4}{3} \pi r_o^3} \right] 4 \pi r_o^2 K_L (C_A - C_A^*)$$

where ϵ is the bed porosity. After equating the rate of inflow minus that outflow to the rate of accumulation in the element $S\Delta z$ for adsorbate A, there results

$$S\Delta z \, (\partial C_A / \partial t) = (vSC_A)_z - (vSC_A)_{z+\Delta z} - \left[\frac{S\Delta z(1-\epsilon)}{\frac{4}{3} \pi r_o^3} \right] 4 \pi r_o^2 K_L (C_A - C_A^*)$$

As $\Delta z \longrightarrow 0$, the above equation reduces to

$$\frac{\partial C_A}{\partial t} = - \left(\frac{v}{\epsilon}\right) \frac{\partial C_A}{\partial z} - \left(\frac{K_L a}{\epsilon}\right) (C_A - C_A^*) \qquad (2A\text{-}1)$$

where the symbol a is the interfacial contact area, defined as the wetted surface area of adsorbent per unit volume of the bed, its mathematical expression may be written as

$$a = \left[\frac{S\Delta z(1-\epsilon)}{\frac{4}{3} \pi r_o^3} \right] * \left[\frac{4 \pi r_o^2}{S \Delta z} \right] = 3(1-\epsilon)/r_o$$

Next, let us consider the material balance of adsorbate on the solid phase. The rate of adsorption that imposed on the solid phase is equal to the rate of adsorbate accumulated on the solid phase. This rate is also equal to the rate of mass transfer of adsorbate from the bulk flow of fluid across the stagnant film around the solid particles. Hence, the material balance of adsorbate on the solid phase can be expressed as

$$4 \pi r_o^2 \frac{\partial C_{As}}{\partial t} = 4 \pi r_o^2 K_L (C_A - C_A^*)$$

or

$$\frac{\partial C_{As}}{\partial t} = K_L (C_A - C_A^*) \qquad (2A\text{-}2)$$

where C_{As} is the concentration of adsorbate A on the solid phase based on the unit surface area of adsorbent particles.

Although the analytic solution of simultaneous partial differential equations, eqs. (2A-1) and (2A-2), is strongly depended upon the form of equilibrium relationship between fluid phase and solid phase, only the linear relationship is adopted here due to mathematical restrictions. The linear equilibrium isotherm is expressed as

$$C_A^* = m C_{As} \qquad (2A\text{-}3)$$

where m is an area based equilibrium constant. The initial

and boundary conditions for solving equations (2A-1) and (2A-2) with (2A-3) are chosen as

$$C_A\ (\ z,\ t=0\ )=\ 0 \qquad (2A\text{-}4a)$$

$$C_{As}(\ z,\ t=0\ )=\ 0 \qquad (2A\text{-}4b)$$

$$C_A\ (\ z=0,\ t\ )=\ C_{Ao}U(t) \qquad (2A\text{-}4c)$$

The first condition states that the bed is free of adsorbate at $t=0$, and the second one states that no adsorbate adsorbed on solid particles initially. The third condition indicates that at entrance(z=0), a step input in adsorbate concentration C_{Ao} is introduced into the column, here U(t) is the step function of time.

If the dimensionless variables are defined as

$$X = C_A/\ C_{Ao}U(t)$$

$$X^*= C_A^*/\ C_{Ao}U(t)$$

$$Y_S= aC_{As}/C_{Ao}U(t)$$

$$\eta'= zK_La/\ v$$

$$\tau'= tmK_L$$

Then equations (2A-1) through (2A-4) become

$$\frac{\partial X}{\partial \tau'} = -\left(\frac{a}{m\epsilon}\right)\frac{\partial X}{\partial \eta'} - \left(\frac{a}{m\epsilon}\right)(X - X^*) \qquad (2A\text{-}5)$$

$$\frac{\partial Y_s}{\partial \tau'} = \left(\frac{a}{m}\right)(X - X^*) \qquad (2A\text{-}6)$$

$$X^* = \left(\frac{a}{m}\right) Y_s \qquad (2A\text{-}7)$$

with the initial and boundary conditions,

$$X(\eta', \tau'=0) = 0 \qquad (2a\text{-}8a)$$

$$Y_s(\eta', \tau'=0) = 0 \qquad (2A\text{-}8b)$$

$$X(\eta'=0, \tau') = 1 \qquad (2A\text{-}9)$$

The analytic solution of simultaneous partial differential equations, eqs. (2A-5),(2A-6) and (2A-7), can be obtained by means of Laplace transformation. With Laplace transform, one may obtain

$$\gamma p\bar{X} = -\frac{d\bar{X}}{d\eta'} - (\bar{X} - \bar{X}^*) \qquad (2A\text{-}10)$$

$$\frac{\gamma p}{\epsilon}\bar{Y}_s = \bar{X} - \bar{X}^* \qquad (2A\text{-}11)$$

$$\bar{X}^* = \left(\frac{\gamma}{\epsilon}\right)\bar{Y}_s \qquad (2A\text{-}12)$$

and

$$\bar{X}(\eta'=0, p) = \frac{1}{p} \qquad (2A\text{-}13)$$

where $\gamma = (m\epsilon/a)$, and the Laplace transformation is defined as

$$\bar{f}(p) = \mathbb{L}\{f(\eta',\tau')\} = \int_0^\infty e^{-p\tau} f(\eta',\tau')\, d\tau'$$

After grouping equations (2A-11) and (2A-12),

$$p\,\bar{X}^* = \bar{X} - \bar{X}^*$$

or

$$\bar{X}^* = \frac{1}{p+1}\,\bar{X} \qquad (2A\text{-}14)$$

Hence

$$\bar{X} - \bar{X}^* = \frac{p}{p+1}\,\bar{X} \qquad (2A\text{-}15)$$

Introducing equation (2A-14) into equation (2A-12) will result

$$\bar{Y}_s = \left(\frac{\epsilon}{\gamma}\right)\left(\frac{1}{p+1}\right)\,\bar{X} \qquad (2A\text{-}16)$$

If one substitutes equation (2A-15) into equation (2A-10), then the following first order ODE is obtained

$$\frac{d\bar{X}}{d\eta'} = -\left(\gamma p + \frac{p}{p+1}\right)\,\bar{X} \qquad (2A\text{-}17)$$

With the aid of boundary condition, equation (2A-13), the complete solution for equation (2A-17) is

$$\bar{X}(\eta',p) = \frac{1}{p}\exp\left\{-\left(\gamma p + \frac{p}{p+1}\right)\eta'\right\} \qquad (2A\text{-}18)$$

From equation (2A-16), the concentration of adsorbate on solid phase is

$$\bar{Y}_s(\eta', p) = \frac{\epsilon}{\gamma p(p+1)} \exp\{-(\gamma p + \frac{1}{p+1})\eta'\} \qquad (2A\text{-}19)$$

The direct inversions of equations (2A-18) and (2A-19) are tedious. Here two kinds of simple methods are used to carry out the inverse Laplace transformation for equations (2A-18) and (2A-19).

Method 1.

Let $b = \gamma\eta'$

$$F'(p) = \frac{1}{p+1} \exp(\frac{\eta'}{p+1})$$

Then equations (2A-18) and (2A-19) can be rewritten as

$$\bar{X}(\eta', p) = e^{-bp} \frac{1}{p} \exp(-\frac{p\eta'}{p+1})$$

$$= e^{-(bp+\eta')}\{\frac{1}{p} \exp(\frac{\eta'}{p+1})\}$$

$$= e^{-(bp+\eta')}\{\frac{\eta'}{p+1} \exp(\frac{\eta'}{p+1}) + \frac{1}{p}(\frac{1}{p+1}\exp(\frac{\eta'}{p+1}))\}$$

$$= e^{-(bp+\eta')}\{F'(p) + \frac{1}{p} F'(p)\} \qquad (2A\text{-}20)$$

and the expression for $\bar{Y}_s$ can be reduced as

$$\bar{Y}_s(\eta',p)=(\frac{\epsilon}{\gamma})e^{-bp}\{\frac{1}{p(p+1)}\ \exp(-\ \frac{p\eta'}{p+1})\ \}$$

$$=(\ \frac{\epsilon}{\gamma}\ )\ e^{-(bp+\eta')}\{\ \frac{1}{p}(\ \frac{1}{p+1}\ \exp(\frac{\eta'}{p+1}))\ \}$$

$$=(\frac{\epsilon}{\gamma})\ e^{-(bp+\eta')}\ \{\ \frac{1}{p}\ F'(p)\ \} \qquad (2A\text{-}21)$$

Referring to the second shifting theorem of Laplace transform,

$$\mathbb{L}^{-1}\{e^{-bp}F'(p)\} = 0 \quad ; \quad \tau' < b$$

$$= f'(\tau' - b) \quad ; \quad \tau' > b$$

and the integral theorem,

$$\mathbb{L}^{-1}\{\ \frac{1}{p}\ F'(p)\}= \int_0^{\tau'} f'(\tau')\ d\tau$$

Also, from the standard table of inverse Laplace transform (26),

$$\mathbb{L}^{-1}\ \{\frac{1}{p+1}\exp(\frac{k}{p+1})\}=\ e^{-\tau'}\ I_0(\ \sqrt{4k\tau'}\ )$$

The inverse Laplace transforms of equations (2A-20) and (2A-21) are then solved. The final solutions are:

$$X(\eta',\tau') = 0 \qquad ; \ \tau' < b$$

$$= e^{-(\eta'+\tau')} I_0(\sqrt{4\eta'\tau'}) + \int_0^{\tau} e^{-(\eta'+\delta)} I_0(\sqrt{4\eta'\delta}\,)\, d\delta \qquad ; \ \tau' > b$$

(2A-22)

and

$$Y_s(\eta',\tau') = 0 \qquad ; \quad \tau' < b$$

$$= \left(\frac{\gamma}{\epsilon}\right) \int_0^{\tau'} e^{-(\eta'+\delta)} \; I_0(\sqrt{4\eta'\delta}\,)\, d\delta \qquad ; \quad \tau' > b$$

(2A-23)

It is also important to know the analytic solution of a model with pulse input in concentration, because it is applicable to the system in which the chromatographic column sequence consists of a series of adsorption-desorption processes, or to cyclic separation processes such as parametric pumping operations. If one defines the pulse input in concentration as

$$C_A(t) = C_{Ao}\{U(t) - U(t-t^*)\}; \text{ at } z=0 \qquad (2A-24)$$

Then the concentration of adsorbate in the fluid phase and on the solid phase are

$$X(\eta',\tau') = 0 \qquad ; \quad \tau' < b$$

$$= H_1(\tau') \qquad ; \quad b < \tau' < \tau^*$$

$$= H_1(\tau') - H_1(\tau'-\tau^*) \qquad ; \quad \tau' > \tau^* \qquad \text{(2A-25)}$$

and

$$Y_s(\eta',\tau') = 0 \qquad ; \quad \tau' < b$$

$$= H_2(\tau') \qquad ; \quad b < \tau' < \tau^*$$

$$= H_2(\tau') - H_2(\tau'-\tau^*) \qquad ; \quad \tau' > \tau^* \qquad \text{(2A-26)}$$

where

$$H_1(\tau') = e^{-(\eta'+\tau')} I_0(\sqrt{4\eta'\tau'}) + \int_0^{\tau'} e^{-(\eta'+\delta)} I_0(\sqrt{4\eta'\delta})\, d\delta$$

$$H_2(\tau') = \int_0^{\tau'} e^{-(\eta'+\delta)} I_0(\sqrt{4\eta'\delta})\, d\delta$$

$$\tau^* = t\ m\ K_L$$

Method 2.

Let $b = \gamma\eta'$

$$F'(p) = \frac{1}{p+1} \exp\left(\frac{\eta'}{p+1}\right)$$

$$F_1(p) = \frac{1}{p} \exp\left(-\frac{p\eta'}{p+1}\right)$$

Then equations (2A-18) and (2A-19) reduce to

$$\bar{X}(\eta', p) = e^{-bp} F_1(p) \qquad (2A\text{-}27)$$

$$\bar{Y}_s(\eta', p) = \left(\frac{\epsilon}{\gamma}\right) e^{-(bp+\eta')}\left\{\frac{1}{p} F'(p)\right\} \qquad (2A\text{-}28)$$

If one defines a function $F_2(p)$ as

$$F_2(p) = \int_o^{\eta'} \frac{1}{p+1} \exp\left(-\frac{p\mu}{p+1}\right) d\mu \qquad (2A\text{-}29)$$

By means of partial integration, the right hand side of equation (2A-29) becomes

$$\int_o^{\eta'} \frac{1}{p+1} \exp\left(-\frac{p\mu}{p+1}\right) d\mu = \int_o^{\eta'} e^{-\mu}\, d\left(\exp\left(\frac{\mu}{p+1}\right)\right)$$

$$= \exp\left(-\frac{p\eta'}{p+1}\right) - 1 + \int_o^{\eta'} \exp\left(-\frac{p\mu}{p+1}\right) d\mu$$

Hence

$$F_2(p) = \frac{1}{p} - \frac{1}{p} \exp\left(-\frac{p}{p+1}\right) \qquad (2A\text{-}30)$$

If the expression of $F_1(p)$ is rewritten as

$$F_1(p) = \frac{1}{p} - \{\frac{1}{p} - \frac{1}{p} \exp(-\frac{p\eta'}{p+1}) \}$$

$$= \frac{1}{p} - \{ \int_0^{\eta'} \frac{1}{p+1} \exp(-\frac{p\mu}{p+1}) d\mu \} \qquad (2A-31)$$

Equation (2A-27) becomes

$$\bar{X}(\eta',p) = e^{-bp}\{ \frac{1}{p} - \int_0^{\eta'} (\frac{1}{p+1}) \exp(-\frac{p\mu}{p+1}) \, d\mu \} \qquad (2A-32)$$

With the experience from Method 1, the inverse Laplace transform of equation (2A-32) is made. The final solution is

$$X(\eta',\tau') = 0 \qquad ; \quad \tau' < b$$

$$= 1 - \int_0^{\eta'} e^{-(\tau'+\mu)} I_0(\sqrt{4\tau'\mu}) \, d\mu \qquad ; \quad \tau' > b \qquad (2A-33)$$

It can be proved that the result expressed in the form of equation (2A-33) is the same as that of equation (2A-22). More detailed discussions of the results are given in chapter IV.

B. Dispersion Model

The effect of axial dispersion in fluid phase in a packed bed operation was first considered by Glueckauf et. al. (16), and extensively studied by Lapidus and Amundson (23). Referring to Figure 4c, the material balance of active component A (adsorbate) in the fluid phase is derived

$$\epsilon S\Delta z \frac{\partial C_A}{\partial t} = (vSC_A)_z - (vSC_A)_{z+\Delta z}$$

$$- (\epsilon SD_L \frac{\partial C_A}{\partial z})_z + (\epsilon SD_L \frac{\partial C_A}{\partial z})_{z+\Delta z}$$

$$- \left[\frac{S\Delta z(1-\epsilon)}{\frac{4}{3}\pi r_o^3} \right] 4\pi r_o^2 K_L(C_A - C_A^*)$$

or

$$\frac{\partial C_A}{\partial t} = - (\frac{v}{\epsilon}) \frac{\partial C_A}{\partial z} - (\frac{K_L a}{\epsilon}) (C_A - C_A^*) + D_L \frac{\partial^2 C_A}{\partial z^2} \qquad (2B\text{-}1)$$

Equation (2B-1) is very similar to equation (2A-1) except for the axial dispersion term, where D_L is the effective axial dispersion coefficient of adsorbate. The material balance of adsorbate on the solid phase and the equilibrium relationship are the same as that in the Simple Model,

$$\frac{\partial C_{AS}}{\partial t} = K_L(C_A - C_A^*) \qquad (2B\text{-}2)$$

$$C_A^* = m C_{As} \qquad (2B\text{-}3)$$

Since equation (2B-1) is a second order partial differential equation, it needs two sets of boundary conditions to obtain the complete soultion. Generally, there are three types of homogeneous boundary conditions that are used to solve the second order linear partial differential equation $\nabla^2 u = 0$ (23):

(a) The Dirichlet boundary condition, which prescribes the value of u at boundaries,

(b) The Neumann boundary condition, which prescribes the value of normal derivatives du/dn of the function u at boundaries,

(c) The Robin boundary condition, which prescribes the value of ku+(du/dn) at boundaries.

The first set of boundary condition in this study belongs to the third type, it is also named the Danckwerts' boundary condition. This boundary condition is derived as follows: In the entrance section, the material balance of adsorbate in fluid phase can be expressed as

$$\epsilon S \Delta z \frac{\partial C_A}{\partial t} = vSC_{Ao}U(t) - (vSC_A)_{\Delta z} + (\epsilon S D_L \frac{\partial C_A}{\partial z})_{\Delta z}$$

$$- \left[\frac{S\Delta z(1-\epsilon)}{\frac{4}{3}\pi r_o^3}\right] 4\pi r_o^2 K_L(C_A - C_A^*)$$

as $\Delta z \longrightarrow 0$, the above equation reduces to

$$C_{Ao}U(t) - C_A\Big|_{z=0} + \left(\frac{\epsilon D_L}{v}\right)\left.\frac{\partial C_A}{\partial z}\right|_{z=0} = 0 \qquad (2B\text{-}4)$$

The second boundary condition can be set up by means of total material balance of adsorbate across the packed column, that is

$$vS\int_o^t (C_{Ao}U(t) - C_A\Big|_{z=L})\,dt = S\epsilon\int_o^L C_A\,dz + \int_o^L C_{As}\,4\pi\,r_o^2\left\{\frac{Sdz(1-\epsilon)}{\frac{4}{3}\pi r_o^3}\right\} \qquad (2B\text{-}5)$$

Here, the left-hand side of equation (2B-5) represents the accumulation of total adsorbate in the packed column during time period t; the first term in the right-hand side of equation (2B-5) is the total amount of adsorbate present in the fluid phase while the second term represents the total amount of adsorbate deposited on the solid phase. After introducing the interfacial contact area a into equation (2B-5), it becomes

$$\int_o^t (C_{Ao}U(t) - C_A\Big|_{z=L})\,dt = \left(\frac{\epsilon}{v}\right)\int_o^L C_A\,dz + \left(\frac{a}{v}\right)\int_o^L C_{As}\,dz \qquad (2B\text{-}6)$$

The initial conditions are the same as those in the Simple Model,

$$C_A\ (z=0,\ t) = 0 \qquad (2B\text{-}7a)$$

$$C_{As}(z=0,\ t) = 0 \qquad (2B\text{-}7b)$$

If the dimensionless variables are defined as

$$X = C_A/C_{Ao}U(t)$$

$$X^* = C_A^*/C_{Ao}U(t)$$

$$Y_s = aC_{As}/C_{Ao}U(t)$$

$$\eta = z/L$$

$$\tau = tD_L/L^2$$

hen the governing equations with initial and boundary onditions are normalized as

Luid Phase

$$\frac{\partial X}{\partial \tau} = -\left(\frac{vL}{\epsilon D_L}\right)\frac{\partial X}{\partial \eta} - \left(\frac{K_L a L^2}{\epsilon D_L}\right)(X-X^*) + \frac{\partial^2 X}{\partial \eta^2}$$

r

$$\frac{\partial X}{\partial \tau} = -A\,\frac{\partial X}{\partial \eta} - \alpha\,(X-X^*) + \frac{\partial^2 X}{\partial \eta^2} \qquad (2B\text{-}8)$$

here

$$A = \frac{vL}{\epsilon D_L} \quad ; \quad \alpha = \frac{K_L a L^2}{\epsilon D_L}$$

Solid Phase

$$\frac{\partial Y_s}{\partial \tau} = \left(\frac{K_L a L^2}{\epsilon D_L}\right) (X - X^*)$$

or

$$\frac{\partial Y_s}{\partial \tau} = \epsilon \, \alpha (X - X^*) \qquad (2B\text{-}9)$$

Equilibrium relationship

$$X^* = (\gamma/\epsilon) \, Y_s \quad ; \text{ where } \quad \gamma = m\epsilon/a \qquad (2B\text{-}10)$$

Initial Conditions

$$X(\eta, \tau=0) = 0 \qquad (2B\text{-}11a)$$

$$Y_s(\eta, \tau=0) = 0 \qquad (2B\text{-}11b)$$

Boundary Conditions

(i) the entrance condition:

$$1 - X\Big|_{\eta=0^+} \left(\frac{1}{A}\right) \frac{\partial X}{\partial \eta}\Big|_{\eta=0} = 0 \qquad (2B\text{-}12)$$

(ii) total material balance:

$$A \int_0^{\tau} (1 - X|_{\eta=1}) \, d\tau = \int_0^1 \left(X + \frac{Y_s}{\epsilon} \right) d\eta \qquad (2B\text{-}13)$$

Taking Laplace transform for equation (2B-8) through (2B-13) will result

$$p\bar{X} = - A \frac{d\bar{X}}{d\eta} - \alpha (\bar{X}-\bar{X}^*) + \frac{d^2X}{d\eta^2} \qquad (2B\text{-}14)$$

$$p\bar{Y}_s = \epsilon\alpha (\bar{X}-\bar{X}^*) \qquad (2B\text{-}15)$$

$$\bar{X}^* = (\gamma/\epsilon) \bar{Y}_s \qquad (2B\text{-}16)$$

with boundary conditions,

$$\frac{1}{p} - \bar{X}\Big|_{\eta=0} + (\frac{1}{A}) \frac{d\bar{X}}{d\eta}\Big|_{\eta=0} = 0 \qquad (2B\text{-}17)$$

$$A(\frac{1}{p} - \bar{X}\Big|_{\eta=1}) = p \int_0^1 (\bar{X} + \frac{\bar{Y}_s}{\epsilon}) d\eta \qquad (2B\text{-}18)$$

Combining equations (2B-15) and (2B-16),

$$p \bar{Y}_s = \epsilon\alpha (\bar{X} - \frac{\gamma}{\epsilon} \bar{Y}_s)$$

or

$$\bar{Y}_s = (\frac{\epsilon\alpha}{p+\alpha\gamma}) \bar{X} \qquad (2B\text{-}19)$$

By substituting equation (2B-19) into equation (2B-15) gives

$$\bar{X}^* = (\frac{\alpha\gamma}{p+\alpha\gamma}) \bar{X} \qquad (2B\text{-}20)$$

and

$$\bar{X} - \bar{X}^* = \left(\frac{p}{p+\alpha\gamma}\right) \bar{X} \qquad (2B\text{-}21)$$

Substituting equation (2B-21) into equation (2B-14) and rearranging it, the result equation is

$$\frac{d^2\bar{X}}{d\eta^2} - A \frac{d\bar{X}}{d\eta} - \left[p + \frac{p\alpha}{p+\alpha\gamma} \right] \bar{X} = 0$$

Let

$$F(p) = p + \frac{p\alpha}{p+\alpha\gamma} \qquad (2B\text{-}22)$$

Then the above differential equation becomes

$$\frac{d^2\bar{X}}{d\eta^2} - A \frac{d\bar{X}}{d\eta} - F(p) \bar{X} = 0 \qquad (2B\text{-}23)$$

Equation (2B-23) is a second order linear ordinary differential equation with constant coefficients. There are two kinds of expression for its general solution which depend upon the value of $A^2+4F(p)$. No matter what type of general solution is adopted initially, the complete solution should be in the same form. Let us assume that the general is expressed as

$$\bar{X}(\eta,p) = e^{\frac{A}{2}\eta} \left\{ c_1 \sinh \frac{\nabla}{2}\eta + c_2 \cosh \frac{\nabla}{2}\eta \right\}$$

where $\nabla = \sqrt{A^2+4F(p)}$ (2B-24)

In order to determine the coefficients c_1 and c_2, the boundary conditions, equations (2B-17) and (2B-18), are employed. It is obvious that equation (2B-18) can be simplified with the aid of equation (2B-19),

$$A\left(\frac{1}{p} - \bar{X}\Big|_{\eta=1}\right) = p\int_0^1 \left(\bar{X} + \frac{\alpha\bar{X}}{p+\alpha\gamma}\right) d\eta$$

$$= F(p)\int_0^1 \bar{X}\, d\eta \qquad (2B\text{-}25)$$

From equation (2B-24), one may have

$$\bar{X}\Big|_{\eta=0} = c_2 \qquad (2B\text{-}26)$$

$$\bar{X}\Big|_{\eta=1} = e^{\frac{A}{2}}\left\{c_1 \sinh\frac{\nabla}{2} + c_2\cosh\frac{\nabla}{2}\right\} \qquad (2B\text{-}27)$$

$$\frac{d\bar{X}}{d\eta}\Big|_{\eta=0} = \frac{A}{2}c_2 + \frac{\nabla}{2}c_1 \qquad (2B\text{-}28)$$

$$\int_0^1 \bar{X}\, d\eta = \int_0^1 \left\{e^{\frac{A}{2}\eta}\left[c_1 \sinh\frac{\nabla}{2}\eta + c_2\cosh\frac{\nabla}{2}\eta\right]\right\} d\eta$$

$$= c_1\int_0^1 e^{\frac{A}{2}\eta}\sinh\frac{\nabla}{2}\eta\, d\eta + c_2\int_0^1 e^{\frac{A}{2}\eta}\cosh\frac{\nabla}{2}\eta\, d\eta$$

$$= -\frac{c_1}{F}\left\{\frac{A}{2}e^{\frac{A}{2}}\sinh\frac{\nabla}{2} - \frac{\nabla}{2}e^{\frac{A}{2}}\cosh\frac{\nabla}{2} + \frac{\nabla}{2}\right\}$$

$$-\frac{c_2}{F}\left\{\frac{A}{2}e^{\frac{A}{2}}\cosh\frac{\nabla}{2} - \frac{\nabla}{2}e^{\frac{A}{2}}\sinh\frac{\nabla}{2} - \frac{A}{2}\right\}$$

(2B-29)

Applying equations (2B-26) and (2B-28) to equation (2B-17),

$$\frac{1}{p} - c_2 + \frac{1}{A}\left(\frac{A}{2}c_2 + \frac{\sqrt{A^2+4F}}{2}c_1\right) = 0$$

or

$$c_2 = \frac{2}{p} + \frac{\sqrt{A^2+4F}}{2}c_1 \qquad (2B\text{-}30)$$

By substituting equations (2B-27) and (2B-29) into equation (2B-18). With the aid of equation (2B-30), the constant c_1 is obtained

$$c_1 = -\frac{A\cosh\frac{\sqrt{A^2+4F}}{2} + \sqrt{A^2+4F}\sinh\frac{\sqrt{A^2+4F}}{2}}{p\left[\sqrt{A^2+4F}\cosh\frac{\sqrt{A^2+4F}}{2} + \left(\frac{A^2+2F}{A}\right)\sinh\frac{\sqrt{A^2+4F}}{2}\right]} \qquad (2B\text{-}31)$$

Substituting equation (2B-31) into equation (2B-30) for c_2,

$$c_2 = \frac{\sqrt{A^2+4F}\cosh\frac{\sqrt{A^2+4F}}{2} + A\sinh\frac{\sqrt{A^2+4F}}{2}}{p\left[\sqrt{A^2+4F}\cosh\frac{\sqrt{A^2+4F}}{2} + \left(\frac{A^2+2F}{A}\right)\sinh\frac{\sqrt{A^2+4F}}{2}\right]} \qquad (2B\text{-}32)$$

Finally, resubstituting the constants c_1 and c_2 into equation (2B-24) and applying the addition formula of hyperbolic function, the complete solution results.

$$\bar{X}(\eta,p)=\frac{e^{\frac{A}{2}\eta}\left\{\cosh\frac{\sqrt{A^2+4F}}{2}(1-\eta)+\frac{A}{\sqrt{A^2+4F}}\sinh\frac{\sqrt{A^2+4F}}{2}(1-\eta)\right\}}{p*\left\{\cosh\frac{\sqrt{A^2+4F}}{2}+\left(\frac{A^2+2F}{A}\right)\frac{1}{\sqrt{A^2+4F}}\sinh\frac{\sqrt{A^2+4F}}{2}\right\}} \qquad (2B\text{-}33)$$

Equation (2B-33) is an expression in Laplace transform, it is desired to inverse this Laplace transform $\bar{X}(\eta,p)$ to get the final solution. The expression of $\bar{X}(\eta,p)$ is so complicated that the discussions of branch point and singularities are necessary before processing the inverse Laplace transformation.

By expanding the hyperbolic functions in terms of infinite series,

$$\cosh\frac{\sqrt{A^2+4F}}{2}=\sum_{n=0}^{\infty}(A^2+4F)^n\left\{\frac{(1/2)^{2n}}{(2n)!}\right\}$$

$$\cosh\frac{\sqrt{A^2+4F}}{2}(1-\eta)=\sum_{n=0}^{\infty}(A^2+4F)^n\left\{\frac{[(1-\eta)/2]^{2n}}{(2n)!}\right\}$$

$$\frac{1}{\sqrt{A^2+4F}}\sinh\frac{\sqrt{A^2+4F}}{2}=\sum_{n=0}^{\infty}(A^2+4F)^n\left\{\frac{(1/2)^{2n+1}}{(2n+1)!}\right\}$$

$$\frac{1}{\sqrt{A^2+4F}}\sinh\frac{\sqrt{A^2+4F}}{2}(1-\eta)=\sum_{n=0}^{\infty}(A^2+4F)^n\left\{\frac{[(1-\eta)/2]^{2n+1}}{(2n+1)!}\right\}$$

Thus, equation (2B-33) can be reduced to

$$\bar{X}(\eta,p)= e^{\frac{A}{2}\eta}\left\{\frac{\sum_{n=0}^{\infty}(A^2+4F)^n\{\frac{[(1-\eta)/2]^{2n}}{(2n)!}+\frac{[(1-\eta)/2]^{2n+1}}{(2n+1)!}\}}{p*\sum_{n=0}^{\infty}(A^2+4F)^n\{\frac{(1/2)^{2n}}{(2n)!}+(\frac{A^2+2F}{A})\frac{(1/2)^{2n+1}}{(2n+1)!}\}}\right\}$$

(2B-34)

If one expands the terms of A^2+4F and $(A^2+2F)/A$ as

$$A^2+4F= A^2+4(p+\frac{p\alpha}{p+\alpha\gamma})= \frac{a_o p^2+a_1 p+a_2}{p+b_o}$$

$$\frac{A^2+2F}{A}= A+\frac{2}{A}(p+\frac{p\alpha}{p+\alpha\gamma})= \frac{l_o p^2+l_1 p+l_2}{p+b_o}$$

Then, equation (2B-34) can be reformed as

$$\bar{X}(\eta,p)= e^{\frac{A}{2}\eta}\left\{\frac{\sum_{n=0}^{\infty}(a_o p^2+a_1 p+a_2)^n(p+b_o)\{\frac{[(1-\eta)/2]^{2n}}{(2n)!}+A\frac{[(1-\eta)/2]^{2n+1}}{(2n+1)!}\}}{p*\sum_{n=0}^{\infty}(a_o p^2+a_1 p+a_2)^n[(p+b_o)\frac{(1/2)^{2n}}{(2n)!}+(l_o p^2+l_1 p+l_2)\frac{(1/2)^{2n+1}}{(2n+1)!}]}\right\}$$

(2B-35)

From equations (2B-34) and (2B-35), it is obvious that there are no branch points and no essential singularities. Therefore, the results deduced from equation (2B-33) are:

(1) there exists one simple pole at p=0,

(2) there exist many simple poles p_k which satisfy

$$\cosh \frac{\sqrt{A^2+4F}}{2} + \left(\frac{A^2+2F}{A}\right)\left(\frac{1}{\sqrt{A^2+4F}}\right)\sinh \frac{\sqrt{A^2+4F}}{2} = 0 \qquad (2B\text{-}36)$$

In general, there are two ways to implement the inverse Laplace transformation. One way is by using the standard tables of special Laplace transform with the existing theorems as shown in part A (Simple Model). The other method which is employed here, is by applying the complex inversion formula and the calculus of residues. Let the Laplace transform $\bar{X}(\eta,p)$ can be expressed as

$$\bar{X}(\eta,p) = J(p)/L(p) \qquad (2B\text{-}37)$$

where the power of p in L(p) is greater than that in J(p). Then by using the residues theorem, the inverse Laplace transform is

$$X(\eta,\tau) = \mathbb{L}^{-1}\{\bar{X}(\eta,p)\} = \sum_k \text{Res}\{ e^{p\tau}\ \bar{X}(\eta,p); p_k\}$$

$$= \lim_{p\to p_k} \left\{\frac{J(p)}{L'(p)}\ e^{p\tau}\right\} \qquad (2B\text{-}38)$$

where the points p_k's are the poles of $\bar{X}(\eta,p)$ and $L'(p)=\frac{dL(p)}{dp}$.

The residues of $\bar{X}(\eta,p)$ are evaluated as follows:

(1) Residue at p=0

Let $\bar{X}(\eta,p)$ be expressed as

$$\bar{X}(\eta,p)= \frac{J(p)}{L(p)}$$

where

$$J(p)= e^{\frac{A}{2}\eta}\{\cosh\frac{\sqrt{A^2+4F}}{2}(1-\eta)+\frac{A}{\sqrt{A^2+4F}}\sinh\frac{\sqrt{A^2+4F}}{2}(1-\eta)\}$$

$$L(p)= p * \{\cosh\frac{\sqrt{A^2+4F}}{2} + (\frac{A^2+2F}{A})(\frac{1}{\sqrt{A^2+4F}})\sinh\frac{\sqrt{A^2+4F}}{2}\}$$

At p=0, F(p)=0; so that

$$J(p=0)= e^{\frac{A}{2}\eta}\{\cosh\frac{A}{2}(1-\eta) + \sinh\frac{A}{2}(1-\eta)\} = e^{\frac{A}{2}}$$

$$L'(p=0)= \cosh\frac{A}{2} + \sinh\frac{A}{2} = e^{\frac{A}{2}}$$

Therefore, the residue evaluated at p=0 is

$$\text{Res } 1 = \lim_{p\to 0}\frac{J(p)}{L'(p)} = 1 \qquad (2B\text{-}39)$$

(2) Residues of $\bar{X}(\eta,p)$ at $p=p_k$'s

There are many simple poles p_k which satisfy equation (2B-36). Equation (2B-36) may be rewritten as

$$\tanh \frac{\sqrt{A^2+4F}}{2} = - \frac{A\sqrt{A^2+4F}}{A^2+2F} \qquad (2B\text{-}40)$$

Two cases will be discussed below in terms of the values values of (A^2+4F): (a) $A^2+4F \geqslant 0$, (b) $A^2+4F < 0$.

Case a.: $A^2+4F \geqslant 0$

Let $A^2+4F=\xi_n^2$, where ξ_n may be positive or negative real numbers. Thus equation (2B-40) reduces to

$$\tanh \frac{\xi_n}{2} = -\frac{2A\xi_n}{A^2+\xi_n^2} \qquad (2B\text{-}41)$$

It can be shown that there are no suitable solutions for equation (2B-41) except the trivial solution $\xi_n=0$.

Case b.: $A^2+4F<0$

Let $A^2+4F=-\beta_n^2$, where β_n may be positive or negative real numbers. Thus equation (2B-40) reduces to

$$\tan (\beta_n/2) = - 2A\beta_n/(A^2 - \beta_n^2) \qquad (2B\text{-}42)$$

Equation (2B-42) is a transcendental equation, there are many eigenvalues β_n which satisfy this eigenfunction as shown in Figure 5. These β_n can be obtained by graphic method or numerical method. Since graphical solution is time consuming, a computer program is developed to search these eigenvalues β_n for equation (2B-42). This computer program is given in Appendix A. The first twenty eigenvalues β_n are shown in Table 1. Knowning the values of β_n, the values of p_k can then be calculated from the relationship, $A^2+4F= -\beta_n^2$.

If one defines $\Phi = (A^2+ \beta_n^2)/4$, then

$$F(p)= p_k+ \frac{\alpha p_k}{p_k+\alpha\gamma} = - \frac{A^2+\beta_n^2}{4} \qquad (2B\text{-}43)$$

Solving equation (2B-43) for p_k, one may obtain

$$p_k= - \frac{G_1}{2} \pm \frac{\sqrt{G_1+4G_2}}{2} \qquad (2B\text{-}44)$$

where

$$G_1= \Phi + \alpha\gamma + \alpha$$

$$G_2= \Phi \alpha\gamma$$

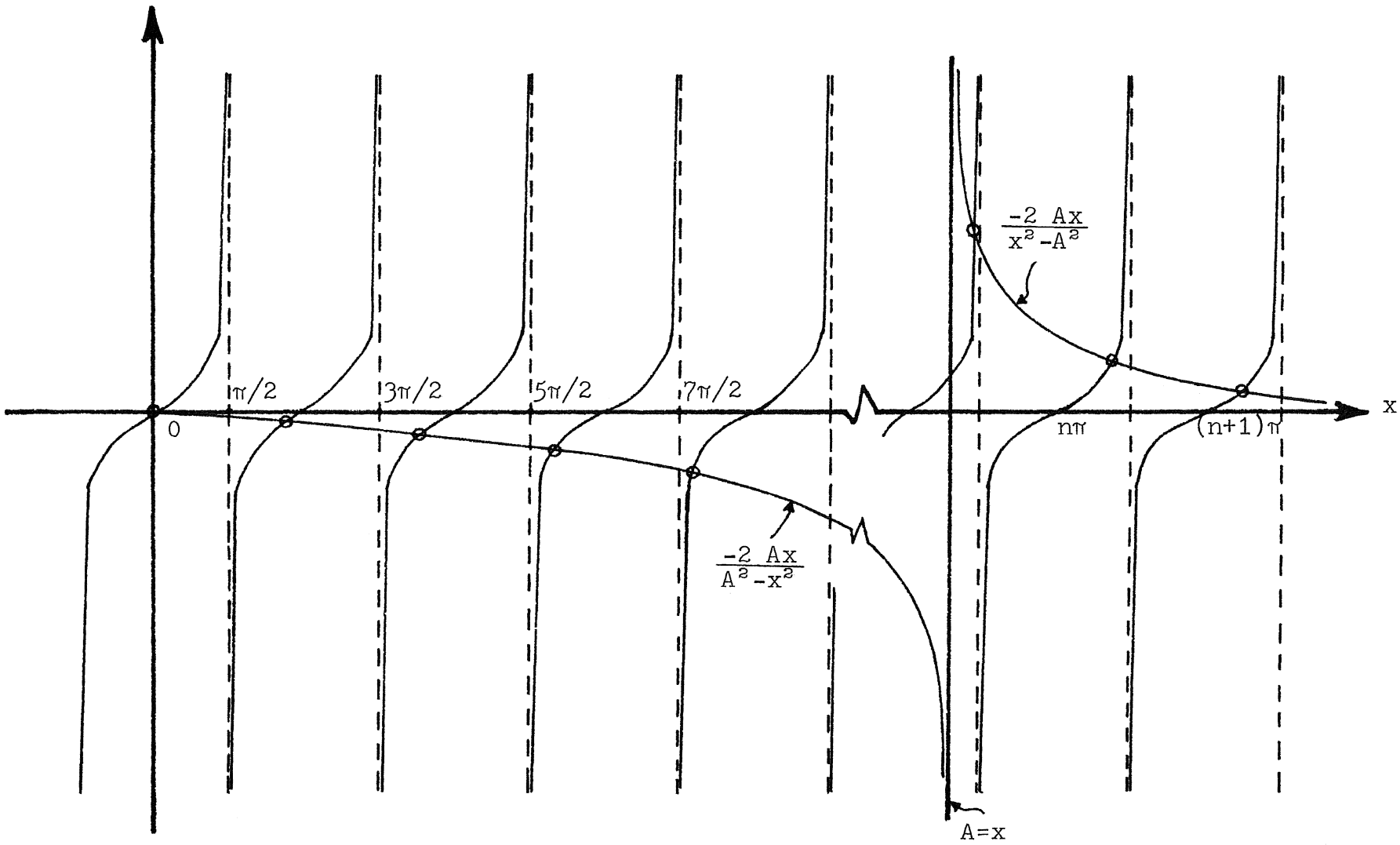

Figure 5. Sketch of eigenfunction, $\tan(x/2) = -2Ax/(A^2-x^2)$

Table 1.

Eigenvalues of $\tan(\beta_n/2) = -2A\beta_n/(A^2-\beta_n^2)$

** For the case of A= 13.3333

β_1	=	0.487981 E01
β_2	=	0.999360 E01
β_3	=	0.154184 E02
β_4	=	0.211035 E02
β_5	=	0.269693 E02
β_6	=	0.329538 E02
β_7	=	0.451313 E02
β_8	=	0.512829 E02
β_9	=	0.574607 E02
β_{10}	=	0.636577 E02
β_{11}	=	0.698693 E02
β_{12}	=	0.760921 E02
β_{13}	=	0.823237 E02
β_{14}	=	0.885623 E02
β_{15}	=	0.948067 E02
β_{16}	=	0.101056 E03
β_{17}	=	0.113565 E03
β_{18}	=	0.119824 E03
β_{19}	=	0.126085 E03
β_{20}	=	0.132349 E03

By applying the residues theorem, the residues of $\bar{X}(\eta,p)$ at $p=p_k$ can be expressed as

$$\text{Res } 2 = \lim_{p\to p_k} \left\{ \frac{J(p)}{L'(p)} e^{p\tau} \right\} \qquad (2B\text{-}45)$$

where

$$J(p)= e^{\frac{A}{2}\eta}\left\{\cosh\frac{\sqrt{A^2+4F}}{2}(1-\eta) + \frac{A}{\sqrt{A^2+4F}} \sinh \frac{\sqrt{A^2+4F}}{2}(1-\eta)\right\}$$

$$L(p)= p* \left\{\cosh \frac{\sqrt{A^2+4F}}{2} +\left(\frac{A^2+2F}{A}\right) \frac{1}{\sqrt{A^2+4F}} \sinh \frac{\sqrt{A^2+4F}}{2}\right\}$$

Differentialting L(p) with respect to p,

$$L'(p)= \left\{\cosh \frac{\sqrt{A^2+4F}}{2} +\left(\frac{A^2+2F}{A}\right) \frac{1}{\sqrt{A^2+4F}} \sinh \frac{\sqrt{A^2+4F}}{2} \right\}$$

$$+p*\left(\frac{dF}{dp}\right)*\left\{\left[\frac{A^2+ 2F}{A(A^2+4F)}\right]\cosh\frac{\sqrt{A^2+4F}}{2}+\left[1 +\frac{2}{A} - \frac{2(A^2+2F)}{A(A^2+4F)}\right]\frac{\sinh\frac{\sqrt{A^2+4F}}{2}}{\sqrt{A^2+ 4F}}\right\} \qquad (2B\text{-}46)$$

and

$$\frac{dF}{dp}= \frac{d}{dp}\left(p+ \frac{p\alpha}{p+\alpha\gamma}\right)= 1 + \frac{\alpha^2\gamma}{(p+\alpha\gamma)^2} \qquad (2B\text{-}47)$$

At $p=p_k$, $A^2+4F= -\beta_n^2$ and $\sqrt{A^2+4F}= i\beta_n$; so that

$$J(p_k)= e^{\frac{A}{2}\eta}\{\cos\frac{\beta_k}{2}(1-\eta)+ \frac{A}{\beta_k}\sin\frac{\beta_k}{2}(1-\eta)\} \qquad (2B\text{-}48)$$

$$L'(p_k)=p_k*[1+ \frac{\alpha^2\gamma}{(p_k+\alpha\gamma)^2}]*\{[\frac{A^2+\beta_k+A^2\beta_k}{A\,\beta_k^3}]\sin\frac{\beta_k}{2} -[\frac{A^2-\beta_k^2}{2A\beta_k^2}]\cos\frac{\beta_k}{2}\}$$

(2B-49)

Substituting equations (2B-48) and (2B-49) into equation (2B-45) results in:

$$\text{Res } 2=\sum_{k=0}^{\infty}\frac{[\ \beta_k\cos\frac{\beta_k}{2}(1-\eta)\ +\ A\ \sin\frac{\beta_k}{2}(1-\eta)]*\ e^{\frac{A}{2}\eta\ +p_k\tau}}{p_k*[1+\frac{\alpha^2\gamma}{(p_k+\alpha\gamma)^2}]*\{[\frac{A^2+A\beta_k^2+\beta_k^2}{A\,\beta_k^3}]\sin\frac{\beta_k}{2} -[\frac{A^2-\beta_k^2}{2A\beta_k^2}]\cos\frac{\beta_k}{2}\ \}}$$

(2B-50)

After combining equations (2B-39) and (2B-50), the complete final solution is obtained

$$X(\eta,\tau)= 1-\sum_{k=0}^{\infty}\frac{[\ \beta_k\cos\frac{\beta_k}{2}(1-\eta)+\ A\ \sin\frac{\beta_k}{2}(1-\eta)]*\ e^{\frac{A}{2}\eta\ +p_k\tau}}{p_k*[1+\frac{\alpha^2\gamma}{(p_k+\alpha\gamma)^2}]*\{[\frac{A^2-\beta_k^2}{2A\beta_k^2}]\cos\frac{\beta_k^2}{2}\ -\ [\frac{A^2+\beta_k^2+A\beta_k^2}{A\,\beta_k^3}]\sin\frac{\beta_k}{2}\}}$$

(2B-51)

Equation (2B-51) describes the local concentration of adsorbate at any position η and at any time τ in the packed column. Hence, from equation (2B-51), the effluent concentration of adsorbate ($\eta = 1$) is

$$X(1,\tau) = 1 - \sum_{k=1}^{\infty} \frac{\beta_k^{*}\, e^{\frac{A}{2}+p_k\tau}}{p_k^{*}\left[1+\frac{\alpha^2\gamma}{(p_k+\alpha\gamma)^2}\right]*\left\{\left[\frac{A^2-\beta_k^2}{2A\beta_k^2}\right]\cos\frac{\beta_k}{2} - \left[\frac{A^2+\beta_k^2+A\beta_k^2}{A\,\beta_k^3}\right]\sin\frac{\beta_k}{2}\right\}}$$

** $\beta_0 = 0$ (2B-52)

Similarily, for a pulse input in adsorbate concentration such as

$$C_A(t) = C_{Ao}\{\, U(t) - U(t-t^{*}) \,\}$$

The effluent concentration of adsorbate in dimensionless form is

$$\begin{aligned} X(1,\tau) &= 1 - V(1,\tau) && ;\ 0 < \tau < \tau^{*} \\ &= V(1,\tau) - V(1,\tau-\tau^{*}) && ;\ \tau > \tau^{*} \end{aligned}$$

where

$$\tau^{*} = tD_L/L^2 \qquad \text{(2B-53)}$$

$$V(1,\tau)=\sum_{k=1}^{\infty}\frac{\beta_k^{*}\, e^{\frac{A}{2}+p_k\tau}}{p_k^{*}\left[1+\frac{\alpha^2\gamma}{(p_k+\alpha\gamma)^2}\right]*\left\{\left[\frac{A^2-\beta_k^2}{2A\beta_k^2}\right]\cos\frac{\beta k}{2}-\left[\frac{A^2+\beta_k^2+A\beta_k^2}{A\beta_k^3}\right]\sin\frac{\beta k}{2}\right\}}$$

The calculated results of equations (2B-52) and (2B-53) are given in Chapter IV.

CHAPTER III

PORE DIFFUSION MODEL

The adsorption processes in a packed bed are generally characterized by the diffusion transport of adsorbate molecules and the interactions between the adsorbate molecules (fluid phase) and the adsorbent particles (solid phase). Although the interaction between the adsorbate molecule and adsorbent depends on the nature of adsorbent and the chemical properties of adsorbate, it can usually be expressed in terms of the equilibrium isotherm. For the sake of simplicity, a linear equilibrium isotherm is assumed throughout this study.

Apart from the axial dispersion in fluid phase, the diffusion rate processes of a given adsorbate molecule in a packed bed operation may be divided into two categories: (i) the external diffusion of adsorbate in fluid phase, (ii) the internal diffusion of adsorbate molecule within porous adsorbent particles. The significance of internal diffusion has been neglected in the previous chapter where it was assumed that the adsorbate molecules are adsorbed on the outer surface of adsorbent particles. In this chapter, the pore diffusion model is assumed that the resistance of in-

ternal diffusion is as significant as that in fluid phase. As in Chapter II, two different cases of pore diffusion models are considered; one with axial dispersion and the other without it.

It is assumed that the porous adsorbent particles in the packed bed may be treated as homogeneous media in which the diffusion process within particles follows the Fick's first law. In addition to the assumptions stated in Chapter II, the following assumptions are made:

(1) The diffusional transport within adsorbent particles is radial, there is no variation in concentration with angular position.

(2) The concentration of adsorbate within adsorbent particles is zero initially, and the concentration of adsorbate at the center of adsorbent particle is specified at any time.

(3) The fluid film resistance is specified at the surface of adsorbent particle, and it is equal to the mass flux of adsorbate diffusing into the adsorbent particle.

As illustrated in Figure 6, the rate equation of adsorbate A within a single particle can be derived from the shell mass balance of adsorbate. The mass balance for adsorbate A over a spherical shell of thickness Δr at a distance r from the center of particle can be expressed as

$$4\pi r^2 N_{Ar}\Big|_r - 4\pi(r+\Delta r)^2 N_{Ar}\Big|_{r+\Delta r} = 4\pi r^2 \Delta r \frac{\partial C_s}{\partial t} \qquad (3\text{-}1)$$

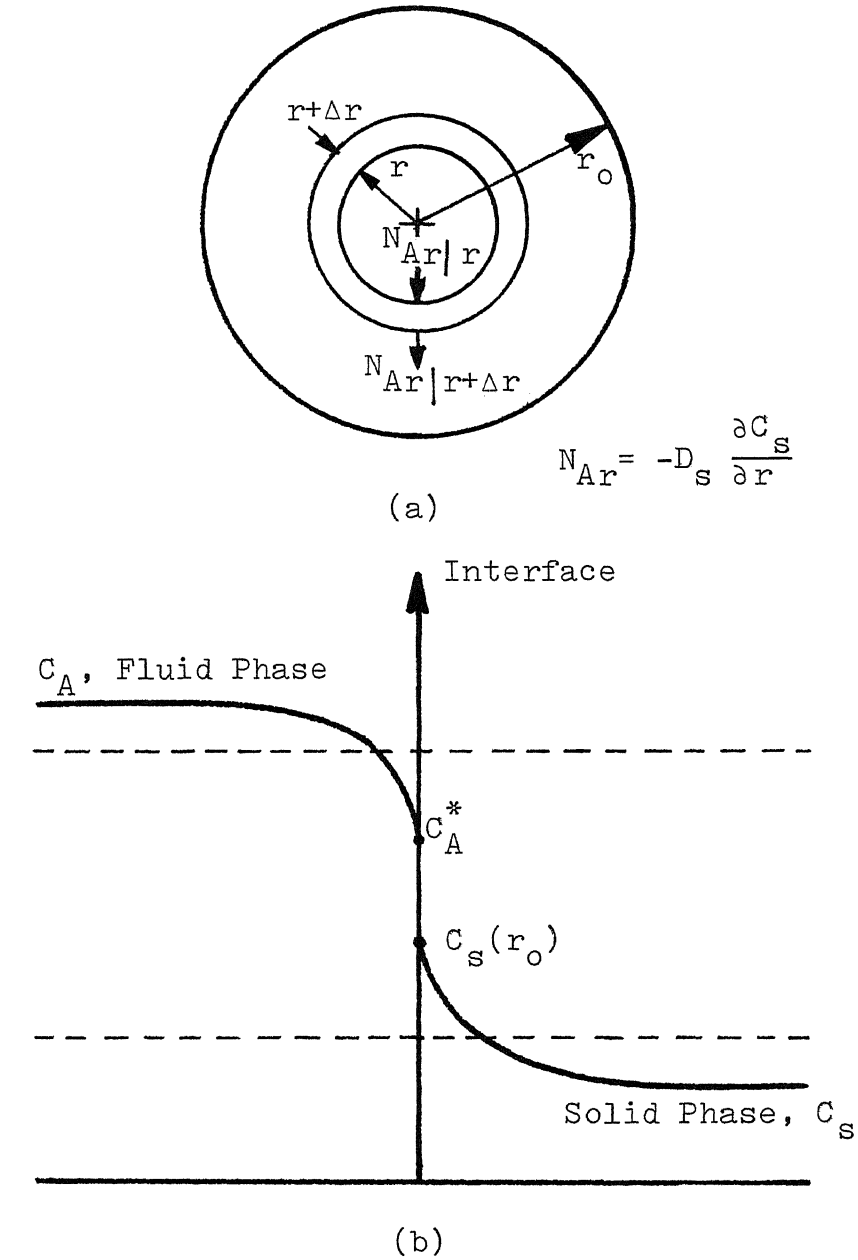

Figure 6. (a) Schematic description of diffusion process within solid particle.

(b) Concentration profile of adsorbate A in the neighborhood of a liquid-solid interface.

where $N_{Ar}|_r$ is the number of moles of adsorbate A passing in the r-direction through an imaginary spherical surface at a distance r from the center of sphere. The source term $4\pi r^2 \Delta r \frac{\partial C_s}{\partial t}$ gives the number of moles of adsorbate A being accumulated in a shell of thickness Δr where C_s is the local concentration of adsorbate A in solid phase expressed as moles of adsorbate per unit volume of packed bed. Dividing equation (3-1) by $4\pi\Delta r$ and letting $\Delta r \longrightarrow 0$, gives

$$\lim_{\Delta r \to 0} \frac{(r^2 N_{Ar})_{r+\Delta r} - (r^2 N_{Ar})_r}{\Delta r} = - r^2 \frac{\partial C_s}{\partial t} \qquad (3\text{-}2)$$

or

$$\frac{1}{r^2} \frac{\partial}{\partial r} (r^2 N_{Ar}) = - \frac{\partial C_s}{\partial t} \qquad (3\text{-}3)$$

The Fick's first law is defined as

$$N_{Ar} = - D_s \frac{\partial C_s}{\partial r} \qquad (3\text{-}4)$$

where D_S is the effective diffusivity for adsorbate A in the porous adsorbent particle. The effective diffusivity D_s must be measured experimentally; it generally depends on pressure, temperature, pH, or other control variables of the specific system. In this study, the effective diffusivity D_s is assumed constant. After substituting equation

(3-4) into equation (3-3), it results

$$\frac{\partial C_s}{\partial t} = \frac{D_s}{r^2} \frac{\partial}{\partial r}\left(r^2 \frac{\partial C_s}{\partial r} \right) \qquad (3\text{-}5)$$

or

$$\frac{\partial C_s}{\partial t} = D_s \left(\frac{\partial^2 C_s}{\partial r^2} + \frac{2}{r} \frac{\partial C_s}{\partial r} \right) \qquad (3\text{-}6)$$

The solution of equation (3-6) is generally subjected to the following two boundary conditions:

(i) $$\left.\frac{\partial C_s}{\partial r}\right|_{r=0} = 0 \ ,$$

(ii) $$D_s \left.\frac{\partial C_s}{\partial r}\right|_{r=r_o} = K_L \left(C_A - C_A^* \right)$$

The first boundary condition states that the concentration of adsorbate A at center of adsorbent particle is constant, so that the rate change with respect to radial position is zero. The second boundary condition indicates that the rate of mass transfer of adsorbate A from the bulk fluid of flow to the particle surface($r=r_o$) is equal to the mass flux of adsorbate A at which it diffuses into the adsorbent particle.

A. Simple Model (neglecting axial dispersion)

The governing equations of simple model with pore diffusion are formulated as

$$\frac{\partial C_A}{\partial t} = - \left(\frac{v}{\epsilon}\right) \frac{\partial C_A}{\partial z} - \left(\frac{K_L a}{\epsilon}\right)(C_A - C_A^*) \qquad (3A\text{-}1)$$

$$\frac{\partial C_s}{\partial t} = D_s \left(\frac{\partial^2 C_s}{\partial r^2} + \frac{2}{r} \frac{\partial C_s}{\partial r} \right) \qquad (3A\text{-}2)$$

$$C_A^* = \lambda C_s(r=r_o, z, t) \qquad (3A\text{-}3)$$

with initial and boundary conditions,

$$C_A (z, t=0) = 0 \qquad (3A\text{-}4a)$$

$$C_s (r, z, t=0) = 0 \qquad (3A\text{-}4b)$$

$$C_A (z=0, t) = C_{Ao} U(t) \qquad (3A\text{-}5)$$

$$\left.\frac{\partial C_s}{\partial r}\right|_{r=0} = 0 \qquad (3A\text{-}6)$$

$$D_s \left.\frac{\partial C_s}{\partial r}\right|_{r=r_o} = K_L(C_A - C_A^*) \qquad (3A\text{-}7)$$

Introducing the dimensionless variables as follows

$$X = C_A / C_{Ao} U(t)$$

$$X^* = C_A^*/C_{A_o}U(t)$$

$$Y = C_s/C_{A_o}U(t)$$

$$R = r/r_o$$

$$\eta = z/L$$

$$\tau = tD_s/r_o^2$$

Then the governing equations become

$$\frac{\partial X}{\partial \tau} = -\theta \frac{\partial X}{\partial \eta} - \omega(X - X^*) \qquad (3A\text{-}8)$$

$$\frac{\partial Y}{\partial \tau} = \left(\frac{\partial^2 Y}{\partial R^2} + \frac{2}{R} \frac{\partial Y}{\partial R} \right) \qquad (3A\text{-}9)$$

$$X^* = \lambda Y(R=1, \eta, \tau) \qquad (3A\text{-}10)$$

with initial and boundary conditions,

$$X(\eta, \tau=0) = 0 \qquad (3A\text{-}11a)$$

$$Y(R, \eta, \tau=0) = 0 \qquad (3A\text{-}11b)$$

$$X(\eta=0, \tau) = 1 \qquad (3A\text{-}12)$$

$$Y\Big|_{R=0} = \text{finite} \qquad (3A\text{-}13)$$

$$\frac{\partial Y}{\partial R}\Big|_{R=1} = B_i\,(X - X^*) \qquad (3A\text{-}14)$$

where

$$\theta = \frac{v r_o^2}{\epsilon L D_s}$$

$$\omega = \frac{K_L a r_o^2}{\epsilon D_s}$$

$$B_i = \frac{K_L r_o}{D_s}$$

The simultaneous differential equations, eqs. (3A-8) to (3A-10) can be solved by means of the Laplace transformation. With the definition of Laplace transform stated in Chapter II, equations (3A-8) through (3A-14) become

$$p\bar{X} = - \theta \frac{d\bar{X}}{d\eta} - \omega \, (\bar{X} - \bar{X}^*) \qquad (3A\text{-}15)$$

$$p\bar{Y} = \left(\frac{\partial^2 \bar{Y}}{\partial R^2} + \frac{2}{R} \frac{\partial \bar{Y}}{\partial R} \right) \qquad (3A\text{-}16)$$

$$\bar{X}^* = \lambda \, \bar{Y}(R=1, \eta, p) \qquad (3A\text{-}17)$$

with boundary conditions,

$$\bar{X}(\eta=0, p) = \frac{1}{p} \qquad (3A\text{-}18)$$

$$\bar{Y}\Big|_{R=0} = \text{finite} \qquad (3A\text{-}19)$$

$$D_s \left. \frac{\partial \bar{Y}}{\partial R} \right|_{R=1} = B_i(\bar{X} - \bar{X}^*) \qquad (3A\text{-}20)$$

To solve equation (3A-16), it may be assumed that $\bar{Y}$

is a function of R only for some specific position η in the lapacian domain p. Hence equation (3A-16) reduces to

$$R^2 \frac{d^2\bar{Y}}{dR^2} + 2R \frac{d\bar{Y}}{dR} - pR^2\bar{Y} = 0 \qquad (3A\text{-}21)$$

Introducing a new variable f as

$$f = R\bar{Y} \qquad (3A\text{-}22)$$

Then substituting equation (3A-22) into equation (3A-21), it results

$$\frac{d^2f}{dR^2} - pf = 0 \qquad (3A\text{-}23)$$

The general solution of equation (3A-23) is

$$f = c_1 \sinh\sqrt{p}R + c_2 \cosh\sqrt{p}R \qquad (3A\text{-}24)$$

where c_1 and c_2 are arbitary constants. By substituting equation (3A-24) into equation (3A-23), one may obtain

$$\bar{Y} = \frac{c_1}{R} \sinh\sqrt{p}R + \frac{c_2}{R} \cosh\sqrt{p}R \qquad (3A\text{-}25)$$

By applying the second boundary condition, eq.(3A-19), the coefficient c_2 has to be equal to zero; otherwise $\bar{Y}$ will be undefinited at R=0. Thus equation (3A-25) reduces to

$$\bar{Y} = \frac{c_1}{R} \sinh\sqrt{p}R \qquad (3A\text{-}26)$$

Differentiating equation (3A-26) with respect to R,

$$\frac{d\bar{Y}}{dR} = \frac{c_1\sqrt{p}}{R}\cosh\sqrt{p}R - \frac{c_1}{R^2}\sinh\sqrt{p}R \qquad (3A\text{-}27)$$

The constant c_1 can be determined with the aid of third boundary condition, eq.(3A-20). Substituting equations (3A-27) and (3A-17) into equation (3A-20) and letting R=1, it results

$$c_1\sqrt{p}\cosh\sqrt{p} - c_1\sinh\sqrt{p} = B_i[\bar{X} - \lambda(c_1\sinh\sqrt{p})]$$

or

$$c_1 = \frac{B_i\,\bar{X}}{\sqrt{p}\cosh\sqrt{p} + (\lambda B_i - 1)\sinh\sqrt{p}} \qquad (3A\text{-}28)$$

Thus, the complete solution for $\bar{Y}$ is

$$\bar{Y} = \frac{B_i R^{-1}\sinh\sqrt{p}R\;\bar{X}}{\sqrt{p}\cosh\sqrt{p} + (\lambda B_i - 1)\sinh\sqrt{p}} \qquad (3A\text{-}29)$$

From equation (3A-29), one may have

$$\bar{X}^* = \frac{\lambda B_i\sinh\sqrt{p}\,\bar{X}}{\sqrt{p}\cosh\sqrt{p} + (\lambda B_i - 1)\sinh\sqrt{p}} \qquad (3A\text{-}30)$$

and

$$\bar{X} - \bar{X}^* = \frac{(\sqrt{p}\cosh\sqrt{p} - \sinh\sqrt{p})\,\bar{X}}{\sqrt{p}\cosh\sqrt{p} + (\lambda B_i - 1)\sinh\sqrt{p}} \qquad (3A\text{-}31)$$

Putting equation (3A-31) into equation (3A-15) results in:

$$\theta \frac{d\bar{X}}{d\eta} + \{p + [\frac{\omega(\sqrt{p}\cosh\sqrt{p} - \sinh\sqrt{p})}{\sqrt{p}\cosh\sqrt{p} + (\lambda B_i - 1)\sin\sqrt{p}}]\} \bar{X} = 0 \qquad (3A-32)$$

The general solution of equation (3A-32) is

$$\bar{X} = c_3 \exp\{-(\frac{\eta}{\theta})[p + \frac{\omega(\sqrt{p}\cosh\sqrt{p} - \sinh\sqrt{p})}{\sqrt{p}\cosh\sqrt{p} + (\lambda B_i - 1)\sinh\sqrt{p}}]\} \qquad (3A-33)$$

The constant c_3 can be determined with the aid of equation (3A-18),

$$c_3 = \frac{1}{p}$$

Therefore, the complete solution for $\bar{X}$ is

$$\bar{X} = \frac{1}{p} \exp\{-(\frac{\eta}{\theta})[p + \frac{\omega(\sqrt{p}\cosh\sqrt{p} - \sinh\sqrt{p})}{\sqrt{p}\cosh\sqrt{p} + (\lambda B_i - 1)\sinh\sqrt{p}}]\} \qquad (3A-34)$$

The final solution of equation (3A-34) may be obtained by applying the technique of inverse Laplace transformation. In order to find out all the residues, equation (3A-34) is rewritten as a series expression. By introducing the definition of hyperbolic function, equation (3A-34) becomes

$$\bar{X} = \frac{1}{p} \exp\{-(\frac{\eta}{\theta})[p + \frac{\omega\left(\sum_k \frac{(1/2)^{2k}}{(2k)!} p^k - \sum_k \frac{(1/2)^{2k+1}}{(2k+1)!} p^k\right)}{\sum_k \frac{(1/2)^{2k}}{(2k)!} p^k + (\lambda B_i - 1)\sum_k \frac{(1/2)^{2k+1}}{(2k+1)!} p^k}]\} \qquad (3A-35)$$

From equation (3A-35), it is obvious that there are no branch points, but there are a simple pole at p=0 and many simple poles p_k which satisfy

$$\sqrt{p}\cosh\sqrt{p} + (\lambda B_i - 1)\sinh\sqrt{p} = 0 \qquad (3A\text{-}36)$$

From the results of Chapter II, we knew that there are only the negative values of p_k which satisfy equation (3A-36). Let $p = -\beta_n^2$, where β_n may be positive or negative real numbers. Then, equation (3A-36) reduces to

$$\tan\beta_n = -\left(\frac{\beta_n}{\lambda B_i - 1}\right) \qquad (3A\text{-}37)$$

Equation (3A-37) is a characteristic equation of β_n, there are many β_n which satisfy this equation.

The expression of $\bar{X}(\eta,p)$ may be rewritten as

$$\bar{X}(\eta,p) = e^{-(\frac{\eta}{\theta})p} G(\eta,p) \qquad (3A\text{-}38)$$

where

$$G(\eta,p) = \frac{1}{p}\exp\left(-\frac{B\eta(\sqrt{p}\cosh\sqrt{p} - \sinh\sqrt{p}}{\sqrt{p}\cosh\sqrt{p} + (\lambda B_i - 1)\sinh\sqrt{p}}\right) \qquad (3A\text{-}39a)$$

$$B = \frac{\omega}{\theta} = \frac{K_L a\, L}{v} \qquad (3A\text{-}39b)$$

Applying the shifting theorem of Laplace transform results in:

$$X(\eta,\tau) = 0 \qquad ; \tau < \frac{\eta}{\theta}$$

$$= g(\eta, \tau - \frac{\eta}{\theta}) \qquad ; \tau > \frac{\eta}{\theta}$$

where (3A-40)

$$g(\eta, \tau) = \mathbb{L}^{-1}\{G(\eta,p)\} = \mathbb{L}^{-1}\left\{\frac{1}{p}\exp\left[-\frac{B\eta(\sqrt{p}\cosh\sqrt{p} - \sinh\sqrt{p})}{\sqrt{p}\cosh\sqrt{p} + (\lambda B_i - 1)\sinh\sqrt{p}}\right]\right\} \quad (3A\text{-}41)$$

To solve equation equation (3A-41), the exponential function $G(\eta,p)$ is expanded into a series and then by applying the residues theorem to carry out the inversion term by term.

$$G(\eta,p) = \frac{1}{p} - \frac{1}{p}\left[\frac{\sqrt{p}\cosh\sqrt{p} - \sinh\sqrt{p}}{\sqrt{p}\cosh\sqrt{p} + (\lambda B_i - 1)\sinh\sqrt{p}}\right](B\eta)$$

$$+ \frac{1}{p}\left[\frac{\sqrt{p}\cosh\sqrt{p} - \sinh\sqrt{p}}{\sqrt{p}\cosh\sqrt{p} + (\lambda B_i - 1)\sinh\sqrt{p}}\right]^2 \frac{(B\eta)^2}{2!}$$

$$- \frac{1}{p}\left[\frac{\sqrt{p}\cosh\sqrt{p} - \sinh\sqrt{p}}{\sqrt{p}\cosh\sqrt{p} + (\lambda B_i - 1)\sinh\sqrt{p}}\right]^3 \frac{(B\eta)^3}{3!}$$

$$+ \text{----------}, \text{etc}$$

$$= G_o(\eta,p) - G_1(\eta,p)(B\eta) + G_2(\eta,p)\frac{(B\eta)^2}{2!} - G_3(\eta,p)\frac{(B\eta)^3}{3!}$$

$$+ \text{----------}, \text{ etc} \qquad (3A\text{-}42)$$

$$= \sum_k (-1)^k G_k(\eta,p)\frac{(B\eta)^k}{k!} \qquad (3A\text{-}43)$$

The residues of $G(\eta,p)$ are evaluated as follows:

(1) Residue of $G(\eta,p)$ at $p=0$,

By applying the residues theorem,

$$\text{Res}[G_o(\eta,p)\ e^{p\tau};\ p=0] = 1$$

$$\text{Res}[G_1(\eta,p)\ e^{p\tau};\ p=0] = 0$$

$$\text{Res}[G_2(\eta,p)\ e^{p\tau};\ p=0] = 0$$

$$\text{Res}[G_3(\eta,p)\ e^{p\tau};\ p=0] = 0$$

---

thus,

$$\text{Res}\ [G(\eta,p)\ e^{p\tau};\ p=0\ ]= 1 \qquad (3A\text{-}44)$$

(2) Residues of $G(\eta,p)$ at $p=p_n=\beta_n^2$

$$\text{Res}\{G(\eta,p)e^{p\tau};p=p_n\}= \text{Res}\{\sum_n(-1)^n G_n(\eta,p)\frac{(B\eta)^n}{n!}\ e^{p\tau};p=p_n\} \qquad (3A\text{-}45)$$

** (2a) $\text{Res}\{G_1(\eta,p)\ e^{p\tau};\ p=p_n\}$

$$=\sum_n \lim_{p\to p_n}\left\{\frac{(p-p_n)(\sqrt{p}\cosh\sqrt{p}-\sinh\sqrt{p})e^{p\tau}}{p(\sqrt{p}\cosh\sqrt{p}+(\lambda B_i-1)\sinh\sqrt{p}}\right\} = \sum_n \frac{e^{p_n\tau}J_1(p_n)}{dL(p_n)} \qquad (3A\text{-}46)$$

where

$$J_1(p)=(\sqrt{p}\cosh\sqrt{p}-\sinh\sqrt{p})/p$$

$$L(p)=\sqrt{p}\cosh\sqrt{p}+(\lambda B_i-1)\sinh\sqrt{p}$$

and

$$J_1(p_n)=\frac{-i}{\beta_n^2}(\beta_n\cos\beta_n-\sin\beta_n)$$

$$dL(p_n)=\frac{dL(p)}{dp}\Big|_{p=p_n}=\frac{-i}{2\beta_n}(\lambda B_i\cos\beta_n-\beta_n\sin\beta_n)$$

Hence,

$$\text{Res}\{G_1(\eta,p)\ e^{p\tau};p=p_n\}=\sum_n \frac{2\ e^{-\beta_n^2\tau}(\beta_n\cos\beta_n-\sin\beta_n)}{\beta_n(\lambda B_i\cos\beta_n-\beta_n\sin\beta_n)} \qquad (3A\text{-}47)$$

** (2b) $\text{Res}\{G_2(\eta,p)\ e^{p\tau};\ p=p_n\}$

$$=\sum_n \lim_{p\to p_n}\frac{d}{dp}\left\{\frac{(p-p_n)^2(\sqrt{p}\cosh\sqrt{p}-\sinh\sqrt{p})^2e^{p\tau}}{p(\sqrt{p}\cosh\sqrt{p}+(\lambda B_i-1)\sinh\sqrt{p})^2}\right\}$$

$$=\sum_n \lim_{p\to p_n}\left\{\frac{d}{dp}\left[\frac{(p-p_n)^2J_2(p)\ e^{p\tau}}{(\ L(p)\ )^2}\right]\right\}$$

$$=\sum_{n=1}^{\infty}\left\{\frac{e^{p_n\tau}[\ J_3(p_n)\ dJ_3(p_n)]}{[dL(p_n)]^2}-\frac{e^{p_n\tau}J_3(p_n)d^2L(p_n)}{[\ dL(p_n)\ ]^3}\right\} \qquad (3A\text{-}48)$$

where

$$J_2(p)=(\sqrt{p}\cosh\sqrt{p}-\sinh\sqrt{p})^2/p$$

$$L(p)=\sqrt{p}\cosh\sqrt{p}+(\lambda B_i-1)\sinh\sqrt{p}$$

and

$$J_2(p_n) = (\beta_n \cos \beta_n - \sin \beta_n)^2 / \beta_n^2$$

$$dL(p_n) = \left.\frac{dL(p)}{dp}\right|_{p=p_n} = \frac{-i}{\beta_n}(\lambda B_i \cos \beta_n - \beta_n \sin \beta_n)$$

$$d^2L(p_n) = \left.\frac{d^2L(p)}{dp^2}\right|_{p=p_n} = \frac{i}{4\beta_n^3}[(\beta_n^2 - \lambda B_i)\cos \beta_n - \lambda B_i \beta_n \sin \beta_n]$$

$$dJ_2(p_n) = \left.\frac{dJ_2(p)}{dp}\right|_{p=p_n} = \frac{-1}{\beta_n^4}(\beta_n \cos \beta_n - \sin \beta_n)*$$

$$*[(1+\beta_n^2)\sin \beta_n - \beta_n \cos \beta_n]$$

Substituting the above relations into eq.(3A-48), it results

$$\mathrm{Res}\{G_2(\eta,p)e^{p\tau}; p=p_n\}$$

$$= \sum_{n=1}^{\infty} \left\{ \frac{(\beta_n \cos \beta_n - \sin \beta_n)[(1+\beta_n^2)\sin \beta_n - \beta_n \cos \beta_n]\, e^{-\beta_n^2 \tau}}{\beta_n^2(\lambda B_i \cos \beta_n - \beta_n \sin \beta_n)^2} \right.$$

$$- \frac{(\beta_n \cos \beta_n - \sin \beta_n)^2 \tau e^{-\beta_n^2 \tau}}{(\lambda B_i \cos \beta_n - \beta_n \sin \beta_n)^2}$$

$$\left. - \frac{2(\beta_n \cos \beta_n - \sin \beta_n)^2[(\beta_n^2 - \lambda B_i)\cos \beta_n - \lambda B_i \beta_n \sin \beta_n] e^{-\beta_n^2 \tau}}{\beta_n^2 (\lambda B_i \cos \beta_n - \sin \beta_n)^3} \right\}$$

(3A-49)

** (2c)

$$\text{Res}\{G_3(\eta,p)\ e^{p\tau};p=p_n\}$$

$$=\sum_n \lim_{p\to p_n}\frac{1}{2!}\frac{d^2}{dp^2}\left\{\frac{(p-p_n)^3(\sqrt{p}\cosh\sqrt{p}-\sinh\sqrt{p})^3e^{p\tau}}{p[\sqrt{p}\cosh\sqrt{p}+(\lambda B_i-1)\sinh\sqrt{p}]^3}\right\}$$

$$=\sum_n \lim_{p\to p_n}\frac{1}{2!}\left\{\left[\frac{p-p_n}{L(p)}\right]^3 d^2[e^{p\tau}J_3(p)]+6\left[\frac{p-p_n}{L(p)}\right]^2 d[e^{p\tau}J_3(p)]d\left[\frac{p-p_n}{L(p)}\right]\right.$$

$$\left.+\ 6\left[e^{p\tau}J_3(p)\right]\left[\frac{p-p_n}{L(p)}\right]\left[d\left(\frac{p-p_n}{L(p)}\right)\right]^2+3\left[e^{p\tau}J_3(p)\right]\left[\frac{p-p_n}{L(p)}\right]^2 d^2\left[\frac{p-p_n}{L(p)}\right]\right\}$$

$$=\sum_{n=1}^{\infty}\left\{\frac{e^{p_n\tau}[\tau^2J_3(p_n)+2\tau\ dJ_3(p_n)+d^2J_3(p_n)]}{2\ [dL(p_n)\ ]^3}\right.$$

$$+\ \frac{3\ d^2L(p_n)\ e^{p_n\tau}[\tau\ J_3(p_n)+dJ_3(p_n)]}{2\ [dL(p_n)]^4}$$

$$\left.+\ \frac{3e^{p_n\tau}J_3(p_n)[d^2L(p_n)]^2}{2[dL(p_n)]^5}-\frac{e^{p_n\tau}J_3(p_n)d^3L(p_n)}{2[dL(p_n)]^4}\right\}$$

(3A-50)

where

$$J_3(p)=(\sqrt{p}\cosh\sqrt{p}-\sinh\sqrt{p})^3/p$$

$$L(p)=\sqrt{p}\ \cosh\sqrt{p}+(\lambda B_i-1)\sinh\sqrt{p}$$

and

$$J_3(p_n) = \frac{i}{\beta_n^2}\,(\beta_n \cos\beta_n - \sin\beta_n)^3$$

$$dJ_3(p_n) = \frac{i}{\beta_n^4}\{(\beta_n\cos\beta_n - \sin\beta_n)^2[\beta_n\cos\beta_n + (\tfrac{3}{2}\beta_n^2 - 1)\sin\beta_n]\}$$

$$d^2J_3(p_n) = \frac{i}{\beta_n^6}\{[\beta_n^2(\beta_n\cos\beta_n - \sin\beta_n)^2][\tfrac{3}{2}\beta_n\cos\beta_n + \sin\beta_n]\}$$

$$- [2(\beta_n\cos\beta_n - \sin\beta_n)^2 + \beta_n^2\sin\beta_n(\beta_n\cos\beta_n - \sin\beta_n)] *$$

$$* [\beta_n\cos\beta_n + (\tfrac{3}{2}\beta_n^2 - 1)\sin\beta_n]\}$$

$$dL(p_n) = \frac{-i}{2\beta_n}(\lambda B_i\cos\beta_n - \beta_n\sin\beta_n)$$

$$d^2L(p_n) = \frac{i}{4\beta_n^3}\,[(\beta_n^2 - \lambda B_i)\cos\beta_n - \lambda B_i\beta_n\sin\beta_n]$$

$$d^3L(p_n) = \frac{i}{8\beta_n^6}\{[\beta_n^2(\lambda B_i - 1) - 3]\beta_n\cos\beta_n - [\beta_n^4 + 3\lambda B_i\beta_n^2]\sin\beta_n\}$$

If we group the first four terms only for $g(\eta,\tau)$, then the final solution for effluent concentration of adsorbate(η=1) is

$$X(\eta=1,\ \tau) = 0 \qquad ;\quad \tau < \frac{1}{\theta}$$

$$= g(\eta=1,\ \tau - \tfrac{1}{\theta}) \ ;\quad \tau > \frac{1}{\theta}$$

where (3A-51)

$$g(\eta=1,\tau) = 1 - \sum_{n=1}^{\infty} \frac{B\, e^{-\beta_n^2 \tau}\, J_1(p_n)}{dL(p_n)}$$

$$+ \sum_{n=1}^{\infty} \left(\frac{B^2}{2!}\right) \left\{ \frac{e^{-\beta_n^2 \tau} \left[J_2(p_n) + dJ_2(p_n)\right]}{\left[dL(p_n)\right]^2} - \frac{e^{-\beta_n^2 \tau}\, J_2(p_n)\, d^2L(p_n)}{\left[dL(p_n)\right]^3} \right\}$$

$$- \sum_{n=1}^{\infty} \left(\frac{B^3}{3!}\right) \left\{ \frac{e^{-\beta_n^2 \tau} \left[\tau^2 J_3(p_n) + 2\tau\, dJ_3(p_n) + d^2J_3(p_n)\right]}{2\left[dL(p_n)\right]^3} \right.$$

$$+ \frac{3\, e^{-\beta_n^2 \tau}\, d^2L(p_n) \left[\tau J_3(p_n) + dJ_3(p_n)\right]}{2\left[dL(p_n)\right]^4}$$

$$+ \frac{3\, e^{-\beta_n^2 \tau}\, J_3(p_n) \left[d^2L(p_n)\right]^2}{2\left[dL(p_n)\right]^5}$$

$$\left. - \frac{e^{-\beta_n^2 \tau}\, J_3(p_n)\, d^3L(p_n)}{2\left[dL(p_n)\right]^4} \right\} + \cdots$$

(3A-52)

where the eigenvalues β_n are calculated from the characteristic equation

$$\tan \beta_n = \frac{-\beta_n}{(\lambda B_i - 1)}$$

B. Dispersion Model

The governing equations of dispersion model with pore diffusion may be formulated as below:

$$\frac{\partial C_A}{\partial t} = -\left(\frac{v}{\epsilon}\right)\frac{\partial C_A}{\partial z} - \left(\frac{K_L a}{\epsilon}\right)(C_A - C_A^*) + D_L\frac{\partial^2 C_A}{\partial z^2} \qquad (3B\text{-}1)$$

$$\frac{\partial C_s}{\partial t} = D_s\left(\frac{\partial^2 C_s}{\partial r^2} + \frac{2}{r}\frac{\partial C_s}{\partial r}\right) \qquad (3B\text{-}2)$$

$$C_A^* = \lambda\, C_s(\, r=r_o,\ z,\ t\,) \qquad (3B\text{-}3)$$

with initial conditions,

$$C_A\ (z,\ t=0) = 0 \qquad (3B\text{-}4a)$$

$$C_s\ (r,\ z,\ t=0) = 0 \qquad (3B\text{-}4b)$$

and boundary conditions,

(i) solid phase:

$$\left.\frac{\partial C_s}{\partial r}\right|_{r=0} = 0 \quad ;\ \text{or}\quad C_s(r=0,\ z,\ t) = 0 \qquad (3B\text{-}5a)$$

$$D_s\left.\frac{\partial C_s}{\partial r}\right|_{r=r_o} = K_L(C_A - C_A^*) \qquad (3B\text{-}5b)$$

(ii) fluid phase:

① at entrance, z=0

$$vSC_{Ao}U(t) - vSC_A\Big|_{z=0} + \epsilon SD_L \frac{\partial C_A}{\partial z}\Big|_{z=0} = 0$$

or

$$C_{Ao}U(t) - C_A\Big|_{z=0} + \left(\frac{\epsilon D_L}{v}\right) \frac{\partial C_A}{\partial z}\Big|_{z=0} = 0 \qquad (3B\text{-}6a)$$

② total material balance of adsorbate,

$$vS \int_o^t (C_{Ao}U(t) - C_A\Big|_{z=L})\, dt = s\epsilon \int_o^L C_A\, dz$$

$$= \int_o^L \int_o^{r_o} \frac{(1-\epsilon)S\, dz}{\frac{4}{3}\pi r_o^3} C_s\, 4\pi r^2\, dr$$

or

$$\left(\frac{v}{\epsilon}\right) \int_o^t (C_{Ao}U(t) - C_A\Big|_{z=L})\, dt$$

$$= \int_o^L C_A\, dz + \left(\frac{a}{\epsilon r_o^2}\right) \int_o^L \int_o^{r_o} C_s\, r^2 dr\, dz \qquad (3B\text{-}6b)$$

Introducing the dimensionless variables as

$$X = C_A/C_{Ao}U(t)$$

$$X^* = C_A^*/C_{Ao}U(t)$$

$$Y = C_s/C_{Ao}U(t)$$

$$R = r/r_o$$

$$\eta = z/L$$

$$\tau = tD_s/r_o^2$$

Then the model equations reduce to

$$\frac{\partial X}{\partial \tau} = -\theta \frac{\partial X}{\partial \eta} - \omega(X - X^*) + \left(\frac{\theta}{A}\right) \frac{\partial^2 X}{\partial \eta^2} \qquad (3B\text{-}7)$$

$$\frac{\partial Y}{\partial \tau} = \left(\frac{\partial^2 Y}{\partial R^2} + \frac{2}{R} \frac{\partial Y}{\partial R} \right) \qquad (3B\text{-}8)$$

$$X^* = \lambda Y(R=1, \eta, \tau) \qquad (3B\text{-}9)$$

with initial conditions,

$$X(\eta, \tau=0) = 0 \qquad (3B\text{-}10a)$$

$$Y(\eta, \tau=0) = 0 \qquad (3B\text{-}10b)$$

and boundary conditions,

(i) solid phase:

$$Y(R=0, \eta, \tau) = 0 \qquad (3B\text{-}11a)$$

$$\left.\frac{\partial Y}{\partial R}\right|_{R=1} = B_i(X - X^*) \qquad (3B\text{-}11b)$$

(ii) fluid phase:

$$1 - X\Big|_{\eta=0} + \frac{1}{A} \left.\frac{\partial X}{\partial \eta}\right|_{\eta=0} = 0 \qquad (3B\text{-}12a)$$

$$\theta \int_0^\tau (1 - X\Big|_{\eta=1}) d\tau = \int_0^1 X \, d\eta + \left(\frac{\omega}{B_i}\right) \int_0^1 \int_0^1 YR^2 dR d \qquad (3B\text{-}12b)$$

where

$$A = \frac{vL}{\epsilon D_L}$$

$$\theta = \frac{vr_o^2}{\epsilon L D_s}$$

$$\omega = \frac{K_L a r_o^2}{\epsilon D_s}$$

$$B_i = \frac{K_L r_o}{D_s}$$

$$a = 3(1-\epsilon)/r_o$$

The simultaneous differential equations, eqs.(3B-7) to (3B-9) with initial and boundary conditions can be solved by means of the Laplace transformation.

With the definition of Laplace transform, one may obtain the model equations in terms of Laplace transform:

Fluid Phase

$$p\,\bar{X} = -\theta \frac{d\bar{X}}{d\eta} - \omega(\bar{X} - \bar{X}^*) + \left(\frac{\theta}{A}\right)\frac{d^2\bar{X}}{d\eta^2} \qquad (3B\text{-}13)$$

with boundary conditions,

$$\frac{1}{p} - \bar{X}\Big|_{\eta=0} + \left(\frac{1}{A}\right)\frac{d\bar{X}}{d\eta}\Big|_{\eta=0} = 0 \qquad (3B\text{-}14a)$$

$$\frac{\theta}{p}\left(\frac{1}{p} - \bar{X}\Big|_{\eta=1}\right) = \int_0^1 \bar{X}\, d\eta + \left(\frac{\omega}{B_i}\right)\int_0^1\int_0^1 \bar{Y}\, R^2 dR d \qquad (3B\text{-}14b)$$

Solid Phase

$$p\,\bar{Y} = \frac{\partial^2 \bar{Y}}{\partial R^2} + \frac{2}{R}\frac{\partial \bar{Y}}{\partial R} \qquad (3B\text{-}15)$$

with boundary conditions,

$$\bar{Y}(R=0, \eta, p) = \text{finite} \qquad (3B\text{-}16a)$$

$$\left.\frac{\partial \bar{Y}}{\partial R}\right|_{R=1} = B_i(\bar{X} - \bar{X}^*) \qquad (3B\text{-}16b)$$

Equilibrium Relationship At Interface

$$\bar{X}^* = \lambda \bar{Y}(R=1, \eta, p) \qquad (3B\text{-}17)$$

For some specific position η, $\bar{Y}$ may be thought of as a function of R only. The solution of equation (3B-15) with equations (3B-16) and (3B-17) has been practiced in part A of this chapter,

$$\bar{Y} = \frac{B_i\, R^{-1} \sinh\sqrt{p}R \;\; \bar{X}}{\sqrt{p}\cosh\sqrt{p} + (\lambda B_i - 1)\sinh\sqrt{p}} \qquad (3B\text{-}18)$$

Substituting equation (3B-18) into equation (3B-17), it results

$$\bar{X}^* = \frac{\lambda\, B_i \sinh\sqrt{p} \;\; \bar{X}}{\sqrt{p}\cosh\sqrt{p} + (\lambda B_i - 1)\sinh\sqrt{p}} \qquad (3B\text{-}19)$$

and

$$\bar{X} - \bar{X}^* = \frac{(\sqrt{p}\cosh\sqrt{p} - \sinh\sqrt{p}) \;\; \bar{X}}{\sqrt{p}\cosh\sqrt{p} + (\lambda B_i - 1)\sinh\sqrt{p}} \qquad (3B\text{-}20)$$

Putting equation (3B-20) into equation (3B-13) and arranging it, a second order ODE is resulted

$$\frac{d^2\bar{X}}{d\eta^2} - A\,\frac{d\bar{X}}{d\eta} - F(p)\,\bar{X} = 0 \qquad (3B\text{-}21)$$

where

$$F(p) = \left(\frac{A}{\theta}\right)\left\{p + \frac{(\sqrt{p}\cosh\sqrt{p} - \sinh\sqrt{p})}{\sqrt{p}\cosh\sqrt{p} + (\lambda B_i - 1)\sinh\sqrt{p}}\right\}$$

Equation (3B-21) can be solved with the aid of boundary conditions given by eqs.(3B-14a) and (3B-14b), its general solution is

$$\bar{X}(\eta,p) = e^{\frac{A}{2}\eta}\left(c_3 \sinh\frac{\nabla}{2}\eta + c_4 \cosh\frac{\nabla}{2}\eta\right) \qquad (3B\text{-}22)$$

where

$$\nabla = \sqrt{A^2+4F(p)}$$

From equation (3B-22), one may derive the following relations,

$$\left.\frac{d\bar{X}}{d\eta}\right|_{\eta=0} = \frac{A}{2}c_4 + \frac{\sqrt{A^2+4F}}{2}c_3 \qquad (3B\text{-}23)$$

$$\int_0^1 \bar{X}\,d\eta = -\left(\frac{1}{F}\right)\left\{c_3\left[\frac{A}{2}\sinh\frac{\nabla}{2} - \frac{\nabla}{2}e^{\frac{A}{2}}\cosh\frac{\nabla}{2} + \frac{\nabla}{2}\right]\right.$$
$$\left. + c_4\left[\frac{A}{2}\cosh\frac{\nabla}{2} - \frac{\nabla}{2}e^{\frac{A}{2}}\sinh\frac{\nabla}{2} - \frac{A}{2}\right]\right\} \qquad (3B\text{-}24)$$

From equation (3B-22),

$$\bar{X}\Big|_{\eta=0} = c_4 \tag{3B-25}$$

$$\bar{X}\Big|_{\eta=1} = e^{\frac{A}{2}} \left(c_3 \sinh \frac{\nabla}{2} + c_4 \cosh \frac{\nabla}{2}\right) \tag{3B-26}$$

Inserting equations (3B-23) and (3B-25) into equation (3B-14a) results in:

$$c_4 = \frac{2}{p} + \frac{\sqrt{A^2+4F}}{A} c_3 \tag{3B-27}$$

From equation (3B-18), it follows that

$$\int_0^1 \int_0^1 \bar{Y}\, R^2 dR d\eta = \int_0^1 \frac{\left(\int_0^1 R \sinh \sqrt{p} R\, dR\right) B_i\, \bar{X}\, d\eta}{\sqrt{p}\cosh\sqrt{p} + (\lambda B_i - 1)\sinh\sqrt{p}}$$

$$= \frac{B_i(\sqrt{p}\cosh\sqrt{p} - \sinh\sqrt{p})}{p\left[\sqrt{p}\cosh\sqrt{p} + (\lambda B_i - 1)\sinh\sqrt{p}\right]} \int_0^1 \bar{X}\, d\eta$$

Hence, equation (3B-14b) becomes

$$A\left(\frac{1}{p} - \bar{X}\Big|_{\eta=1}\right) = \left(\frac{A}{\theta}\right)\left[p + \frac{(\sqrt{p}\cosh\sqrt{p} - \sinh\sqrt{p})}{\sqrt{p}\cosh\sqrt{p} + (\lambda B_i - 1)\sinh\sqrt{p}}\right] \int_0^1 \bar{X} d\eta$$

$$= F(p) \int_0^1 \bar{X}\, d\eta \tag{3B-28}$$

Substituting equations (3B-24) and (3B-26) into equation

(3B-28), the constant c_3 is solved

$$c_3 = -\frac{A\cosh\frac{\sqrt{A^2+4F}}{2} + \sqrt{A^2+4F}\cosh\frac{\sqrt{A^2+4F}}{2}}{p\left[\sqrt{A^2+4F}\cosh\frac{\sqrt{A^2+4F}}{2} + \left(\frac{A^2+2F}{A}\right)\sinh\frac{\sqrt{A^2+4F}}{2}\right]}$$

(3B-29)

Also, the constant c_4 can be obtained by substituting equation (3B-29) into equation (3B-27),

$$c_4 = \frac{\sqrt{A^2+4F}\cosh\frac{\sqrt{A^2+4F}}{2} + A\sinh\frac{\sqrt{A^2+4F}}{2}}{p\left[\sqrt{A^2+4F}\cosh\frac{\sqrt{A^2+4F}}{2} + \left(\frac{A^2+2F}{A}\right)\sinh\frac{\sqrt{A^2+4F}}{2}\right]}$$

(3B-30)

Inserting the constants c_3 and c_4 into equation (3B-22) and by applying the addition formulae of hyperbolic functions, the complete solution for $\bar{X}$ is

$$\bar{X} = \frac{e^{\frac{A}{2}\eta}\left[\cosh\frac{\sqrt{A^2+4F}}{2}(1-\eta) + \frac{A}{\sqrt{A^2+4F}}\sinh\frac{\sqrt{A^2+4F}}{2}(1-\eta)\right]}{p\left[\cosh\frac{\sqrt{A^2+4F}}{2} + \left(\frac{A^2+2F}{A}\right)\frac{1}{\sqrt{A^2+4F}}\sinh\frac{\sqrt{A^2+4F}}{2}\right]}$$

(3B-31)

It is necessary to employ the technique of inverse Laplace transformation for equation (3B-31) to obtain a final solution for $X(\eta,\tau)$. In order to find out all the residues, it is an important concern to examine the analytic properties of $\bar{X}(\eta,p)$ for eq.(3B-31). As in part B of Chapter II, we knew that there are no branch points in eq.(3B-31), but there exist a simple pole at p=0 and many simple poles $p=p_k$ which satisfy the characteristic equation:

$$\cosh\frac{\sqrt{A^2+4F}}{2} + \left(\frac{A^2+2F}{A}\right)\frac{1}{\sqrt{A^2+4F}}\sinh\frac{\sqrt{A^2+4F}}{2} = 0 \qquad (3B\text{-}32)$$

Let

$$\bar{X}(\eta,p) = J(p)/L(p) \qquad (3B\text{-}33)$$

where

$$J(p) = e^{\frac{A}{2}\eta}\left\{\cosh\frac{\sqrt{A^2+4F}}{2}(1-\eta) + \frac{A}{\sqrt{A^2+4F}}\sinh\frac{\sqrt{A^2+4F}}{2}(1-\eta)\right\}$$

$$L(p) = p^*\left\{\cosh\frac{\sqrt{A^2+4F}}{2} + \left(\frac{A^2+2F}{A}\right)\frac{1}{\sqrt{A^2+4F}}\sinh\frac{\sqrt{A^2+4F}}{2}\right\}$$

By applying the residues theorem,

$$X(\eta,\tau) = \mathbb{L}^{-1}\{\bar{X}(\eta,p)\} = \sum_k \text{Res}\left\{e^{p\tau}\bar{X}(\eta,p);\ p_k\right\}$$

$$= \sum_k \lim_{p\to p_k}\left\{\left[J(p)/L'(p)\right]e^{p\tau}\right\} \qquad (3B\text{-}34)$$

where p_k are the poles of $\bar{X}(\eta,p)$ and $L'(p) = dL(p)/dp$.

The resiues of $\bar{X}(\eta,p)$ are evaluated as follows:

(1) Residue of $\bar{X}(\eta,p)$ at p=0,

At p=0, F(p=0)=0 and $\sqrt{A^2+4F} = A$. Hence

$$J(p=0)= e^{\frac{A}{2}\eta}\{\cosh \frac{A}{2}(1-\eta)+ \sinh \frac{A}{2}(1-\eta)\} = \frac{A}{2}$$

$$L'(p=0)= \cosh \frac{A}{2} + \sinh \frac{A}{2} = \frac{A}{2}$$

and,

$$\text{Res } 1 = J(p=0)/L'(p=0)= 1 \qquad (3B\text{-}35)$$

(2) Residues of $\bar{X}(\eta,p)$ at $p=p_k$,

As stated in part B of Chapter II, we knew that there are only the negative values for the term A^2+4F are satisfied with equation (3B-32). Let $A^2+4F = -\beta_n^2$, then equation (3B-32) is reduced to

$$\tan \frac{\beta_n}{2} = \frac{-2A\beta_n}{A^2-\beta_n^2} \qquad (3B\text{-}36)$$

There are many eigenvalues β_n which satisfy eq.(3B-36) as shown in Figure 5 before. The values of p_k can be calculated from the relation $A^2+4F= -\beta_n^2$ after the values of β_n were found.

Since

$$F(p)= \left(\frac{A}{\theta}\right)\left\{p + \frac{\omega(\sqrt{p}\cosh\sqrt{p}- \sinh\sqrt{p})}{\sqrt{p}\cosh\sqrt{p}+(\lambda B_i-1)\sinh\sqrt{p}}\right\} = -\left(\frac{A^2+\beta_n^2}{4}\right)$$

so that,

$$p + \left\{\frac{\omega(\sqrt{p}\cosh\sqrt{p}- \sinh\sqrt{p})}{\sqrt{p}\cosh\sqrt{p}+(\lambda B_i-1)\sinh\sqrt{p}}\right\}= \left(\frac{\theta}{A}\right)\left(\frac{A^2+\beta_n^2}{4}\right)$$

Let $p= - S_{n,m}^2$, then equation (3B-37) is simplified

$$\tan (S_{n,m})= - \frac{S_{n,m}(S_{n,m}^2 - \omega - \Phi_n)}{(S_{n,m}^2 - \Phi_n)(\lambda B_i-1)+ \omega} \qquad (3B\text{-}38)$$

where

$$\Phi_n= \left(\frac{\theta}{A}\right)\left(\frac{A^2+\beta_n^2}{4}\right)$$

There are also many eigenvalues $S_{n,m}$ which satisfy eq. (3B-38) with respect to different values of β_n. Table 2 lists the first five eigenvalues of $S_{n,m}$[from eq.(3B-38)] along with the first ten eigenvalues of β_n[from eq.(3B-36)].

By applying the residues theorem, the residues of $\bar{X}(\eta,p)$ may be expressed as

$$\text{Res } 2 = \sum_k \lim_{p\to p_k} \{J(p)e^{p\tau}/L'(p)\}=\sum_{nm} \lim_{p\to S_{n,m}} \left\{\frac{J(p)}{L'(p)} e^{p\tau}\right\}$$

(3B-39)

ABSTRACT

EXPLOITATION OF INFRARED POLARIMETRIC IMAGERY FOR PASSIVE REMOTE SENSING APPLICATIONS

by
João Miguel Mendes Romano

Polarimetric infrared imagery has emerged over the past few decades as a candidate technology to detect manmade objects by taking advantage of the fact that smooth materials emit strong polarized electromagnetic waves, which can be remotely sensed by a specialized camera using a rotating polarizer in front of the focal plate array in order to generate the so-called Stokes parameters: S_0, S_1, S_2, and DoLP. Current research in this area has shown the ability of using such variations of these parameters to detect smooth manmade structures in low contrast contrast scenarios.

This dissertation proposes and evaluates novel anomaly detection methods for long-wave infrared polarimetric imagery exploitation suited for surveillance applications requiring automatic target detection capability. The targets considered are manmade structures in natural clutter backgrounds under unknown illumination and atmospheric effects. A method based on mathematical morphology is proposed with the intent to enhance the polarimetric Stokes features of manmade structures found in the scene while minimizing its effects on natural clutter. The method suggests that morphology-based algorithms are capable of enhancing the contrast between manmade objects and natural clutter backgrounds, thus, improving the probability of correct detection of manmade objects in the scene. The second method departs from common practices in the polarimetric research community (i.e., using the Stokes vector parameters as input to algorithms) by using instead the raw polarization component imagery (e.g., 0°, 45°, 90°,

where

$$J(p) = e^{\frac{A}{2}\eta}\{\cosh\frac{\sqrt{A^2+4F}}{2}(1-\eta)+ \frac{A}{\sqrt{A^2+4F}} \sinh\frac{\sqrt{A^2+4F}}{2}(1-\eta)\}$$

$$L(p) = p \{ \cosh\frac{\sqrt{A^2+4F}}{2} +(\frac{A^2+2F}{A})\frac{1}{\sqrt{A^2+4F}} \sinh\frac{\sqrt{A^2+4F}}{2} \}$$

Differentiating L(p) with respect to p, it results

$$L'(p)=dL(p)/dp= \left\{\cosh\frac{\sqrt{A^2+4F}}{2} +(\frac{A^2+2F}{A})\frac{1}{\sqrt{A^2+4F}} \sinh\frac{\sqrt{A^2+4F}}{2}\right\}$$

$$+ p \ (\frac{dF}{dp})\left\{[\frac{A^2+2F}{A(A^2+4F)}]\cosh\frac{\sqrt{A^2+4F}}{2}\right.$$

$$\left. + [1+ \frac{2}{A} - \frac{2(A^2+2F)}{A(A^2+4F)}] \frac{\sinh\frac{\sqrt{A^2+4F}}{2}}{\sqrt{A^2+4F}}\right\}$$

(3B-40)

where

$$\frac{dF}{dp} = (\frac{A}{\theta})\left\{ 1+ \frac{(\frac{\omega\lambda B_i}{2})[\sinh^2\sqrt{p}- \cosh^2\sqrt{p} + \frac{1}{\sqrt{p}} \sinh\sqrt{p}\cosh\sqrt{p}]}{[\sqrt{p}\cosh\sqrt{p} +(\lambda B_i-1) \sinh\sqrt{p}]^2}\right\}$$

(3B-41)

At $p=p_k= -S^2_{n,m}$, $A^2+4F = -\beta^2_n$. So that

$$J(S_{n,m})= e^{\frac{A}{2}\eta}\{\cos\frac{\beta_n}{2}(1-\eta)+ \frac{A}{\beta_n} \sin\frac{\beta_n}{2}(1-\eta)\} \qquad (3B-42)$$

$$L'(S_{n,m}) = -S_{n,m}^2 * DF * \left\{ \left[\frac{A^2+\beta_n^2+A\beta_n^2}{A\beta_n^3} \right] \sin\frac{\beta_n}{2} - \left[\frac{A^2-\beta_n^2}{A\beta_n^2} \right] \cos\frac{\beta_n}{2} \right\} \tag{3B-43}$$

and

$$DF = \left. \frac{dF}{dp} \right|_{p=-S_{n,m}^2}$$

$$= \left(\frac{A}{\theta}\right) \left\{ 1 + \frac{\left(\frac{\omega\lambda B_i}{2}\right)\left[\sin^2(S_{n,m}) + \cos^2(S_{n,m}) - \frac{\cos(S_{n,m})\sin(S_{n,m})}{S_{n,m}}\right]}{\left[S_{n,m}\cos(S_{n,m}) + (\lambda B_i - 1)\sin(S_{n,m})\right]^2} \right\} \tag{3B-44}$$

Inserting equations (3B-42) and (3B-44) into equation (3B-39), the residues of $\bar{X}(\eta,p)$ at $p=-S_{n,m}^2$ are

$$\text{Res } 2 = -\sum_n \sum_m \frac{\left[\beta_n \cos\frac{\beta_n}{2}(1-\eta) + A\sin\frac{\beta_n}{2}(1-\eta)\right] e^{\frac{A}{2}\eta - S_{n,m}^2 \tau}}{S_{n,m}^2 * DF * \left[\left(\frac{A^2+\beta_n^2+A\beta_n^2}{A\beta_n^3}\right)\sin\frac{\beta_n}{2} - \left(\frac{A^2-\beta_n^2}{2A\beta_n^2}\right)\cos\frac{\beta_n}{2} \right]} \tag{3B-45}$$

Therefore, the final complete solution for $X(\eta,\tau)$ is

$$X(\eta,\tau) = 1 - \sum_{n=1}^{\infty}\sum_{m=1}^{\infty} \frac{\left[\beta_n \cos\frac{\beta_n}{2}(1-\eta) + A\sin\frac{\beta_n}{2}(1-\eta)\right] e^{\frac{A}{2}\eta - S_{n,m}^2 \tau}}{S_{n,m}^2 * DF * \left[\left(\frac{A^2+\beta_n^2+A\beta_n^2}{A\beta_n^3}\right)\sin\frac{\beta_n}{2} - \left(\frac{A^2-\beta_n^2}{2A\beta_n^2}\right)\cos\frac{\beta_n}{2} \right]} \tag{3B-46}$$

The effluent concentration of adsorbate (at $\eta=1$) is

$$X(\eta,\tau)= 1-\sum_{n=1}^{\infty}\sum_{m=1}^{\infty}\frac{\beta_n^* \, e^{\frac{A}{2}-S_{n,m}^2\tau}}{S_{n,m}^2 * DF * \left[\left(\frac{A^2\beta_n^2 A\beta_n^2}{A\beta_n^3}\right)\sin\frac{\beta_n}{2} - \left(\frac{A^2-\beta_n^2}{2A\beta_n^2}\right)\cos\frac{\beta_n}{2}\right]} \qquad (3B\text{-}47)$$

where

$$DF= \left(\frac{A}{\theta}\right)\left\{1+ \frac{\left(\frac{\omega\lambda B_i}{2}\right)\left[\sin^2(S_{n,m})+\cos^2(S_{n,m})- \frac{\cos(S_{n,m})\sin(S_{n,m})}{S_{n,m}}\right]}{\left[S_{n,m}\cos(S_{n,m}) +(\lambda B_i-1)\sin(S_{n,m})\right]^2}\right\}$$

the eigenvalues β_n and $S_{n,m}$ are evaluated from equations (3B-36) and (3B-38) respectively. The calculated results of equation (3B-47) are discussed in Chapter IV.

CHAPTER IV

RESULTS AND DISCUSSIONS

The central problem in designing the packed bed adsorption processes is the dynamic response of the adsorption column to a step change or a pulse change in input concentration of adsorbate. These dynamic behaviors of an adsorbent fixed bed are usually studied from the breakthrough curves which are expressed as dimensionless effluent concentration of adsorbate versus effluent volume or elapsed time in terms of different operation conditions.

For a given adsorbent-adsorbate system, the shape of breakthrough curves depends on the rate and mechanism of adsorption process, on the nature of adsorption equilibrium, on the physical properties of system such as the bed length and the cross-sectional area of column, on the effective interfacial contact area, and on the transport parameters related to the flow of fluid (i.e. fluid velocity, axial dispersion, etc.).

In this chapter, the equations developed in chapter II and III, namely, eqs(2A-22), (2A-25), (2B-52), (2B-53), and (3B-47) are employed to calculate the breakthrough curves

in terms of different system parameters. Breakthrough curves of two different models are studied. Finally, the proposed models are verified by experimental data of the system of hemoglobin- albumin- CM sepharose- DEAE sepharose.

A. Surface Adsorption Model

Based on equation (2A-22), the calculated breakthrough curves of simple model with surface adsorption in response to a step change in input are shown in Figures 7 to 12. Figure 7 shows the effect of flow rate on the performance of a packed column. As expected, high flow rate was responsible for earlier breakpoint, because the time provided for the contact of adsorbent and adsorbate is reduced at high flow rate and exhausted the bed more rapidly. The effects of bed length and cross-sectional of column on the calculated breakthrough curves are illustrated in Figures 8 and 9 respectively. From these figures, it is shown that the adsorption capacity (loading) can be enhanced by increasing the bed length or the cross-sectional area of column. Figure 10 represents the effect of mass transfer coefficient on predicted breakthrough curves. This figure shows that by increasing the mass transfer coefficient will cause an increase in mass transfer rate and result in increasing the rate of adsorption. The rate of adsorption can also be increased by increasing the effective contact area of adsorbent particles, this phenomenon is shown in

Figure 11. Figure 12 represents the effect of equilibrium constant on calculated breakthrough curves. The equilibrium constant is an important factor in adsorption process, because this factor might affect the reversibility of adsorption/desorption process. The equilibrium constant is generally governed by the thermodynamic intensive variables (such as temperature, pressure, ionic strength, affinity, pH, electric field, etc.). Figure 12 shows the system performance is highly sensitive to the variation in equilibrium constant.

For a pulse change in input concentration of adsorbate, the effects of some system parameters on the predicted breakthrough curves are studied. Based on eq.(2A-25), the results are shown in Figures 13 to 16. Referring to Figures 13 and 14, it can be seen that the breakthrough curve has higher peak for larger mass transfer coefficient, K_L and the breakpoint is delayed for larger contact area, a. This phenomenon implies that the larger K_L and a posses higher mass transfer rate and larger adsorption capability to load the finite amount of adsorbate for the case of pulse input. Figure 15 shows the effect of mass transfer rate ($K_L a$) on calculated breakthrough curves. Figure 16 represents the effect of distribution ratio ($m\epsilon/a$) on calculated breakthrough curves. It is evident that the larger distribution ratio has less adsorption capability, thus the curve has higher peak and smears out the column earlier than the others.

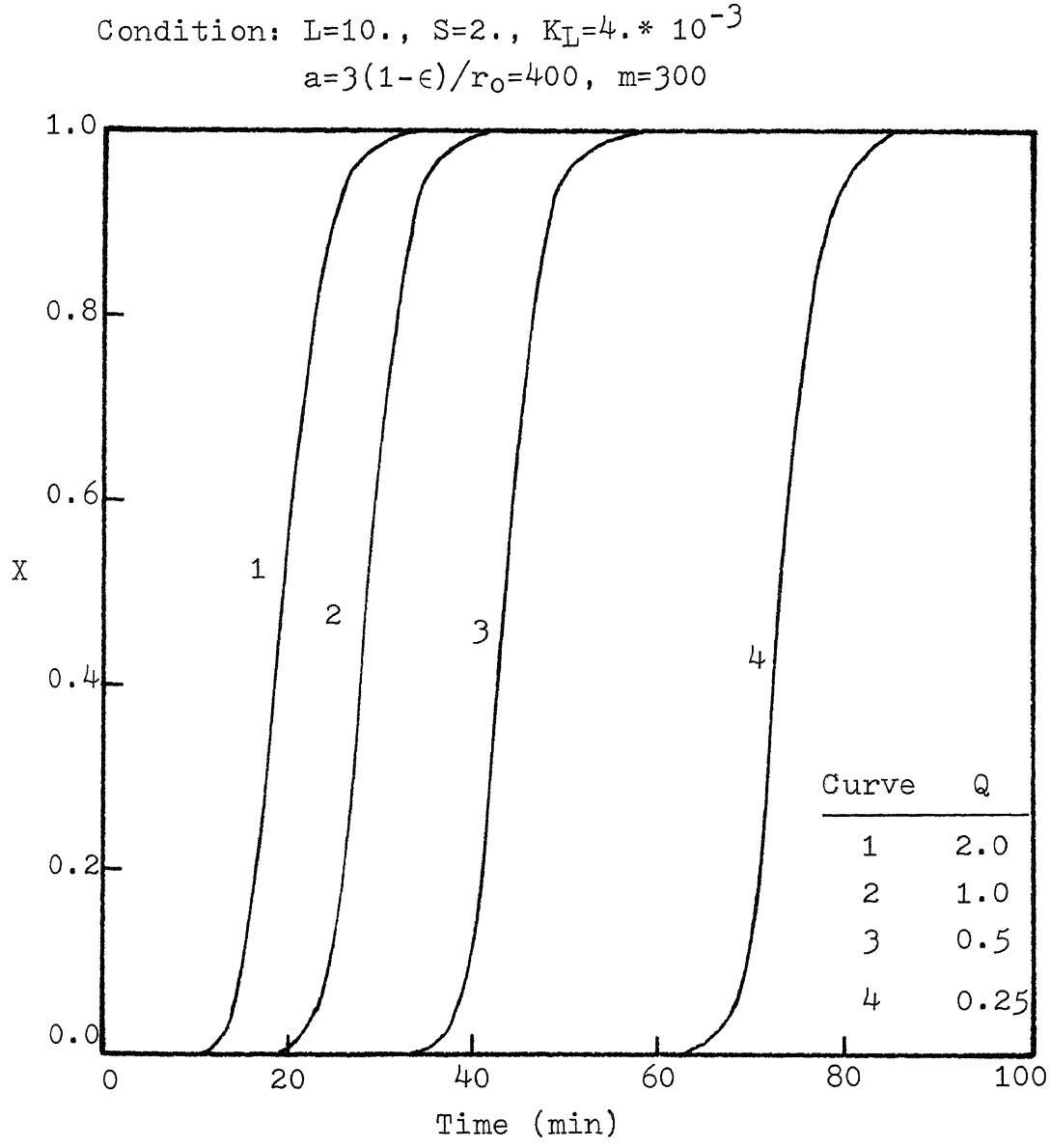

Figure 7. Effect of flow rate Q on predicted greakthrough curves (simple model with surface adsorption)

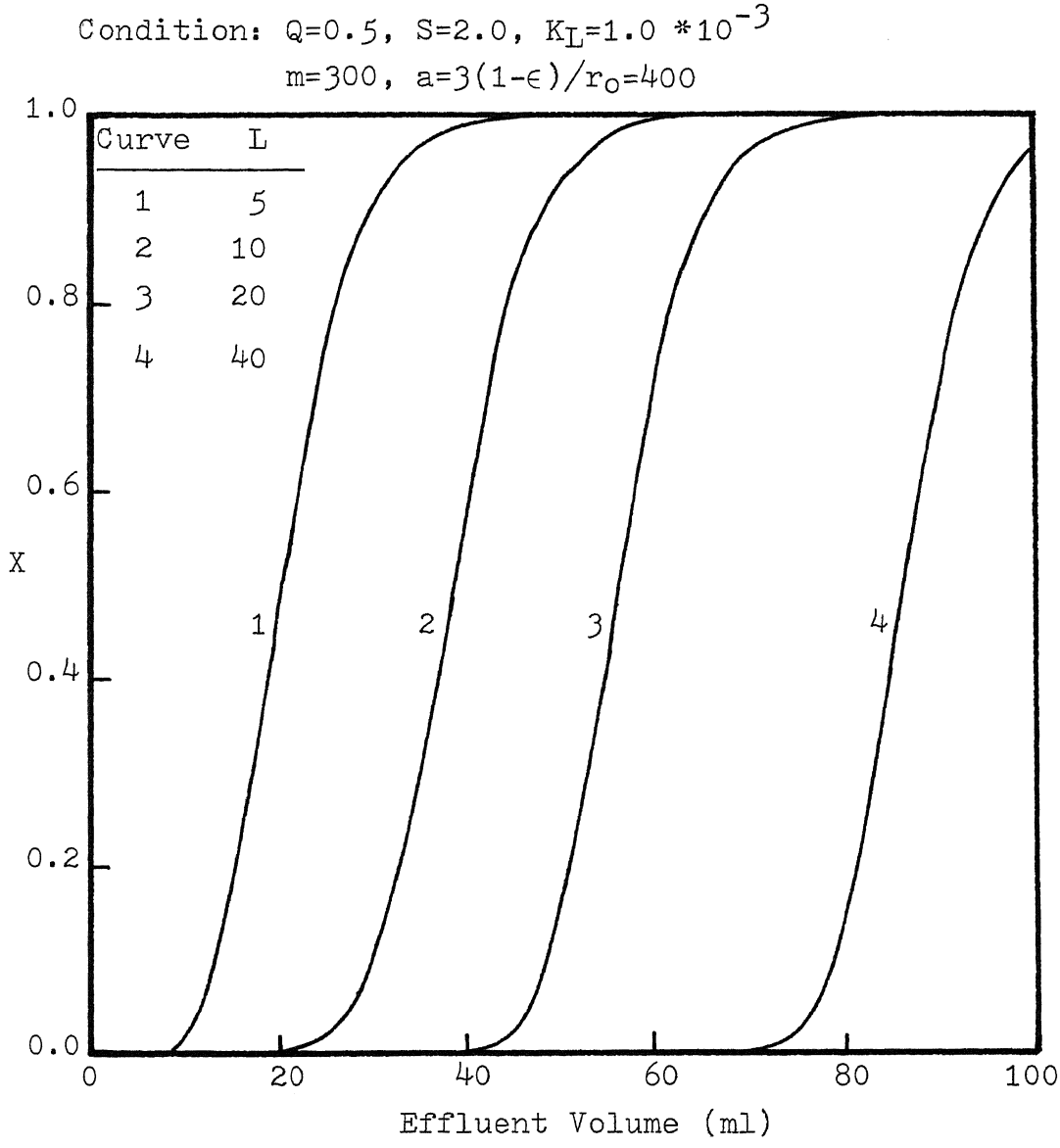

Figure 8. Effect of bed length L on predicted breakthrough curves (simple model with surface adsorption)

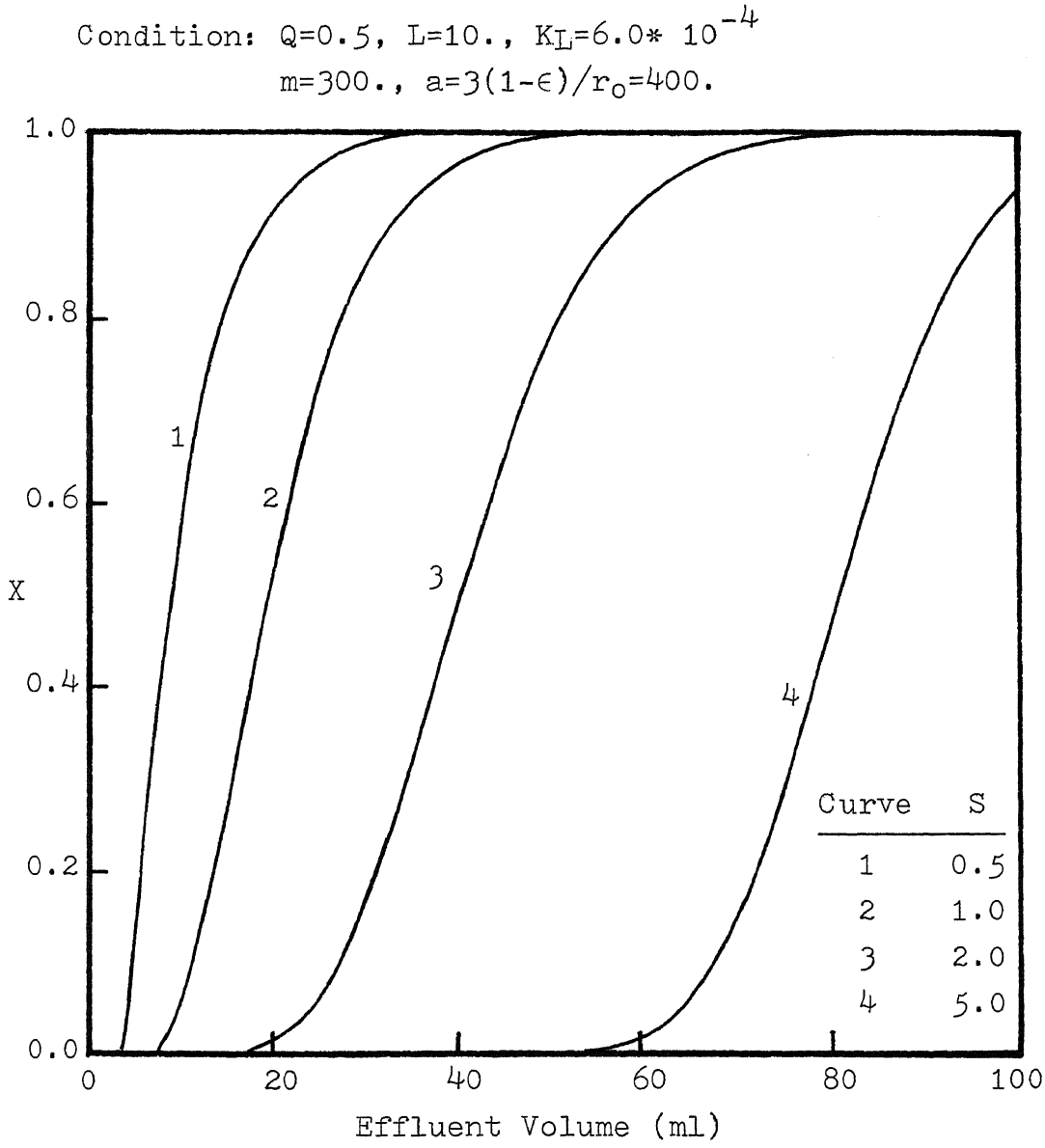

Figure 9. Effect of cross-sectional area of column S on predicted breakthrough corves (simple model with surface adsorption)

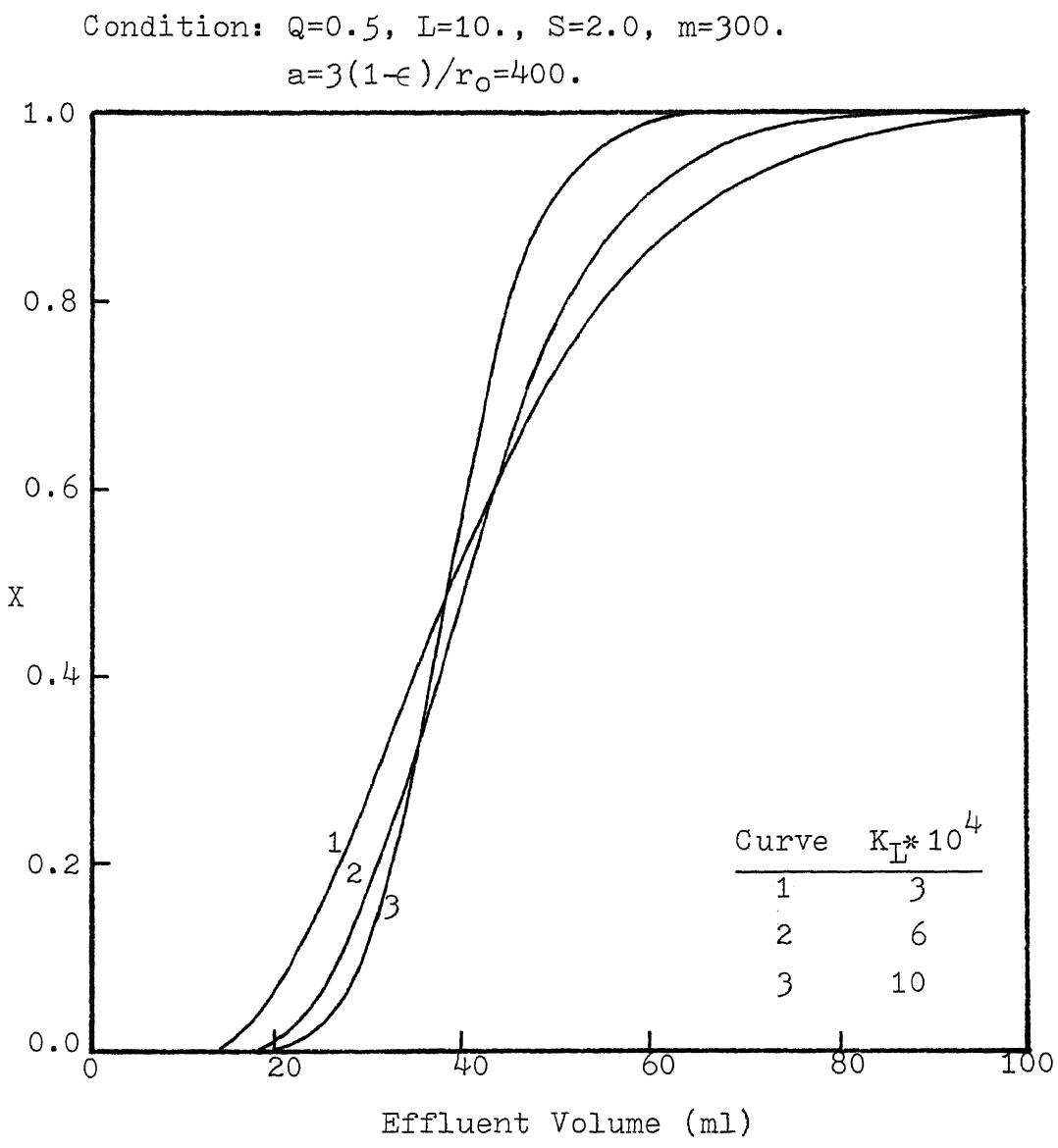

Figure 10. Effect of mass transfer coefficient K_L on predicted breakthrough curves (simple model with surface adsorption)

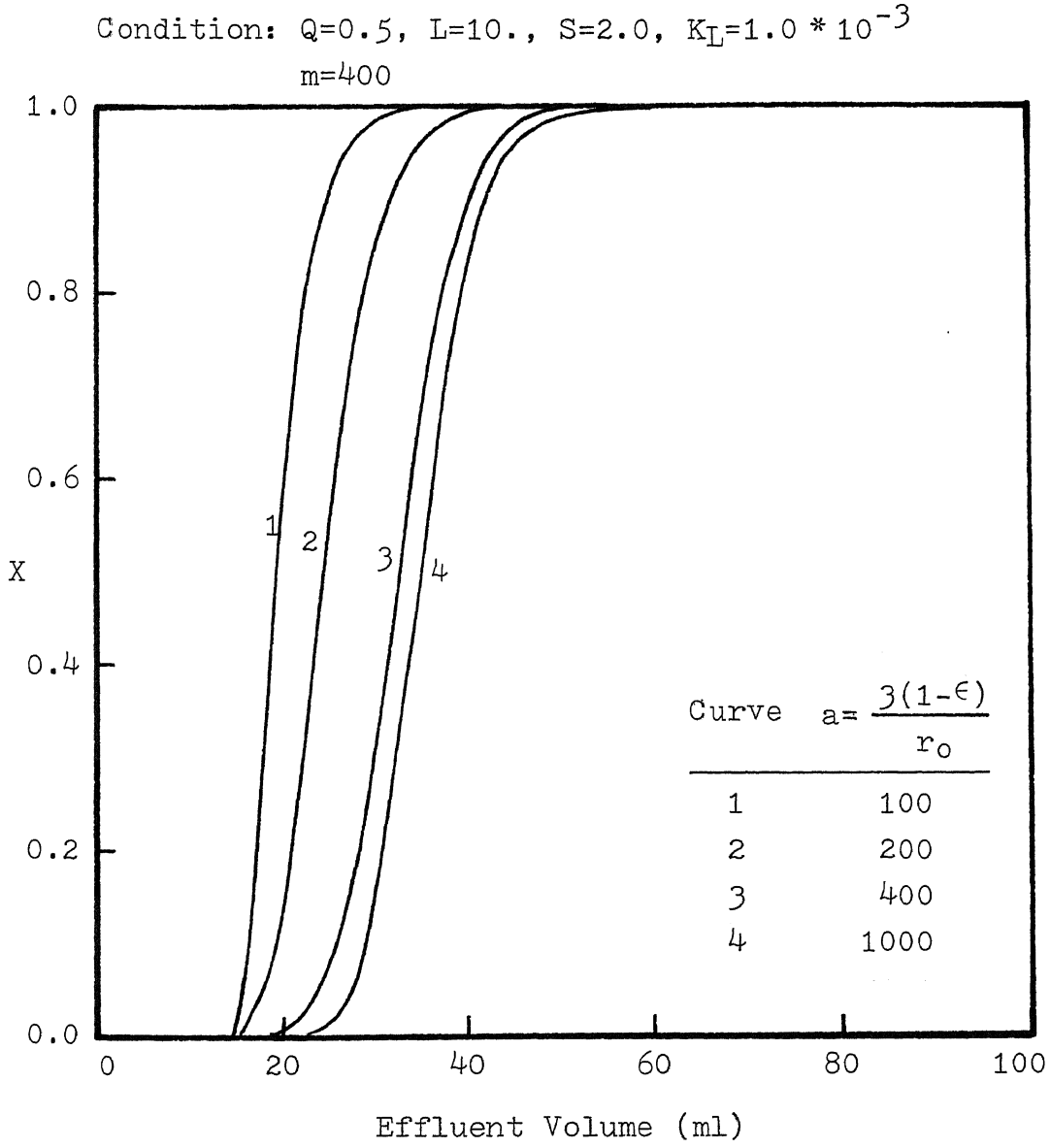

Figure 11. Effect of interfacial contact area a on predicted breakthrough curves (simple model with surface adsorption)

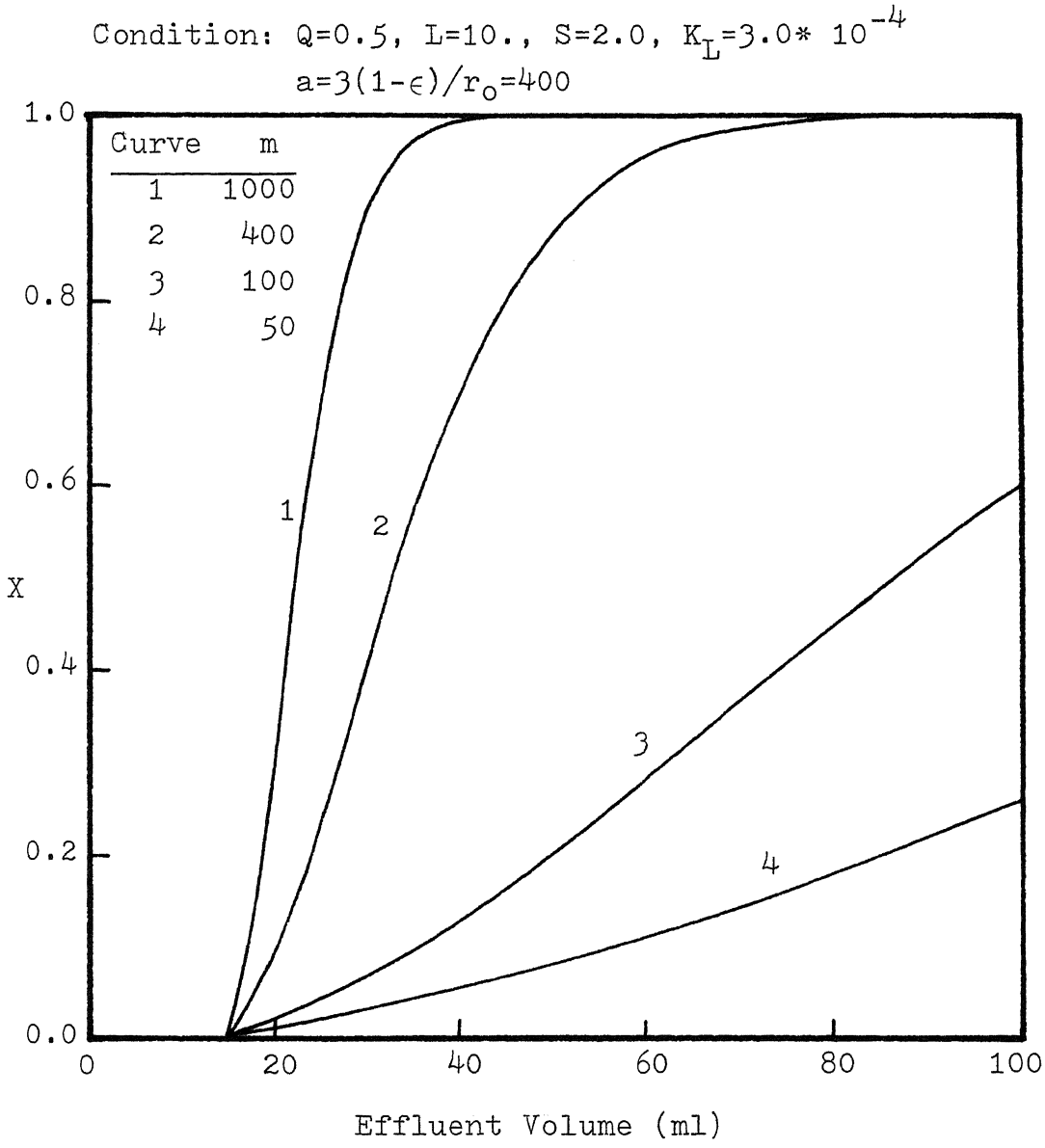

Figure 12. Effect of area based equilibrium constant m on predicted breakthrough curves (simple model with surface adsorption)

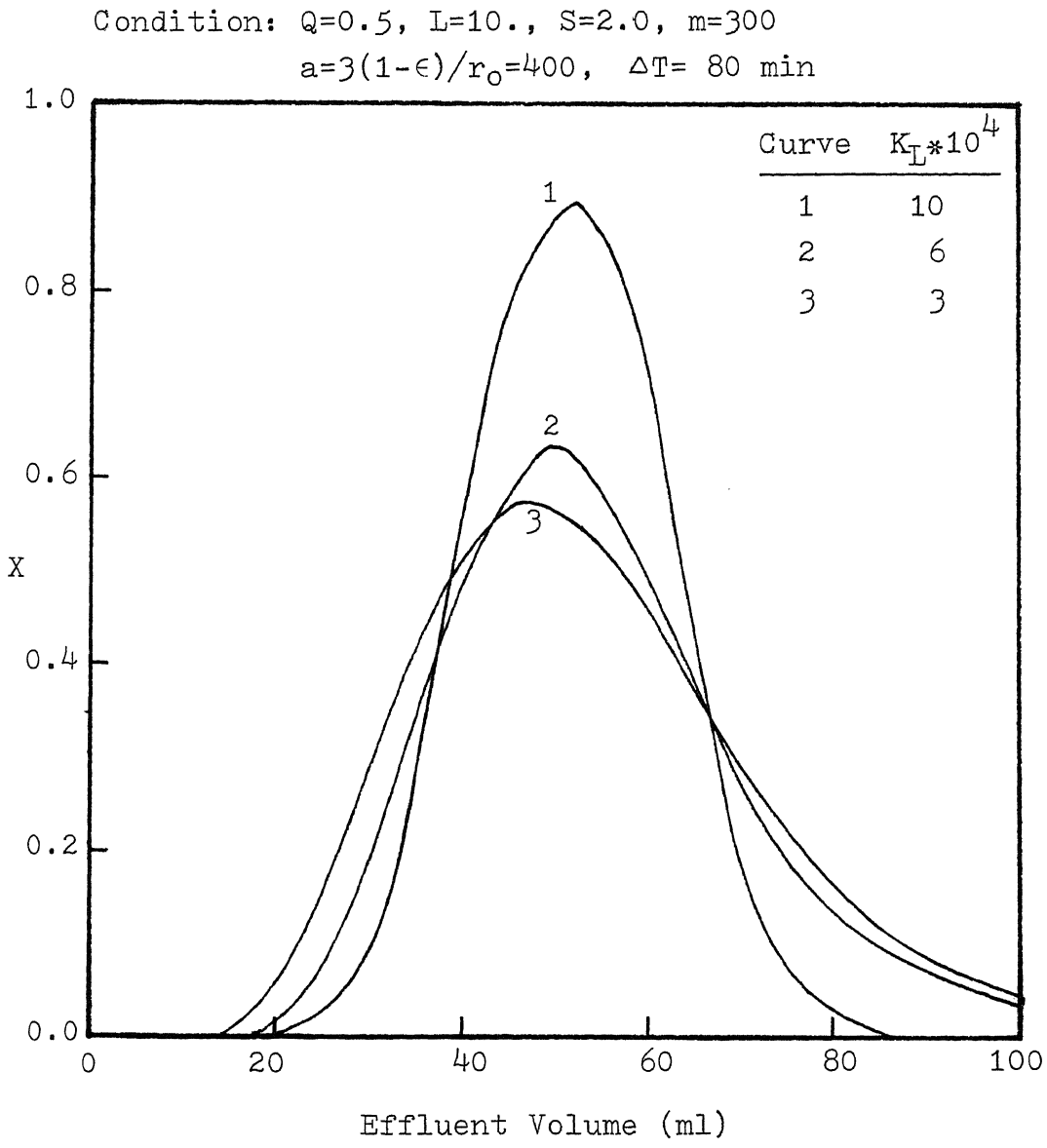

Figure 13. Effect of mass transfer coefficient K_L on predicted breakthrough curves (simple model with surface adsorption)

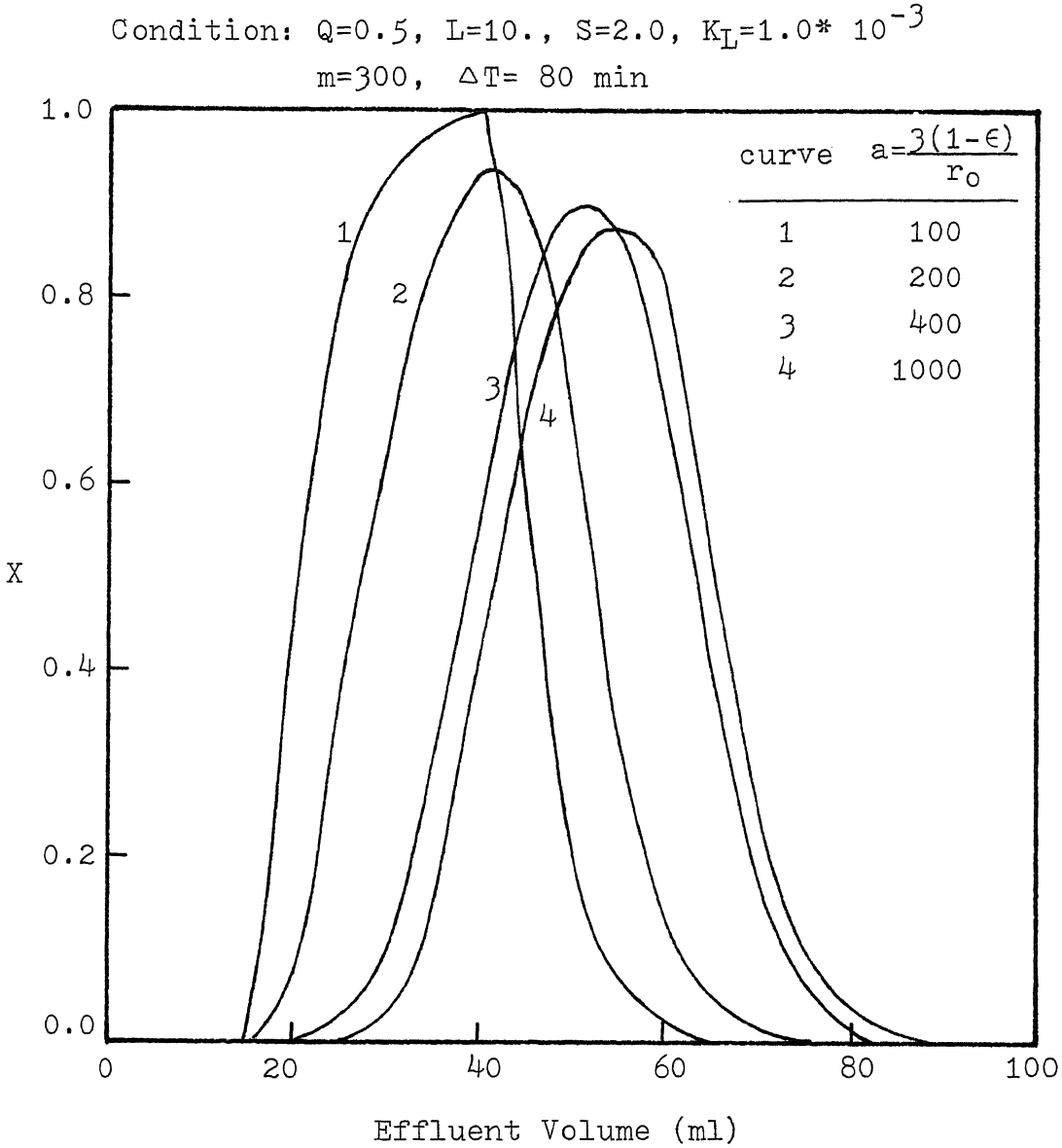

Figure 14. Effect of the interfacial contact area a on predicted breakthrough curves
(simple model with surface adsorption)

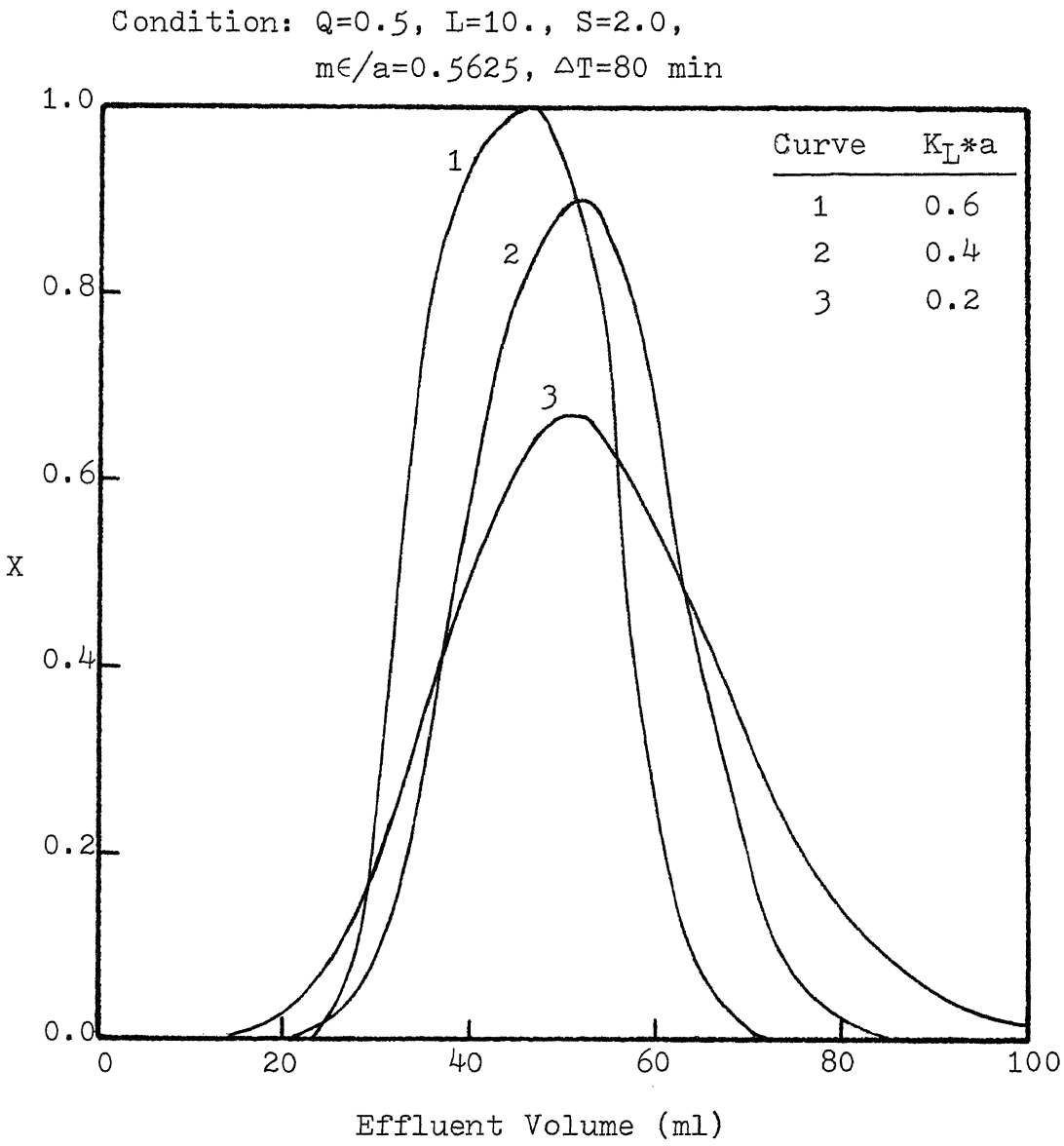

Figure 15. Effect of mass transfer rate K_L*a on predicted breakthrough curves (simple model with surface adsorption)

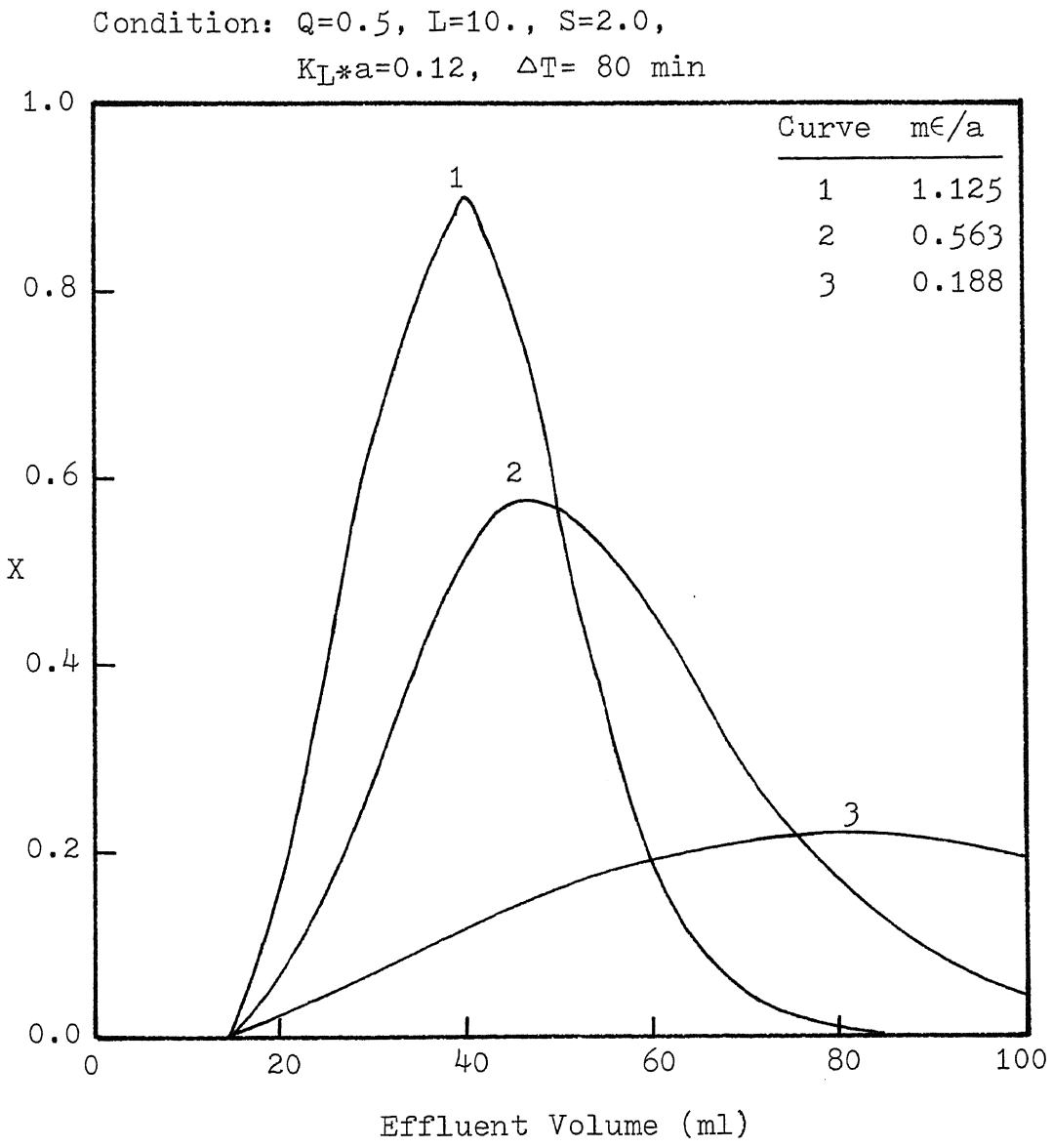

Figure 16. Effect of (mε/a) on predicted breakthrough curves (simple model with surface adsorption)

Figures 17 to 23 represent the calculated breakthrough curves [based on eq.(2B-52)] for the case of dispersion model with surface adsorption in response to a step change in input concentration of adsorbate. Figure 17 shows the influence of axial dispersion on adsorber performance. A comparison with the simple model ($D_L = 0$) shows that the break time decreases by increasing the axial dispersivity D_L. From the definition, it is known that the axial dispersion is the result of eddy diffusion and molecular diffusion. Hence, an increase in axial dispersion will result in a superimposition on the convective flow of fluid and then decrease the column efficiency.

Among the considerations in designing the packed bed adsorber, the most important features of a breakthrough curve are the position of break point, the adsorption capacity of the packed bed, and the steepness of the curve. By comparing the illustrations in Figures 18 to 23 with that in Figures 7 to 12, it can be found that both cases display the same trends of the effects of system parameters Q, L, S, K_L, a, and m on calculated breakthrough curves. However, the appearance of axial dispersion as shown in Figures 18 to 23 causes the curves to have earlier breakpoints, less adsorption capability and less steepness. These phenomena are also noticed in Figures 24 to 28 for the case of dispersion model with surface adsorption in response to a pulse change in input concentration of adsorbate.

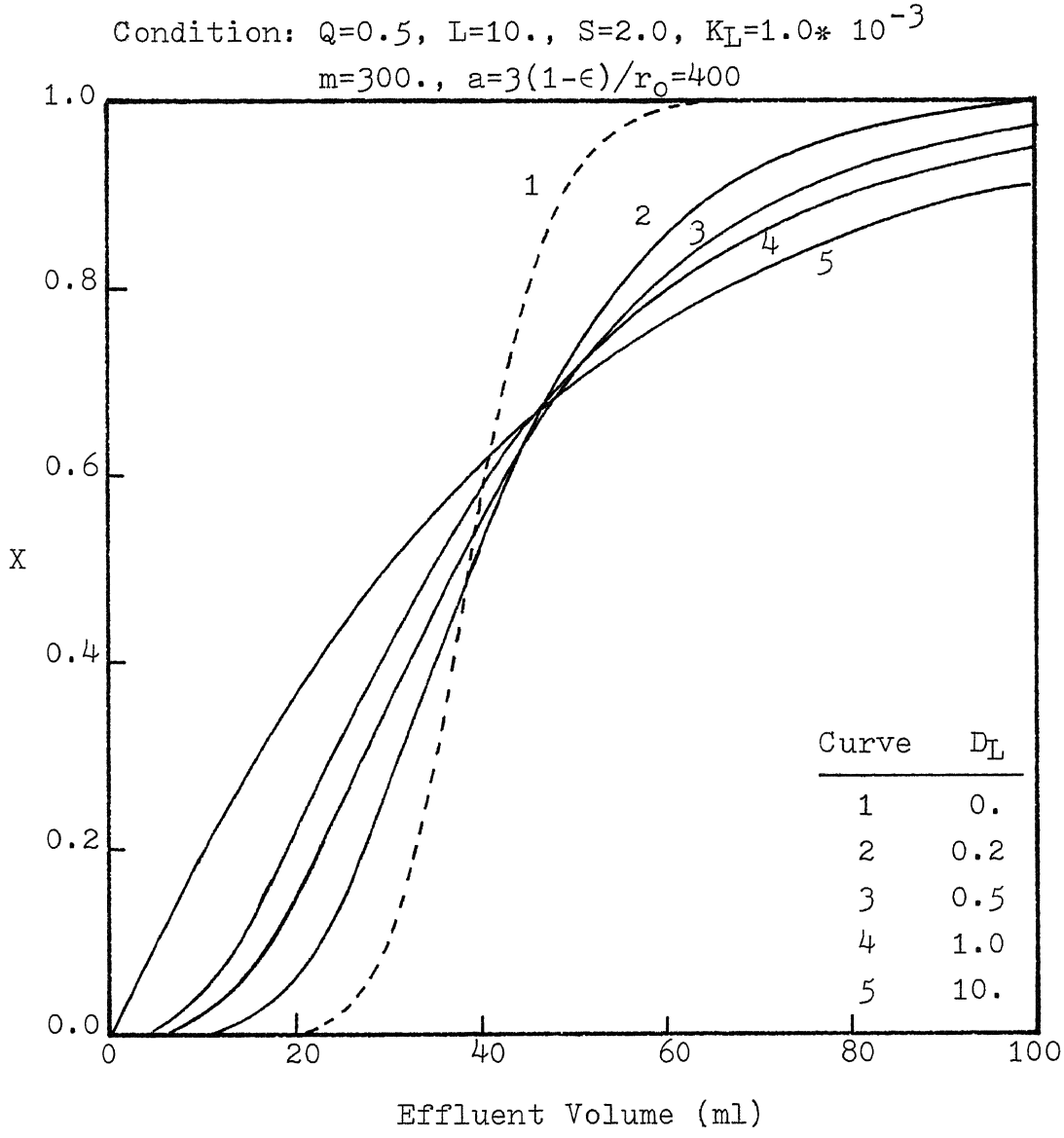

Figure 17. Effect of axial dispersion coefficient D_L on predicted breakthrough curves (dispersion model with surface adsorption)

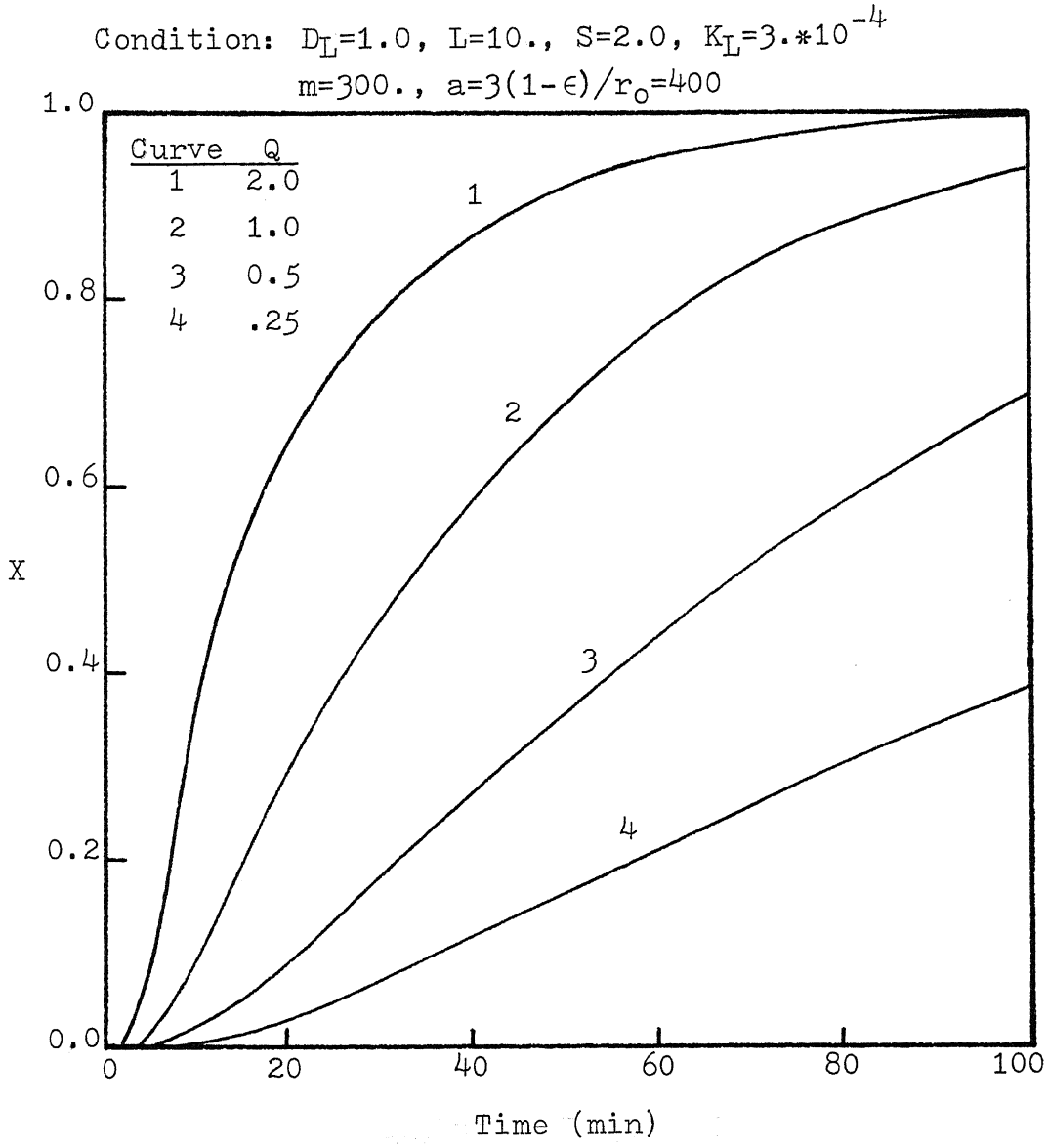

Figure 18. Effect of flow rate Q on predicted breakthrough curves
(dispersion model with surface adsorption)

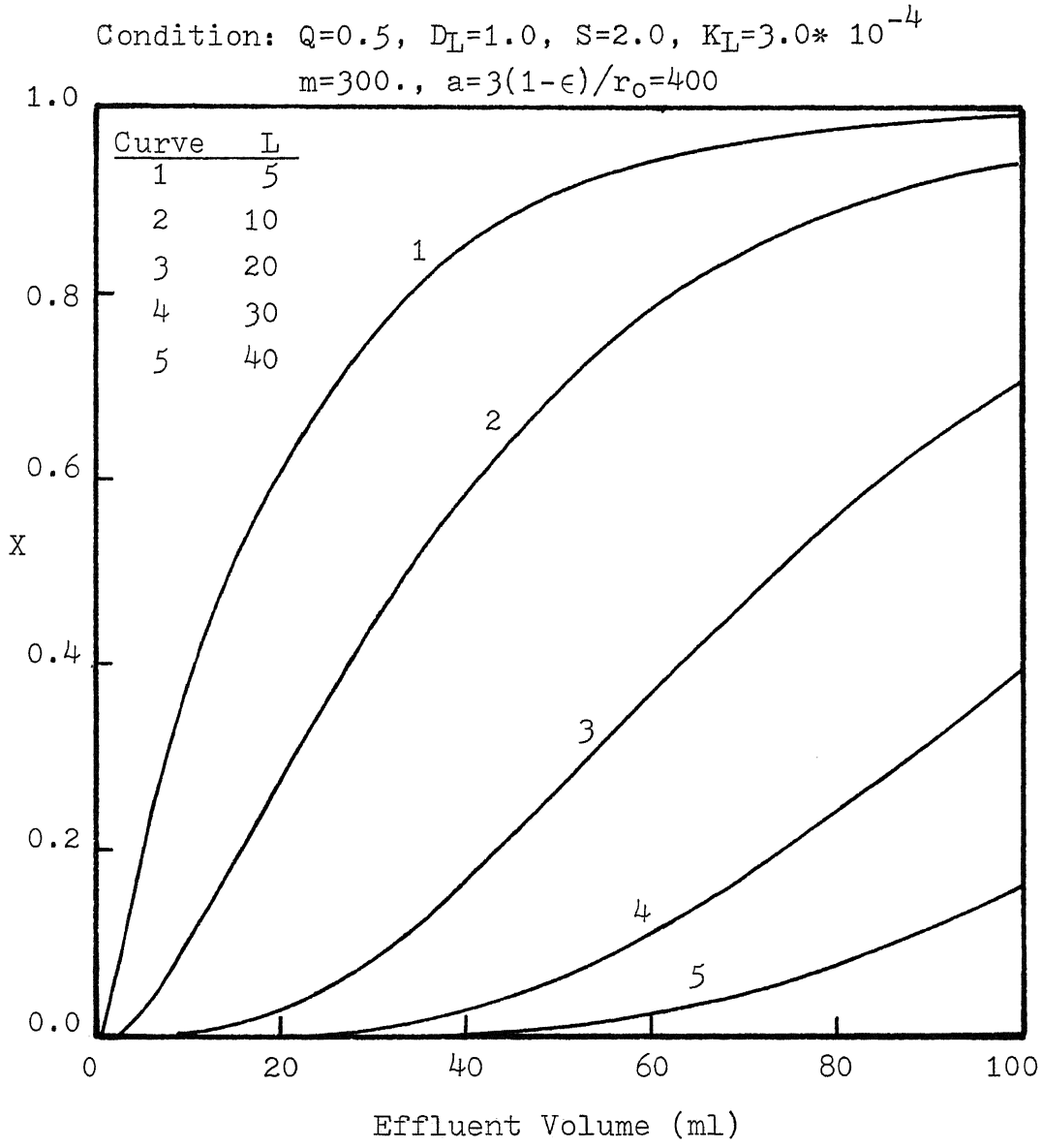

Figure 19. Effect of bed length L on predicted breakthrough curves
(dispersion model with surface adsorption)

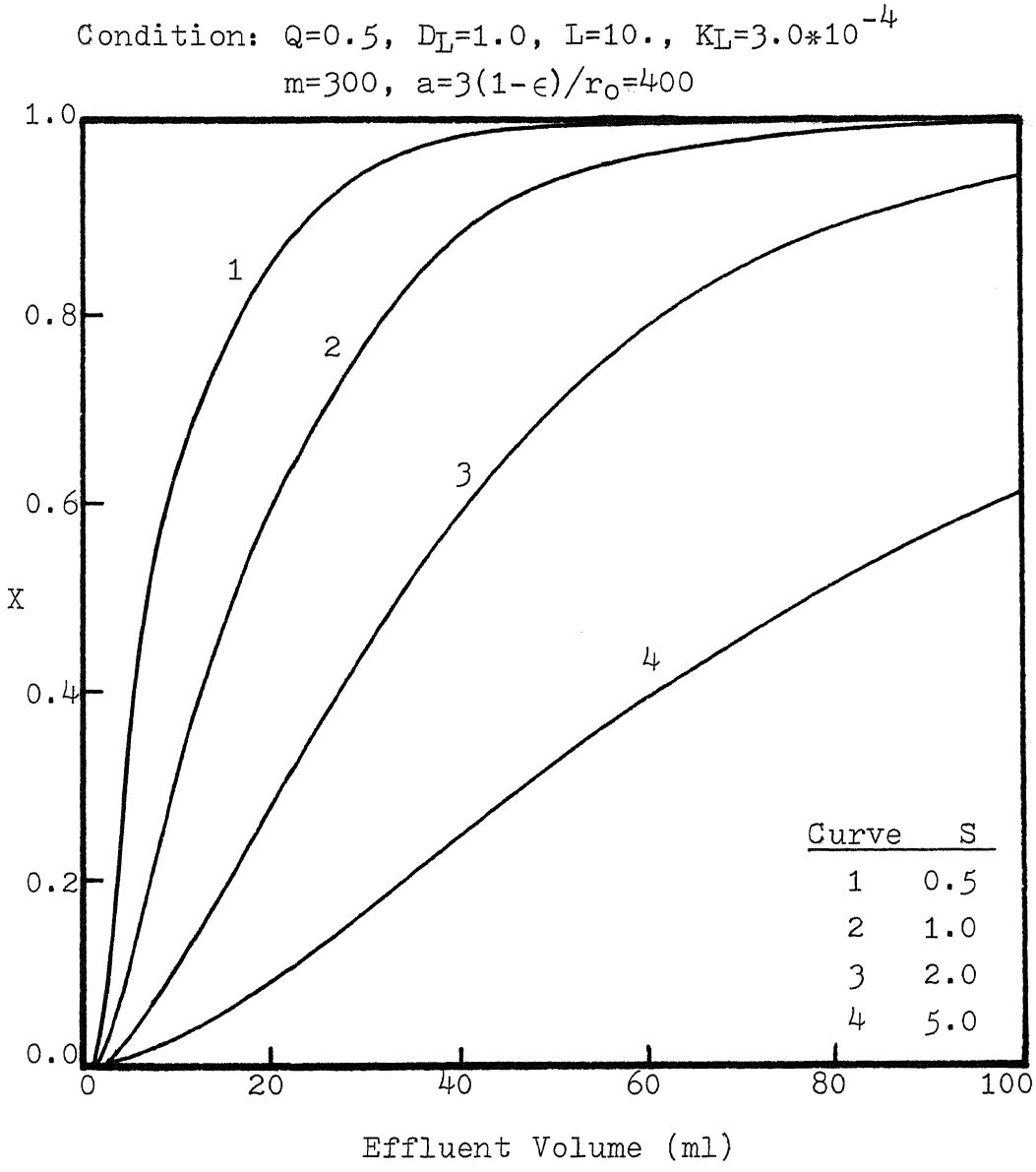

Figure 20. Effect of cross-sectional area of column S on predicted breakthrough curves (dispersion model with surface adsorption)

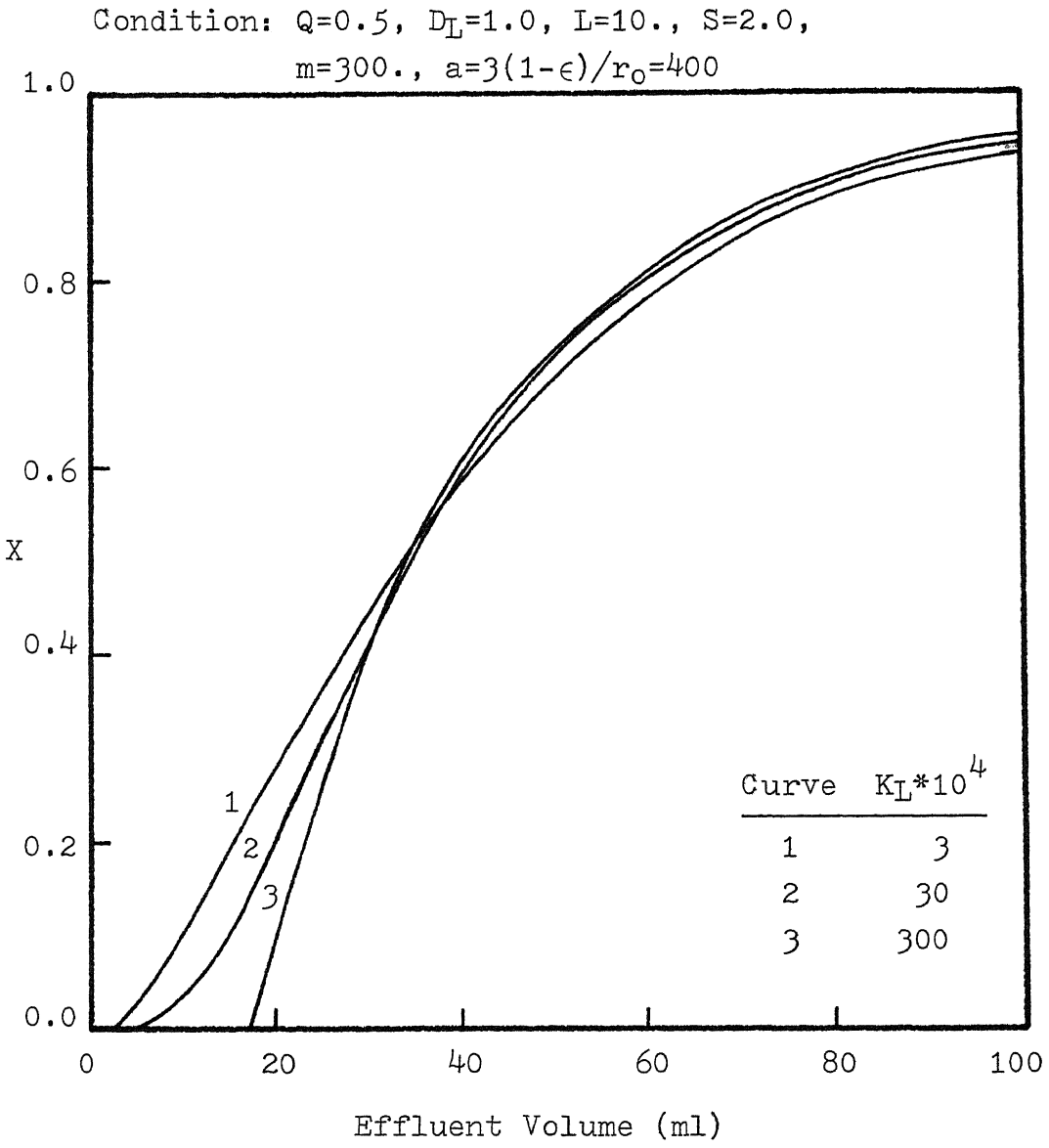

Figure 21. Effect of mass transfer coefficient K_L on predicted breakthrough curves (dispersion model with surface adsorption)

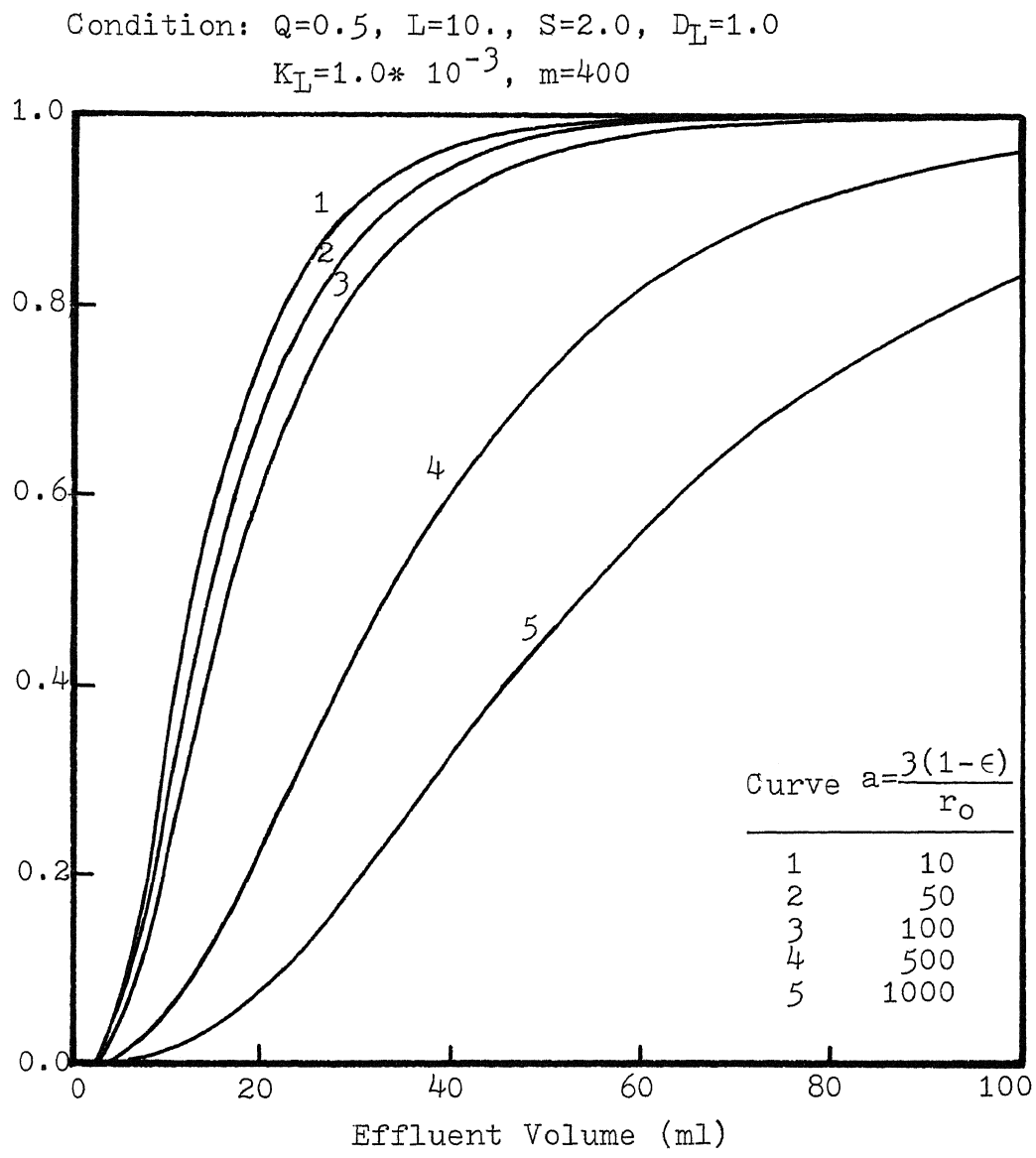

Figure 22. Effect of the interfacial contact area a on predicted breakthrough curves (dispersion model with surface adsorption)

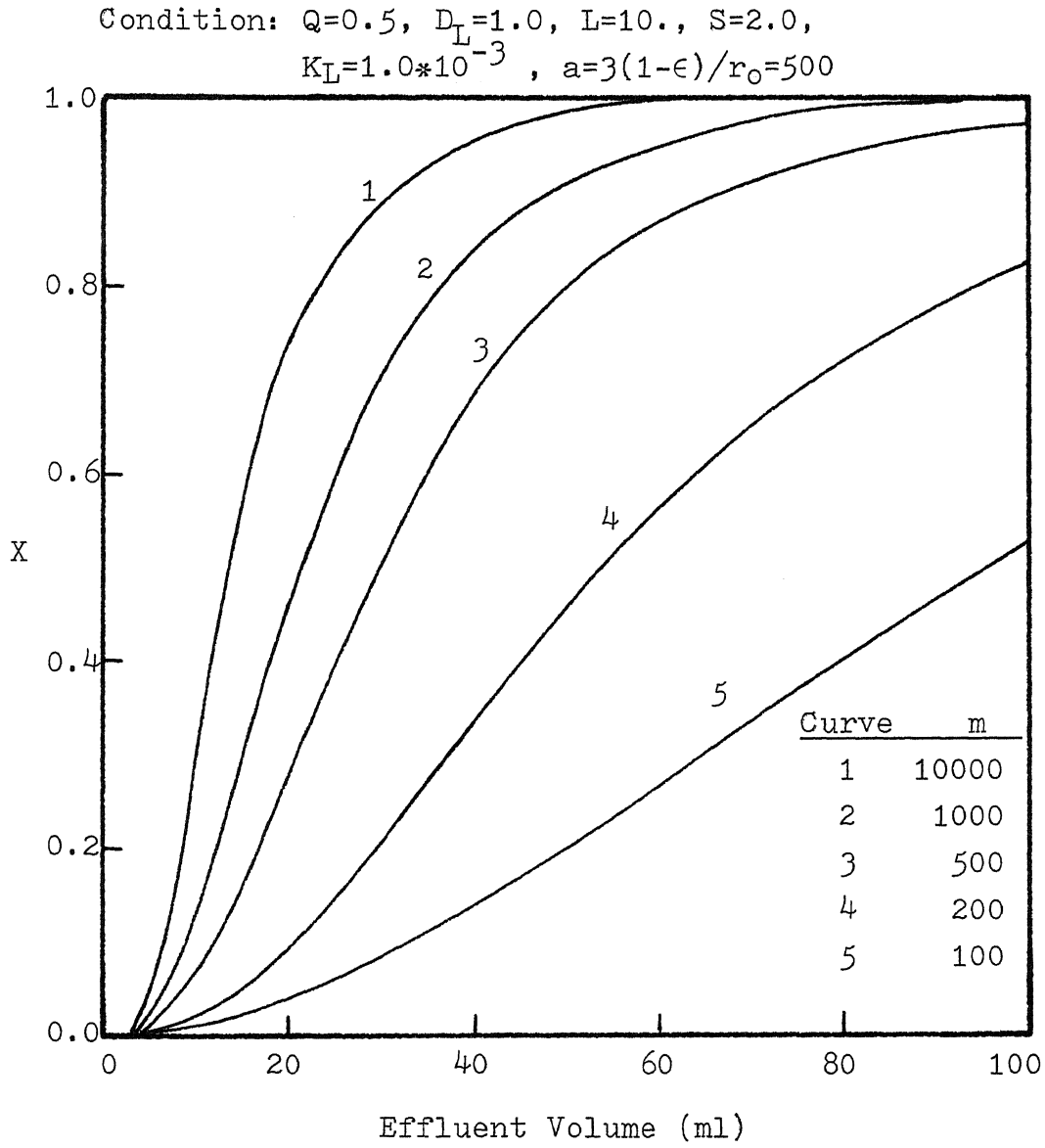

Figure 23. Effect of the area based eqiulibrium constant m on predicted breakthrough curves (dispersion model with surface adsorption)

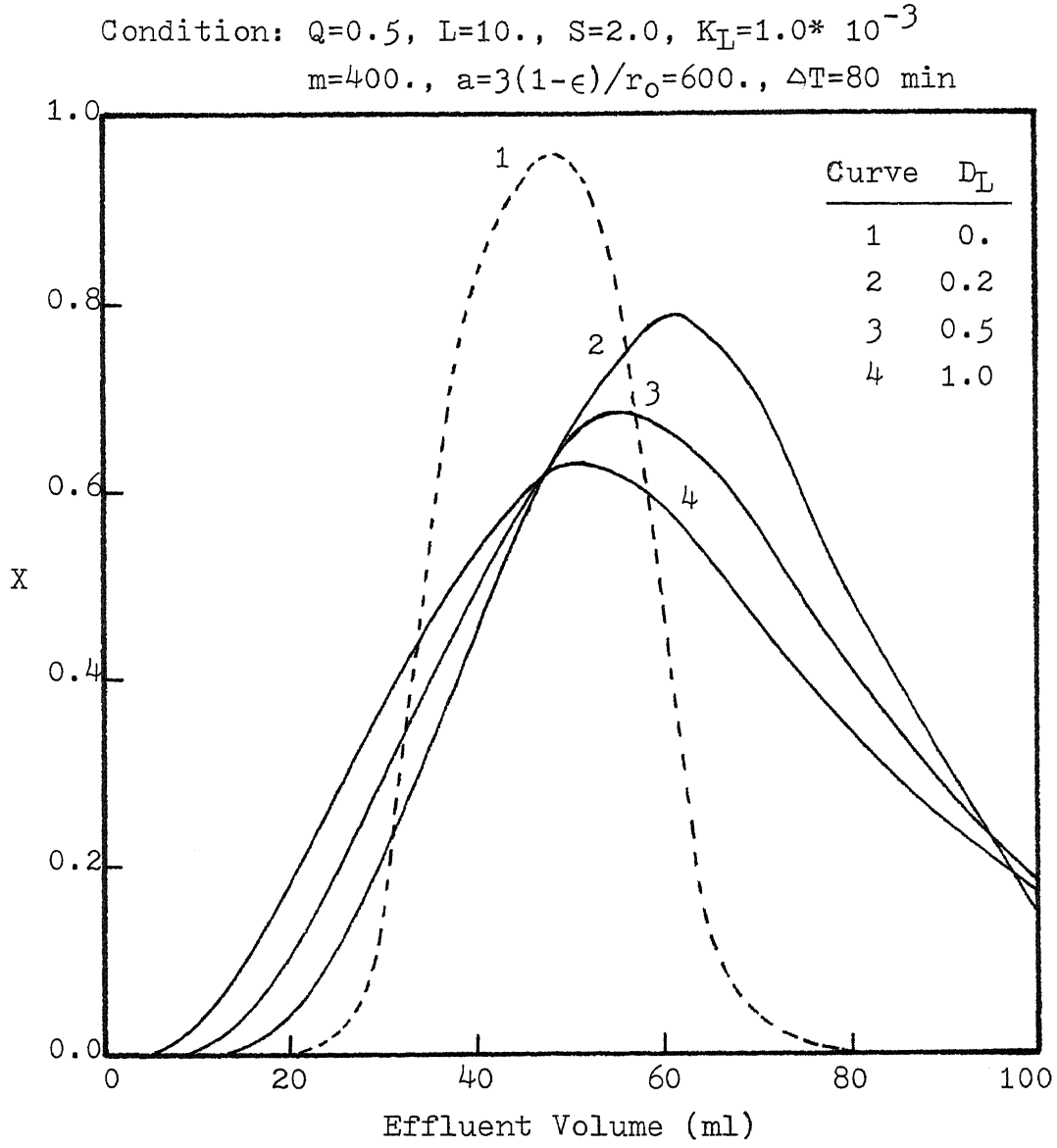

Figure 24. Effect of axial dispersion coefficient D_L on predicted breakthrough curves (dispersion model with surface adsorption)

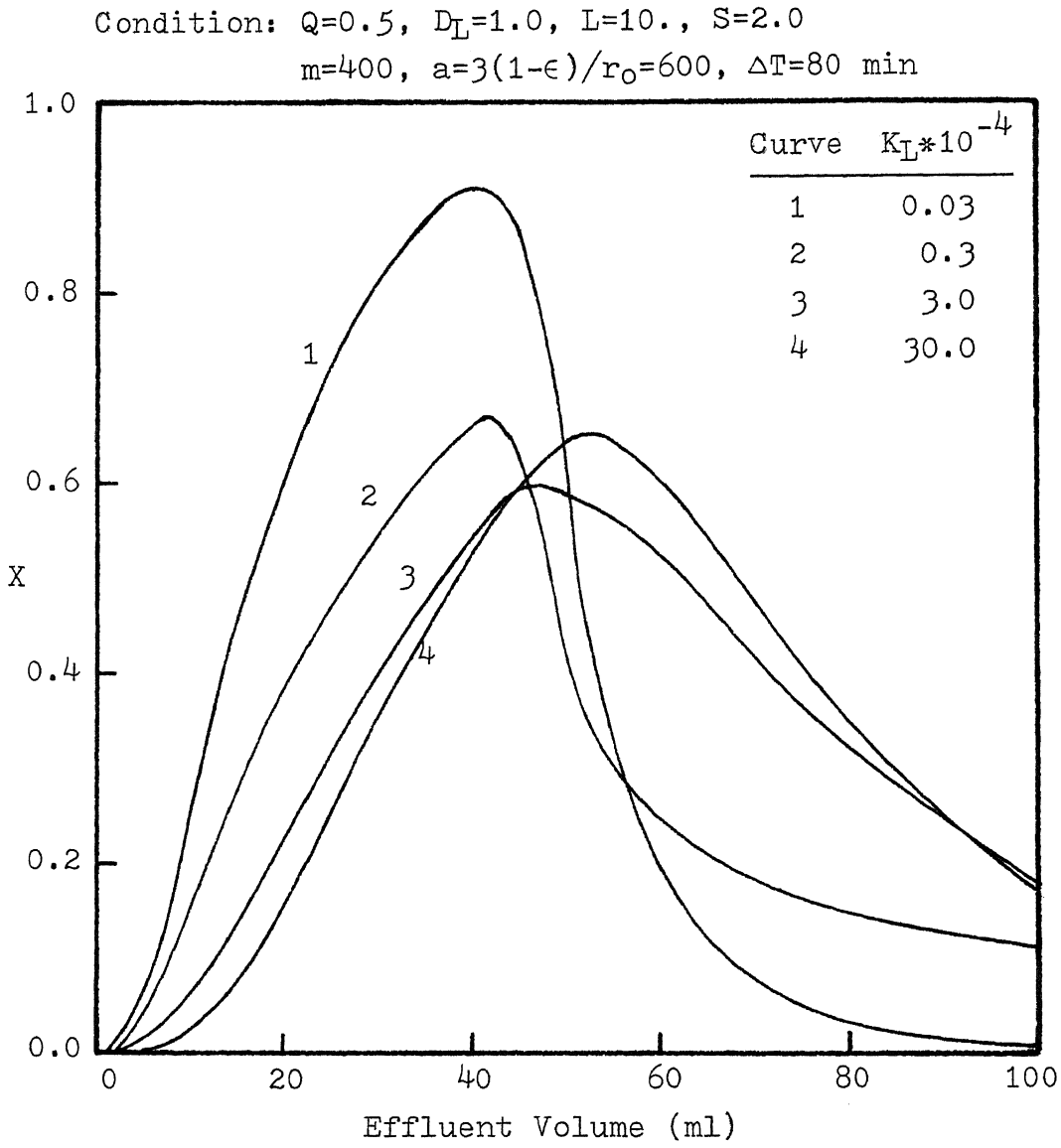

Figure 25. Effect of mass transfer coefficient K_L on predicted breakthrough curves (dispersion model with surface adsorption)

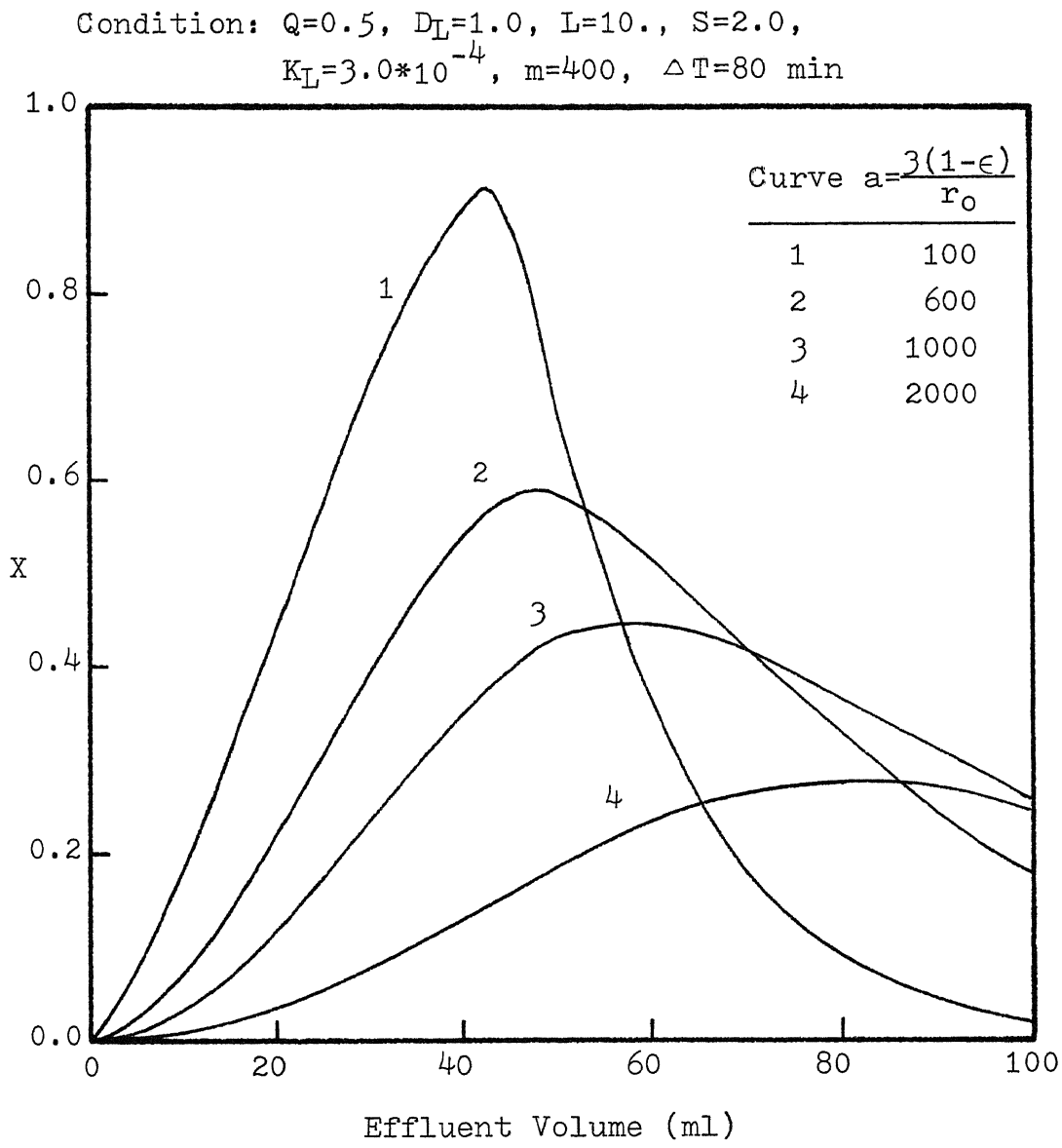

Figure 26. Effect of the interfacial contact area a on predicted breakthrough curves (dispersion model with surface adsorption)

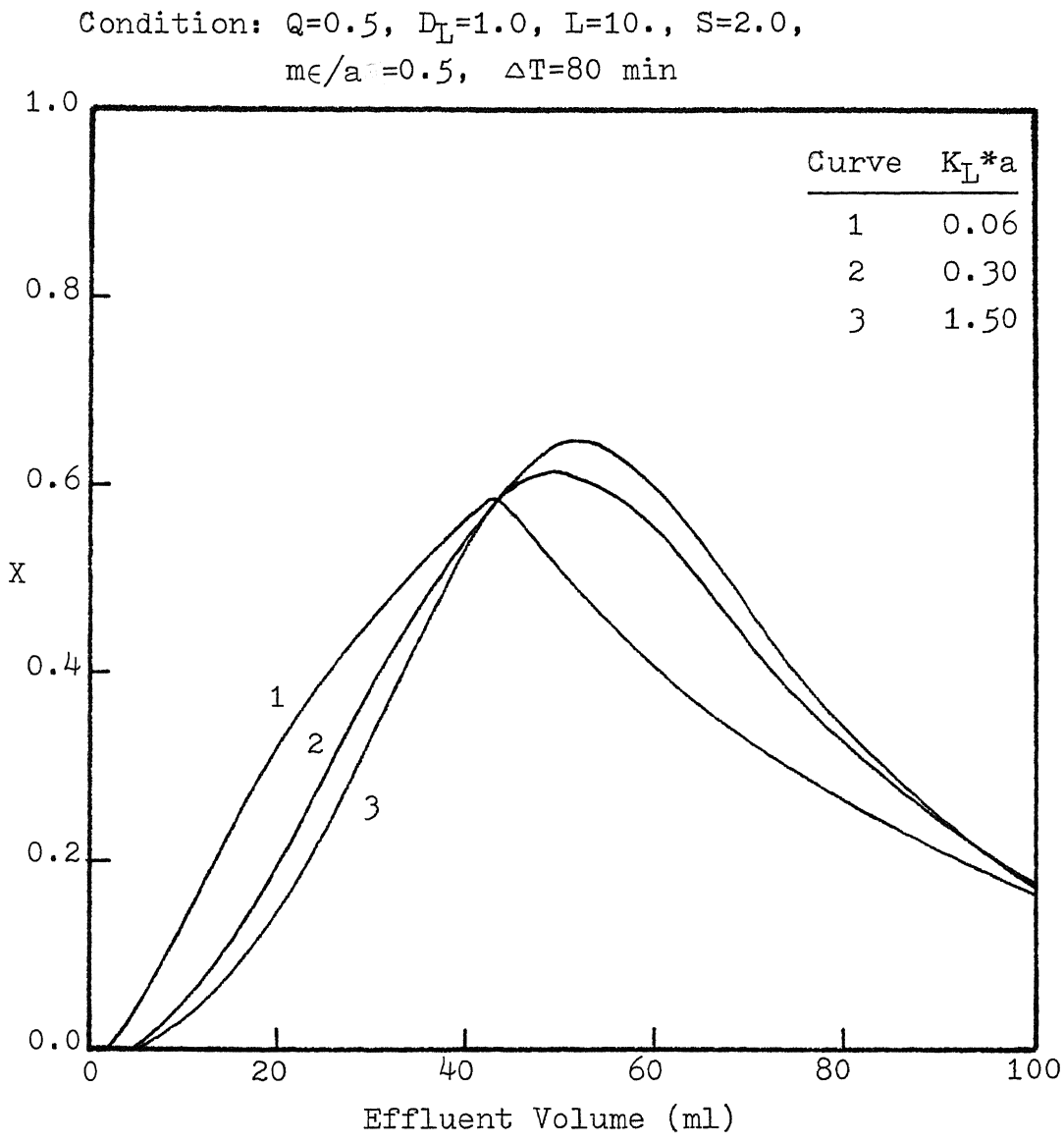

Figure 27. Effect of mass transfer rate K_L*a on predicted breakthrough curves (dispersion model with surface adsorption)

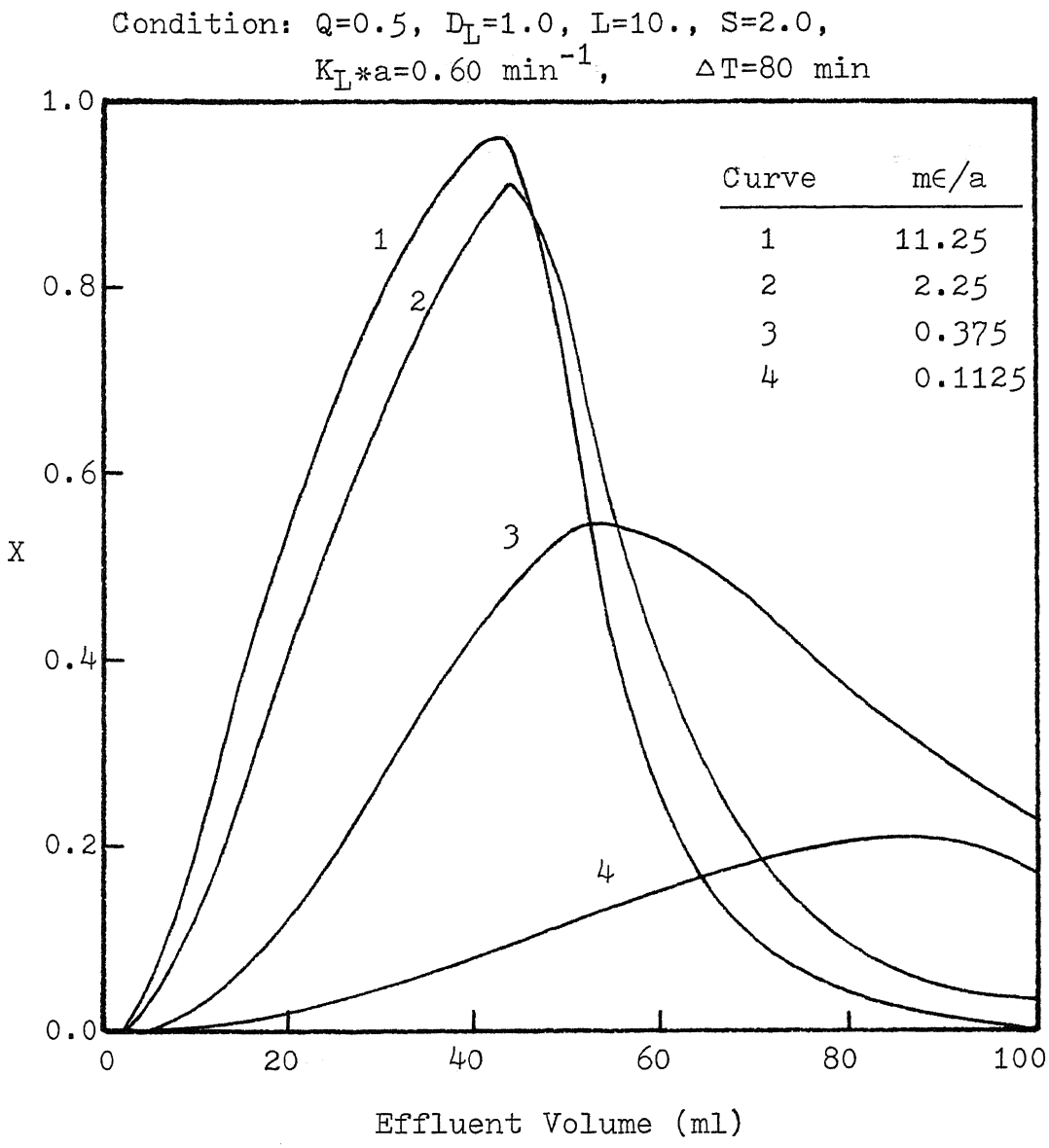

Figure 28. Effect of the distribution ratio mε/a on predicted breakthrough curves (dispersion model with surface adsorption)

B. Pore Diffusion Model

Based on equation (3B-47), Figures 29 to 35 illustrate the effects of some basic parameters on calculated breakthrough curves for the case of dispersion model with pore diffusion in response to a step change in input adsorbate concentration. As compared with the surface adsorption model, it can be seen that the breakthrough curves shown in Figures 29 to 35 have steeper slope at the early stage. This phenomenon is probably due to the effect of internal diffusion, so the bed can be saturated rapidly as the adsorption wave passes through the bed.

Figure 29 shows that the column performance decreases with increasing the axial dispersion. As illustrated before, Figures 30 to 32 show that an increase in flow rate, Q decreases the adsorption rate, and increasing the bed length, L or the cross-sectional area of column, S will cause an increase in adsorption capacity. Figure 33 illustrates the effect of equilibrium constant, λ on the calculated breakthrough curves. In dealing with the pore diffusion model, it seems that the system parameters, K_L, a, and D_s are interrelated, because the adsorption rate is first controlled by the fluid film resistance and then controlled by internal diffusion resistance. Figures 34 and 35 represent the effects of mass transfer rate, $K_L a$ and internal diffusion, $\frac{D_s}{r_o^2}$ on the breakthrough curves. From these figures, it can be

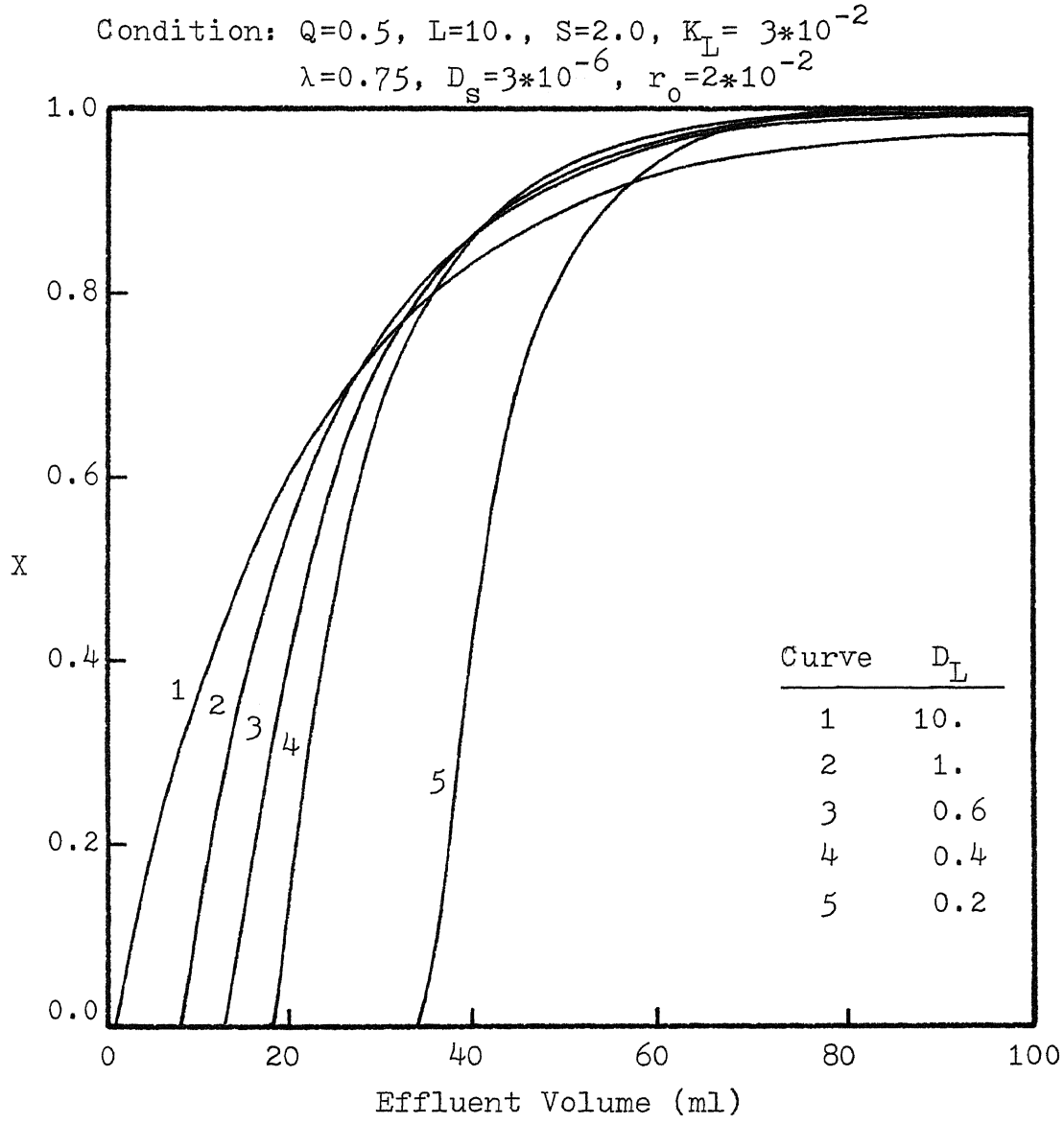

Figure 29. Effect of axial dispersivity D_L on predicted breakthrough curves (dispersion model with pore diffusion)

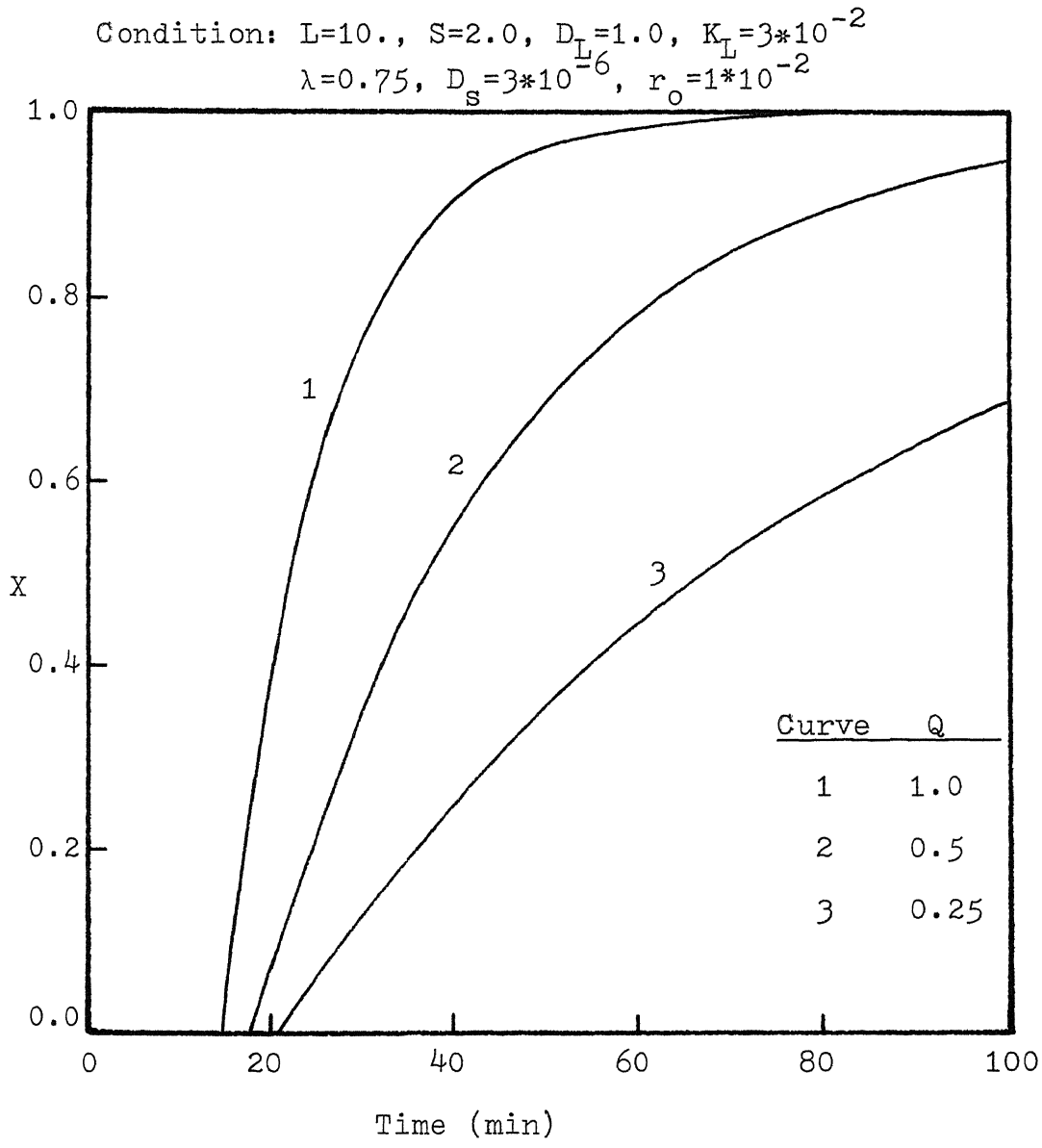

Figure 30. Effect of flow rate Q on predicted breakthrough curves (dispersion model with pore diffusion)

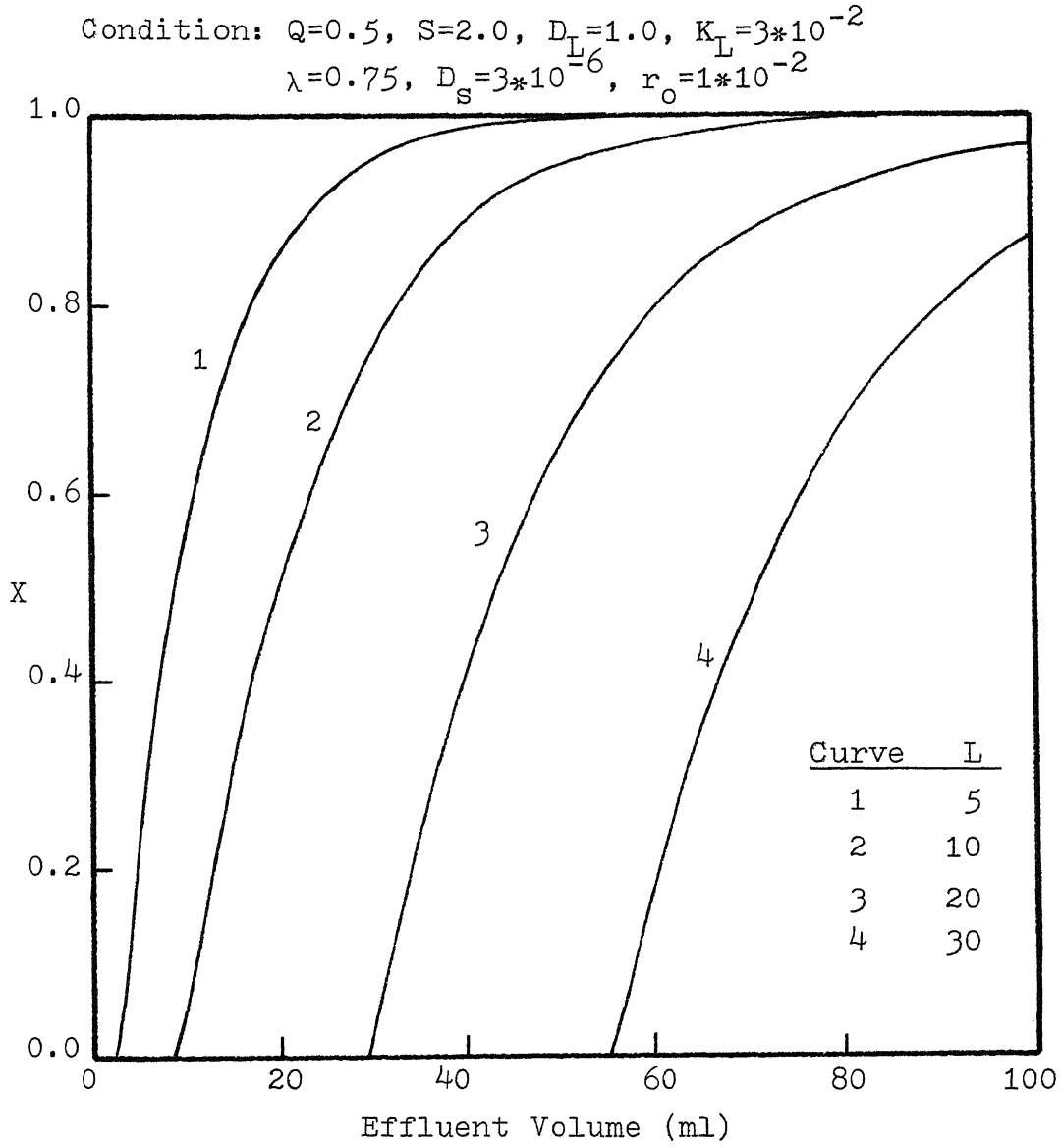

Figure 31. Effect the bed length L on predicted breakthrough curves
(dispersion model with pore diffusion)

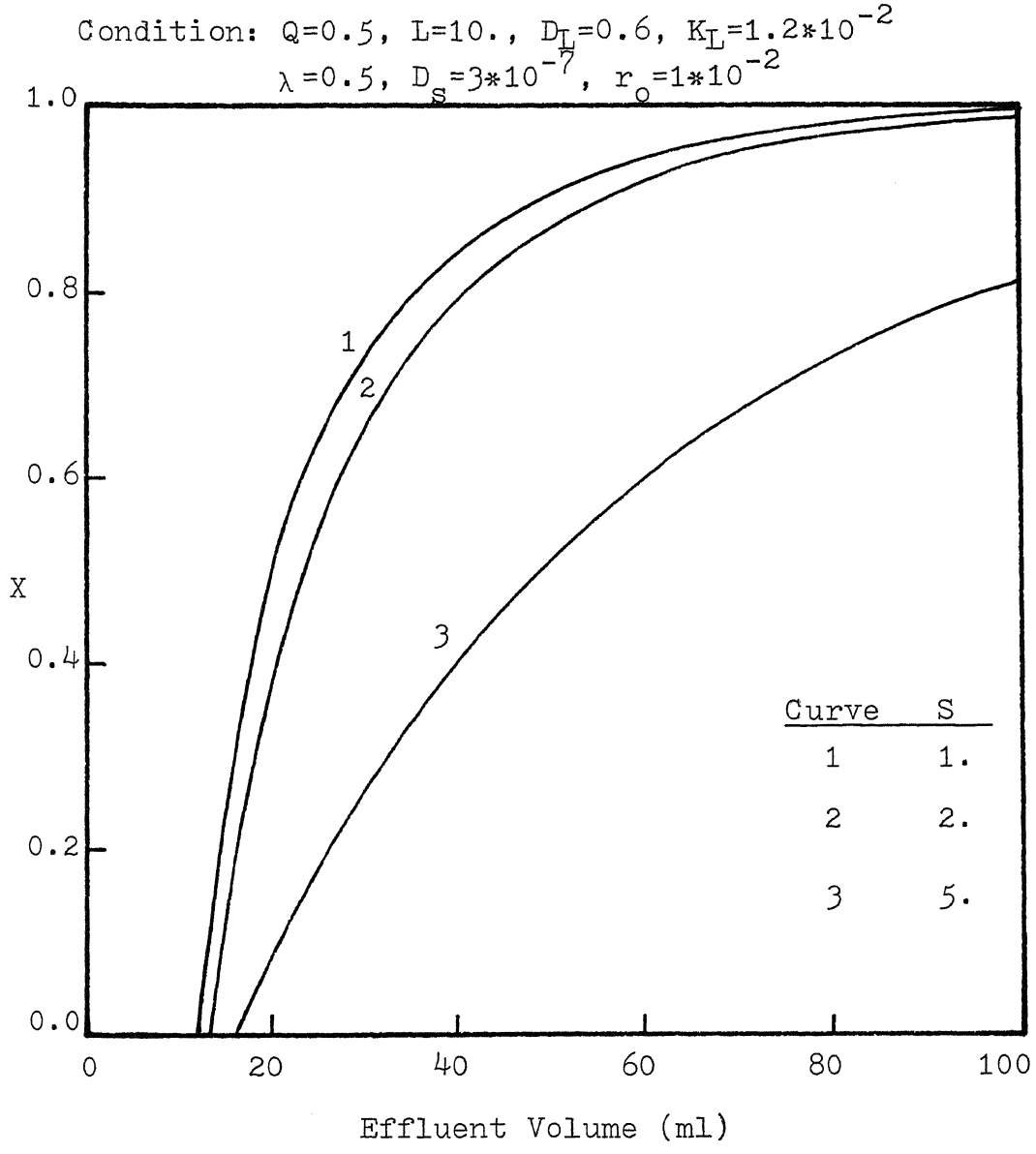

Figure 32. Effect of cross-sectional area of column S on predicted breakthrough curves (dispersion model with pore diffusion)

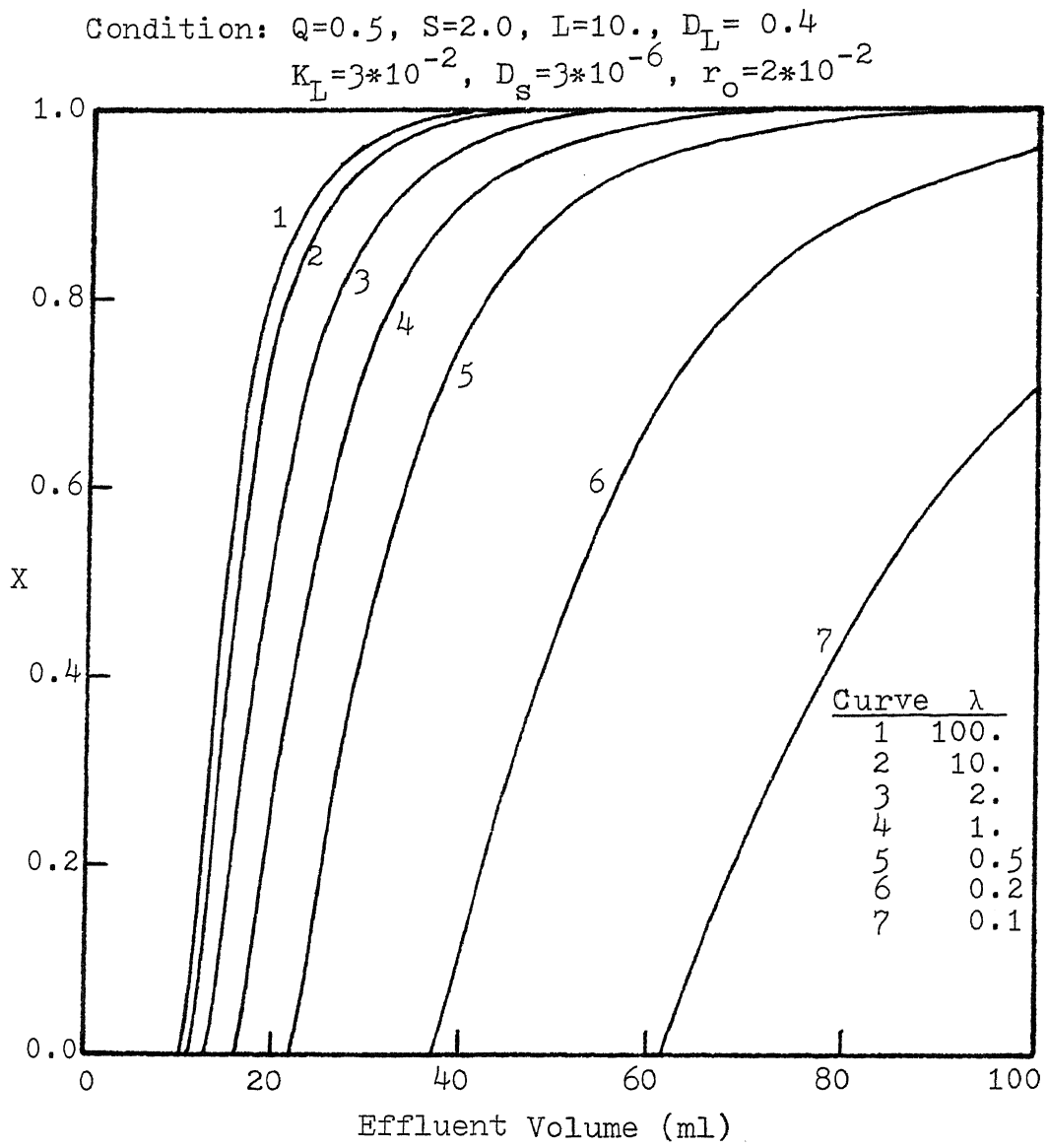

Figure 33. Effect of equilibrium constant λ on predicted breakthrough curves (dispersion model with pore diffusion)

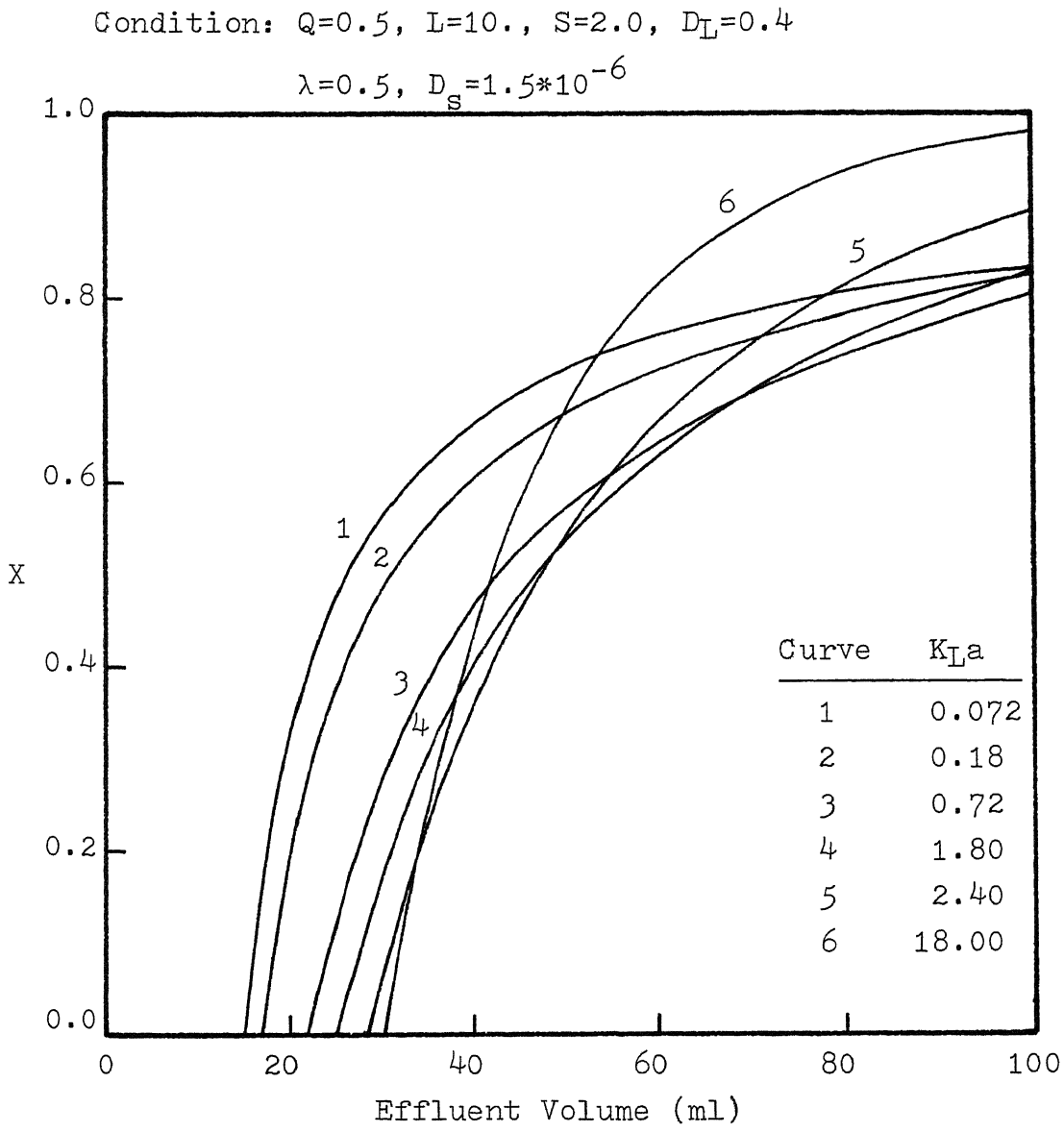

Figure 34. Effect of the mass transfer rate K_La on breakthrough curves (dispersion model with pore diffusion)

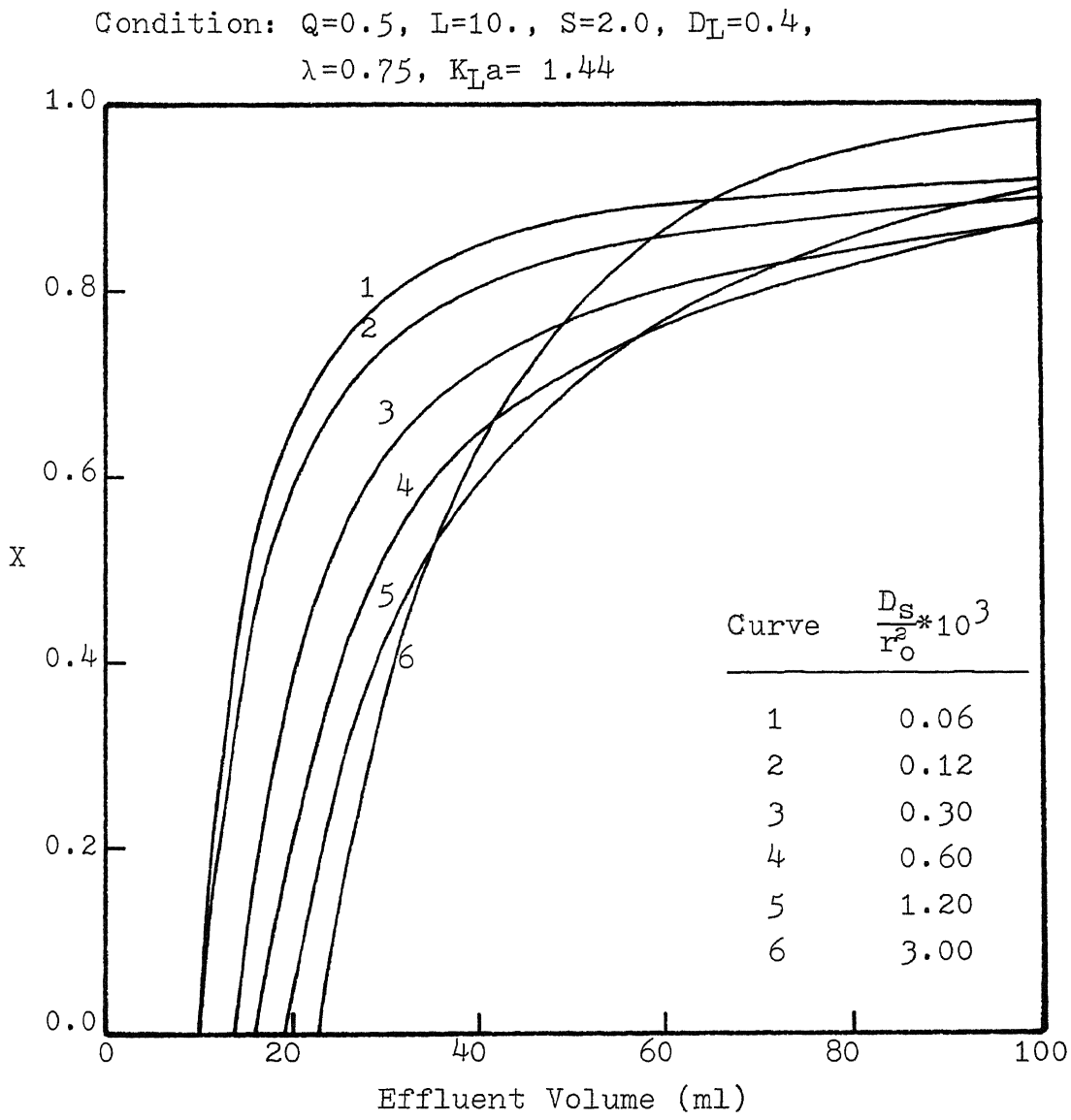

Figure 35. Effect of internal diffusion rate D_s/r_o^2 on predicted breakthrough curves (dispersion model with pore diffusion)

found that an increase in mass transfer rate or internal diffusion rate could improve the performance of adsorption processes.

C. Experimental Verifications

The adsorption of aqueous protein mixture (hemoglobin or albumin) by a fixed bed packed with CM-sepharose cation exchanger or DEAE-sepharose anion exchanger were experimentally investigated. The detailed description of adsorption system is given in Appendix B. Three sets of experimental data were obtained (36). These experimental data are first verified with the surface adsorption model as shown in Figures 36 to 44, and then verified with the pore diffusion model as shown in Figures 45 to 47. The operation conditions used in the experimental verifications are: the flow rate, Q is 1 cm^3/min, the bed length, L is 8 cm, the cross-sectional area of column, S is 2 cm^2, the average radius of resin particles, r_o is 50 μm (d_p = 40 ~ 160 μm), and the area based equilibrium constant, m is chosen as 150 cm^{-1} (or λ=0.75) for lower pH level and 200 cm^{-1} (or λ=1.0) for higher pH level. Some parameters such as axial dispersivity, D_L, the mass transfer coefficient, K_L, and the internal diffusivity D_s are not fixed and treated as variables. The trial values of K_L and D_s are adopted form the literatures (17,21).

Figures 36 to 41 represent the verifications of surface adsorption model with the experimental breakthrough data of hemoglobin on CM-sepharose at pH=4.0 and at pH=6.5. The results indicate that the axial dispersion has more significant effect on the column performance at higher pH level than that at lower pH level. This phenomenon is probably due to the adsorption capability of CM-sepharose to hemoglobin is stronger at pH=4.0 than that at pH=6.5, where the isoelectric point of hemoglobin is pI=6.7 (10). As shown in Figures 38 and 41, the good agreement between the predicted breakthrough curves and the experimental data can be obtained if the interaction of axial dispersion and mass transfer rate is taken into account. However, there is a little deviation between the predicted breakthrough curves and the experimental data at the early stage. This phenomenon is probably due to the fact that the assumption of linear velocity profile can not be effectively used to simulate the adsorption process. For the case of albumin adsorbed onto DEAE-sepharose at pH=6.5, the verifications of surface adsorption model with the experimental breakthrough data are shown in Figures 42 to 44. It can be seen that the disagreement between the predicted breakthrough curves and the experimental data is more noticeable than that in the case of hemoglobin.

With the consideration of internal diffusion, the verifications of pore diffusion model with the experimental

data are shown in Firures 45 to 47. From these demonstrations, it can be seen that the fitting of experimental data is improved a little by the pore diffusion model.

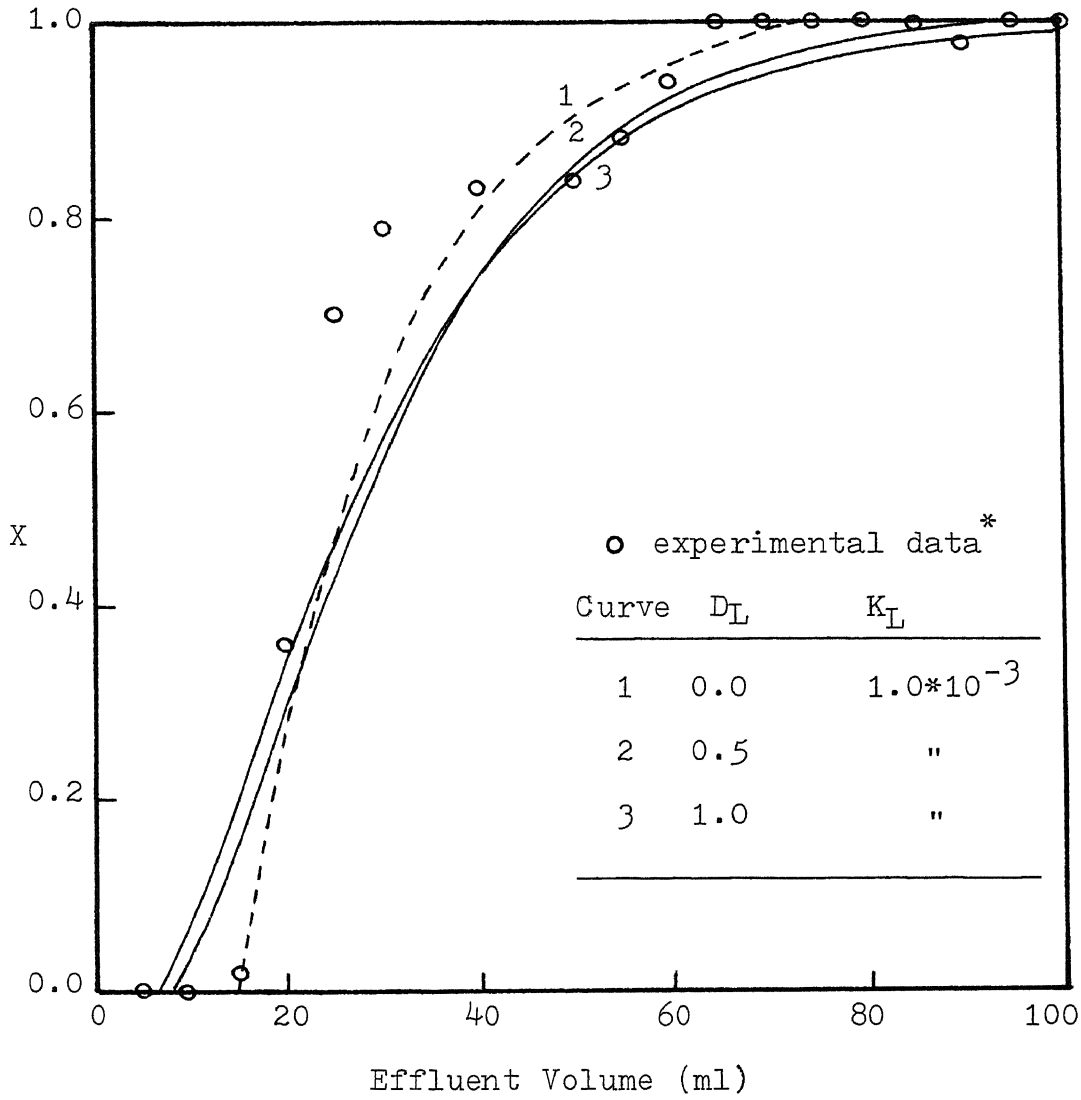

Figure 36. The verification of experimental breakthrough data with surface adsorption model
(Hemoglobin on CM-Sepharose at pH= 4.0)
Condition: Q=1.0, S=2.0, L=8.0, m=150.
ϵ=0.75, r_o=50.μm

*Ref.(36)

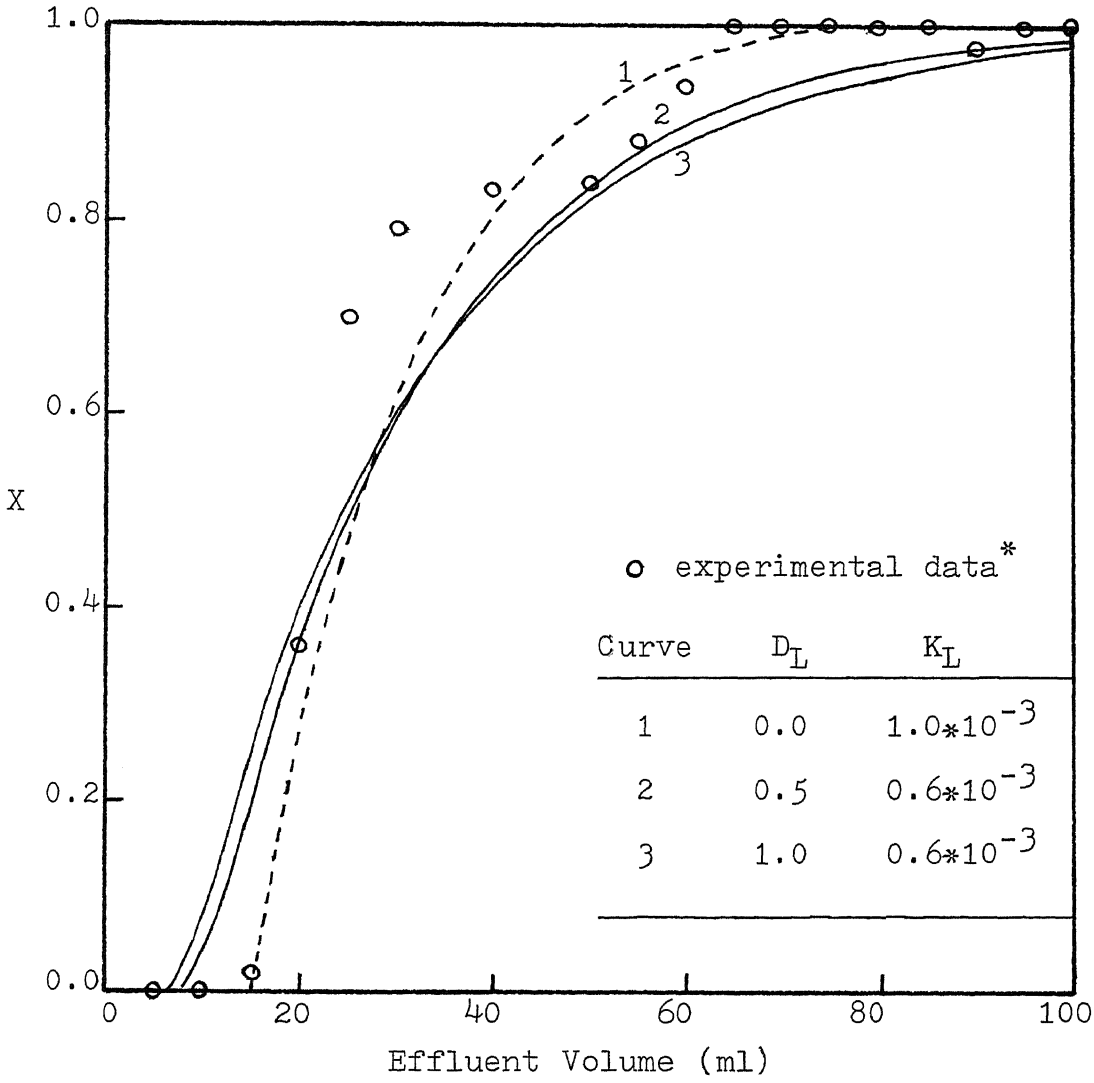

Figure 37. The verification of experimental breakthrough data with surface adsorption model
(Hemoglobin on CM-Sepharose at pH= 4.0)
Condition: Q=1.0, S=2.0, L=8.0, m=150.
ϵ=0.75, r_o=50μm

*Ref.(36)

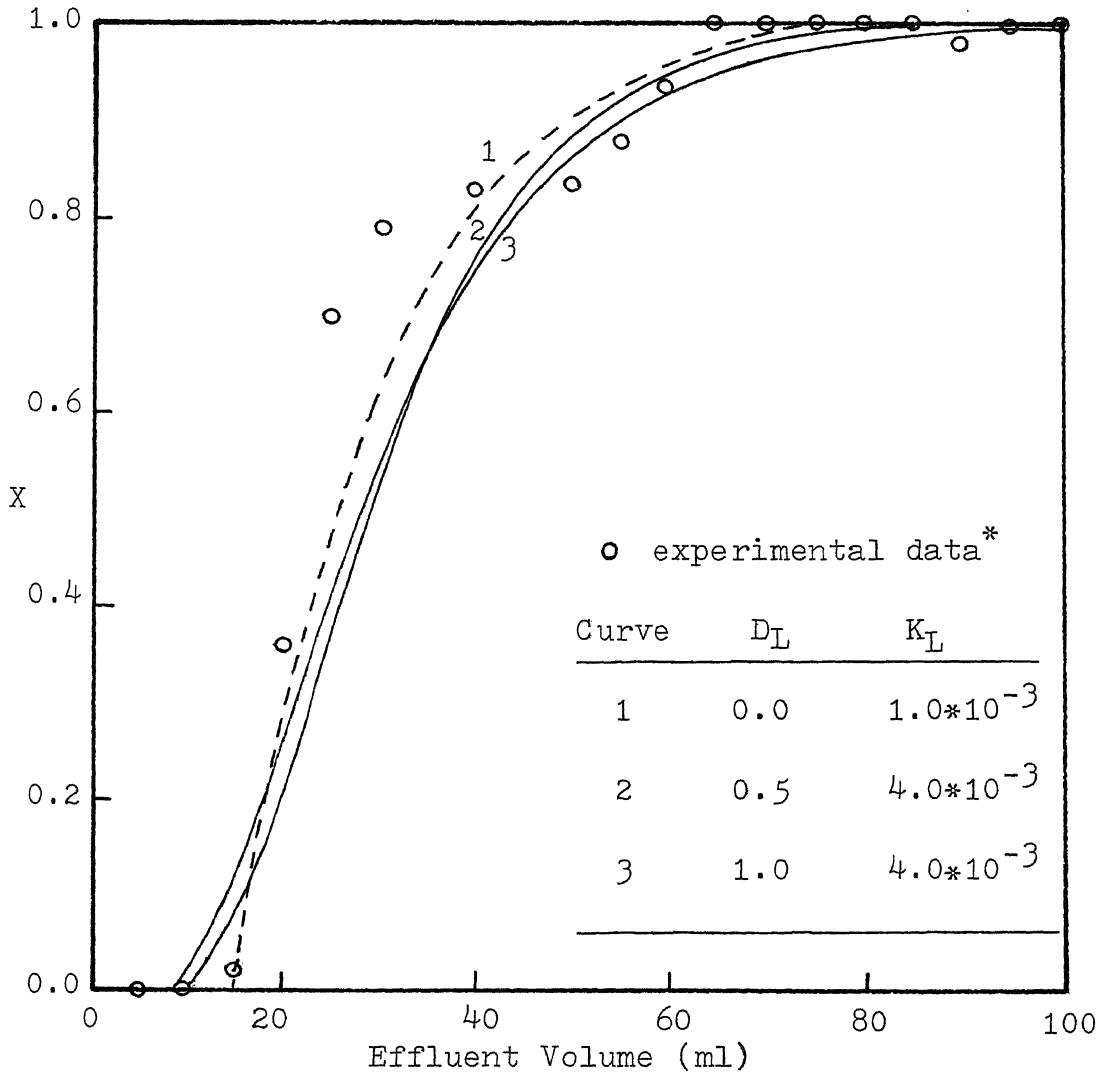

Figure 38. The verification of experimental breakthrough data with surface adsorption model
(Hemoglobin on CM-Sepharose at pH= 4.0)
Condition: Q=1.0, S=2.0, L=8.0, m=150.
ϵ=0.75, r_o= 50 μm

*Ref.(36)

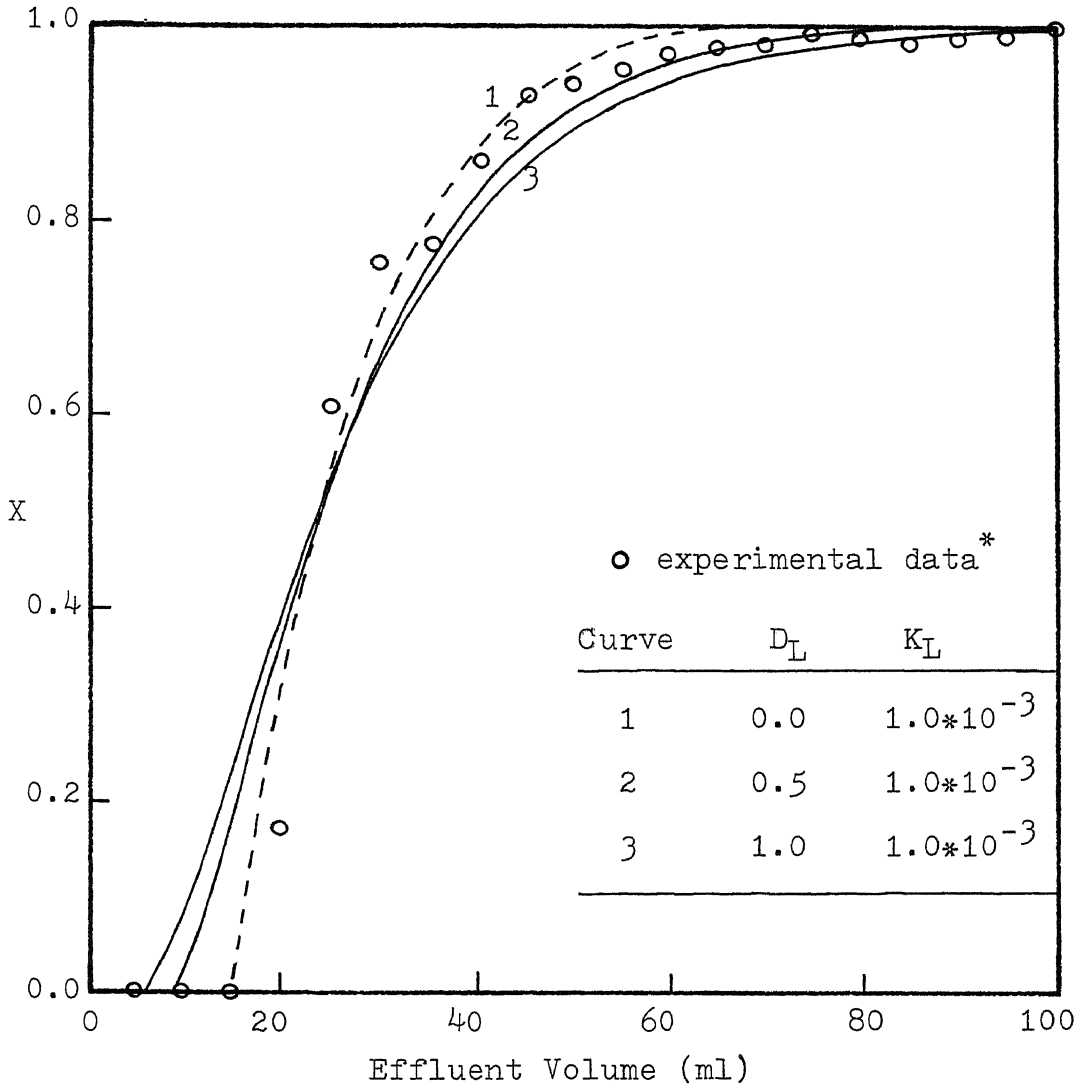

Figure 39. The verification of experimental breakthrough data with surface adsorption model
(Hemoglobin on CM-Sepharose at pH= 6.5)
Condition: Q=1.0, S=2.0, L=8.0, m=200.
ϵ=0.75, r_o= 50 μm

*Ref.(36)

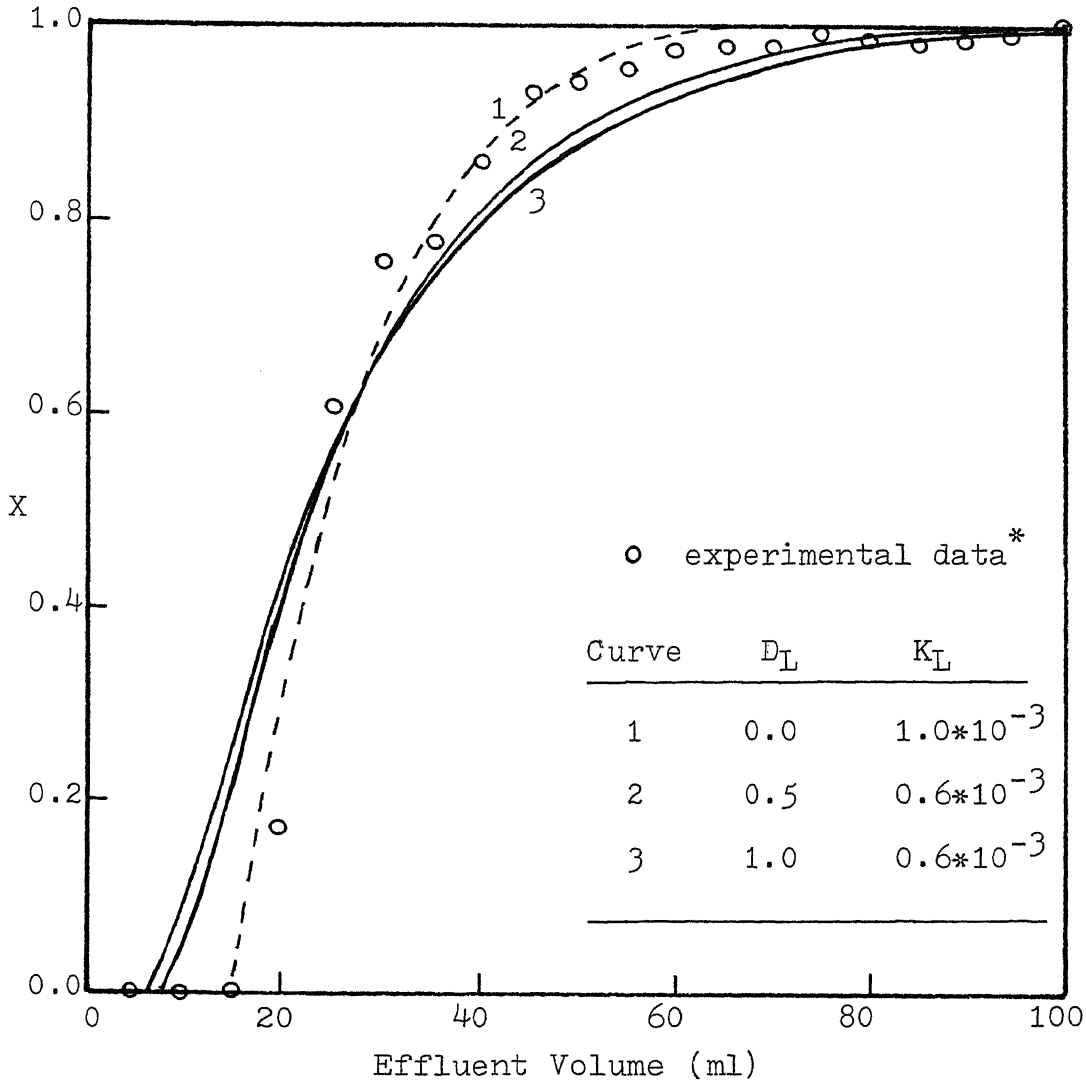

Figure 40. The verification of experimental breakthrough data with surface adsorption model
(Hemoglobin on CM-Sepharose at pH= 6.5)
Condition: Q=1.0, S=2.0, L=8.0, m=200.
ϵ=0.75, r_o= 50 μm

*Ref.(36)

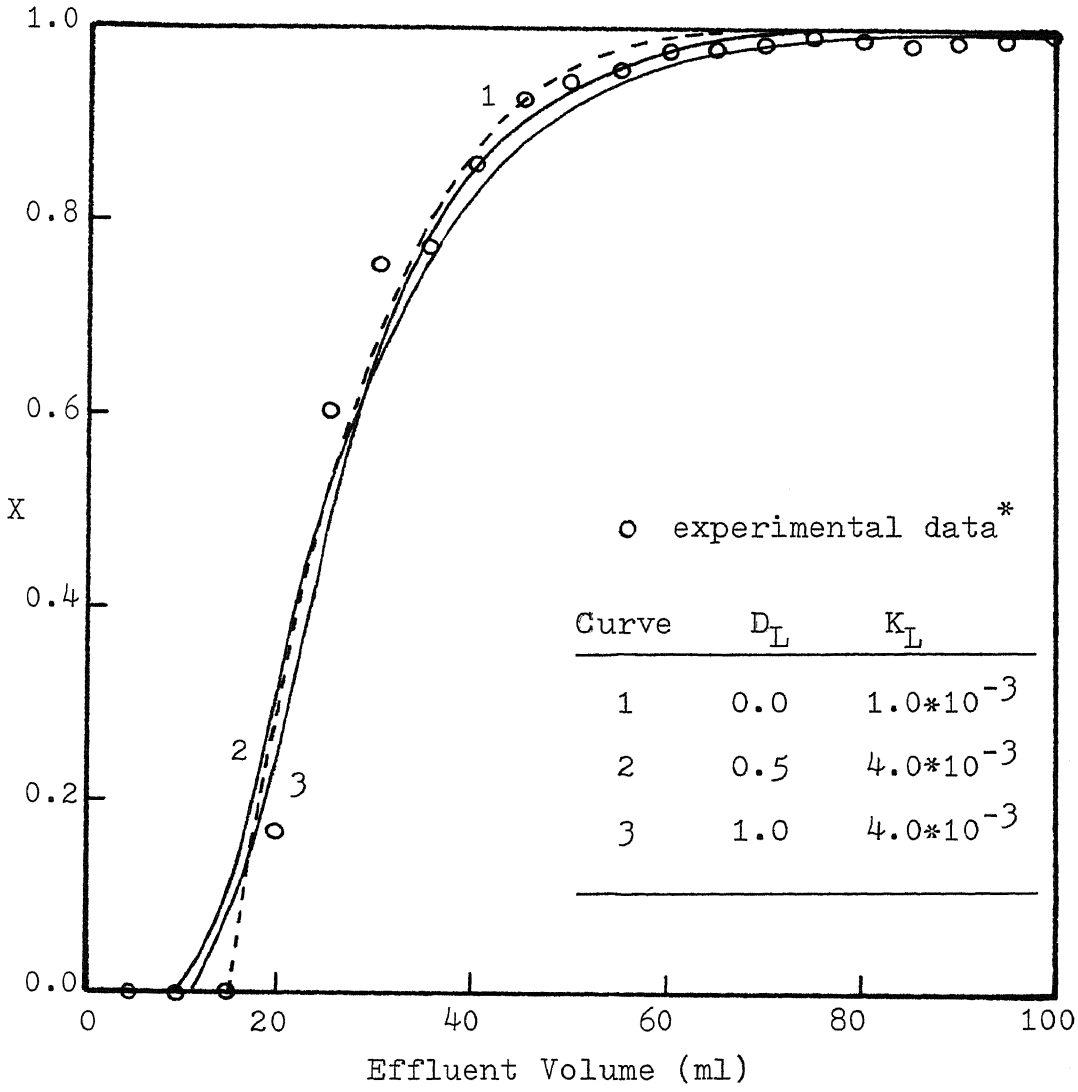

Figure 41. The verification of experimental breakthrough data with surface adsorption model
(Hemoglobin on CM-Sepharose at pH= 6.5)
Condition: Q=1.0, S=2.0, L=8.0, m=200.
ϵ=0.75. r_o= 50 μm

*Ref.(36)

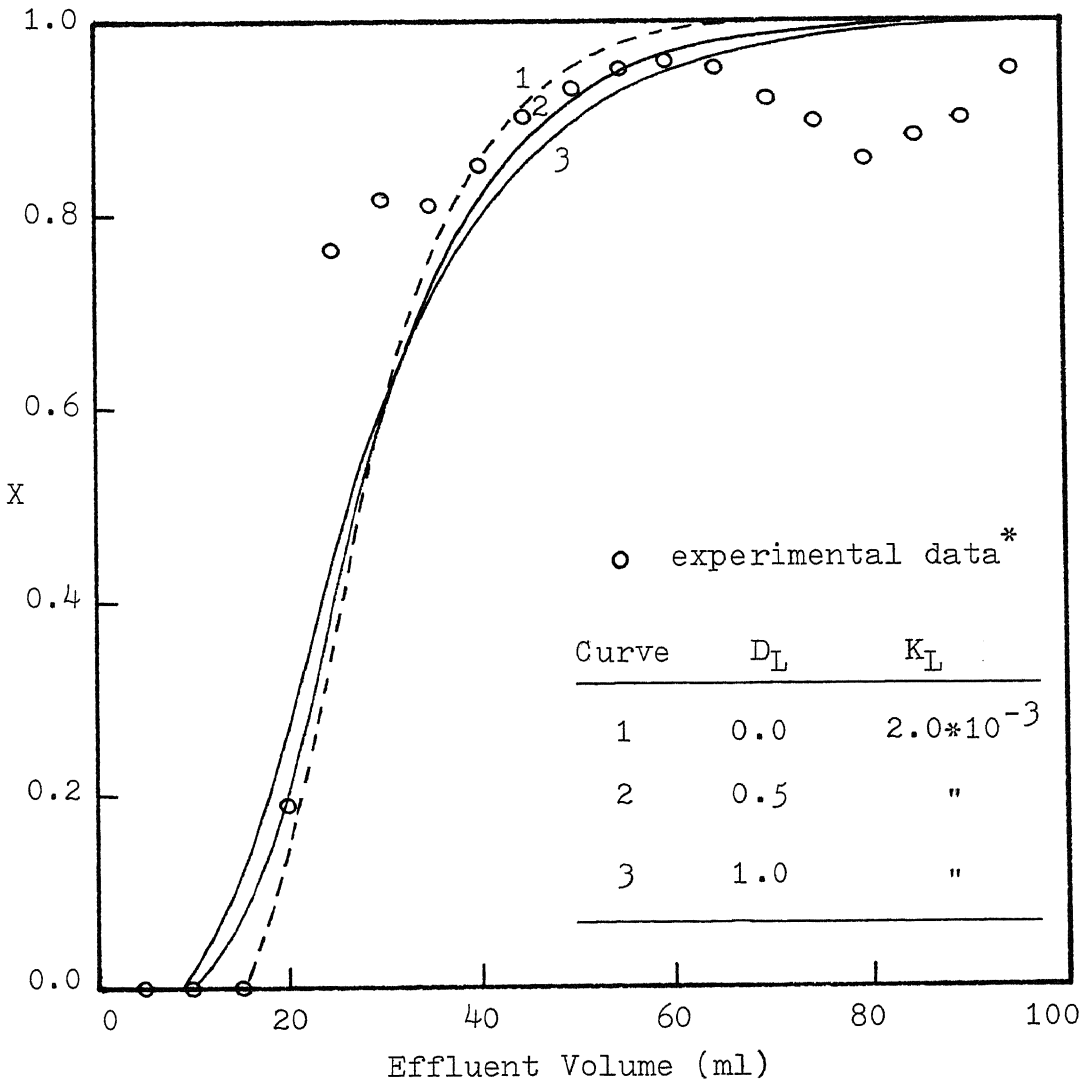

Figure 42. The verification of experimental breakthrough data with surface adsorption model (Albumin on DEAE-Sepharose at pH= 6.5)

Condition: Q=1.0, S=2.0, L=8.0, m=150.

ϵ=0.75, r_o= 50 μm

*Ref.(36)

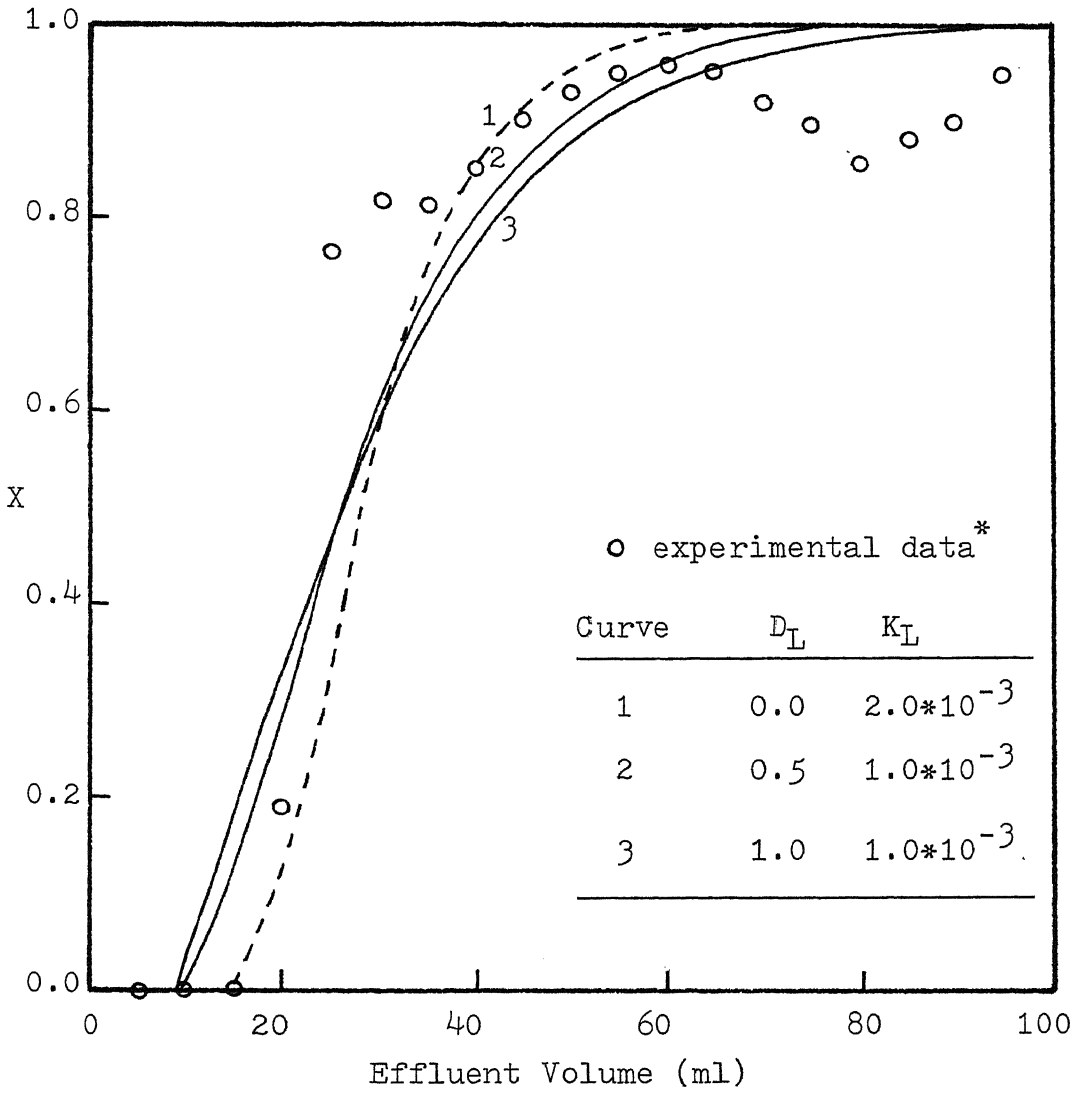

Figure 43. The verification of experimental breakthrough data with surface adsorption model (Albumin on DEAE-Sepharose at pH= 6.5)
Condition: Q=1.0, S=2.0, L=8.0, m=150.
ϵ=0.75, r_o= 50 μm

*Ref.(36)

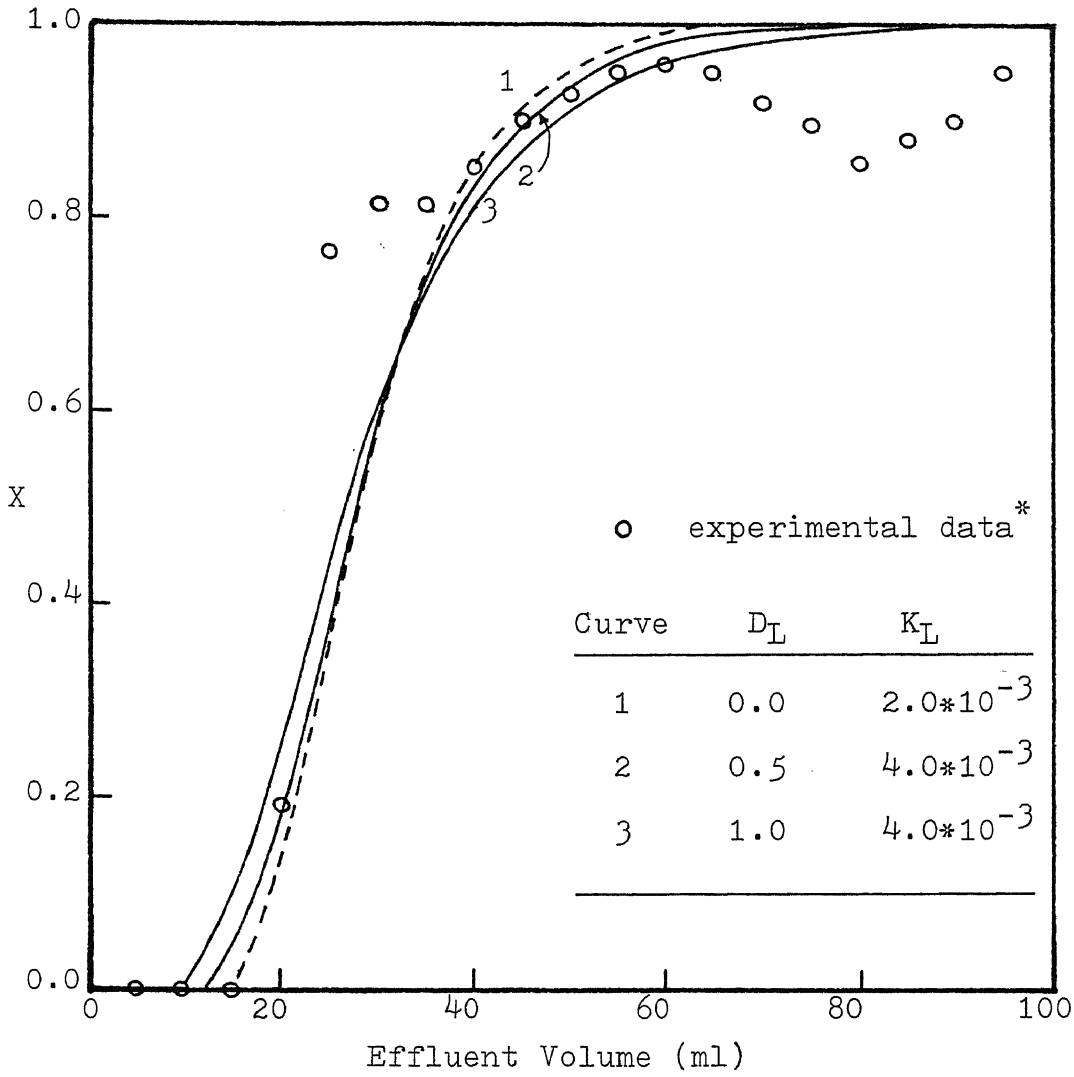

Figure 44. The verification of experimental breakthrough data with surface adsorption model (Albumin on DEAE-Sepharose at pH= 6.5)

Condition: Q=1.0, S=2.0, L=8.0, m=150.
ϵ=0.75, r_o= 50 μm

*Ref.(36)

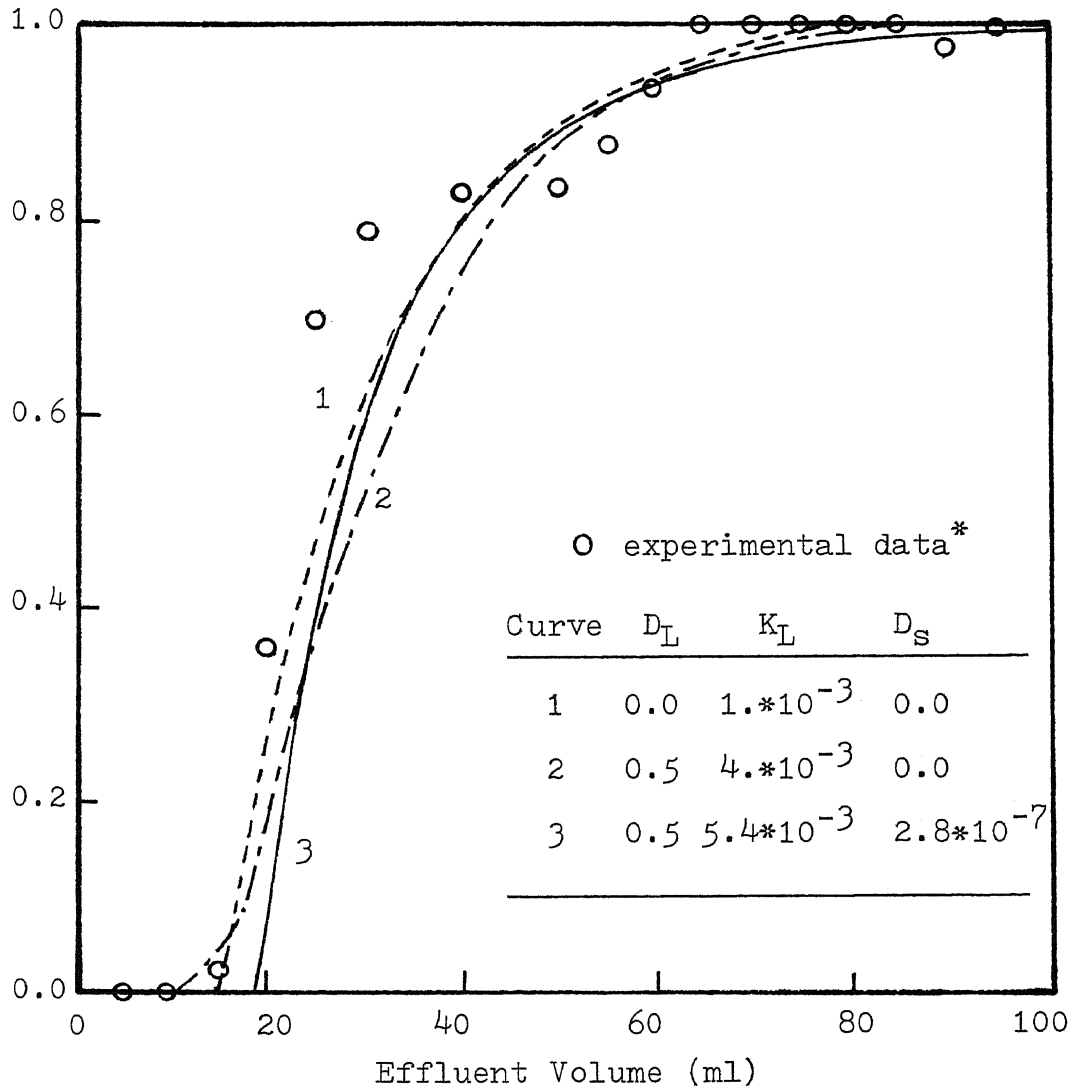

Figure 45. The verification of experimental breakthrough data with pore diffusion model(curve 3)
(Hemoglobin on CM-Sepharose at pH= 4.0)

Condition: Q=1.0, S=2.0, L=8.0, ϵ=0.75
λ=0.75(or mϵ/a=0.75), r_o= 50 μm

*Ref.(36)

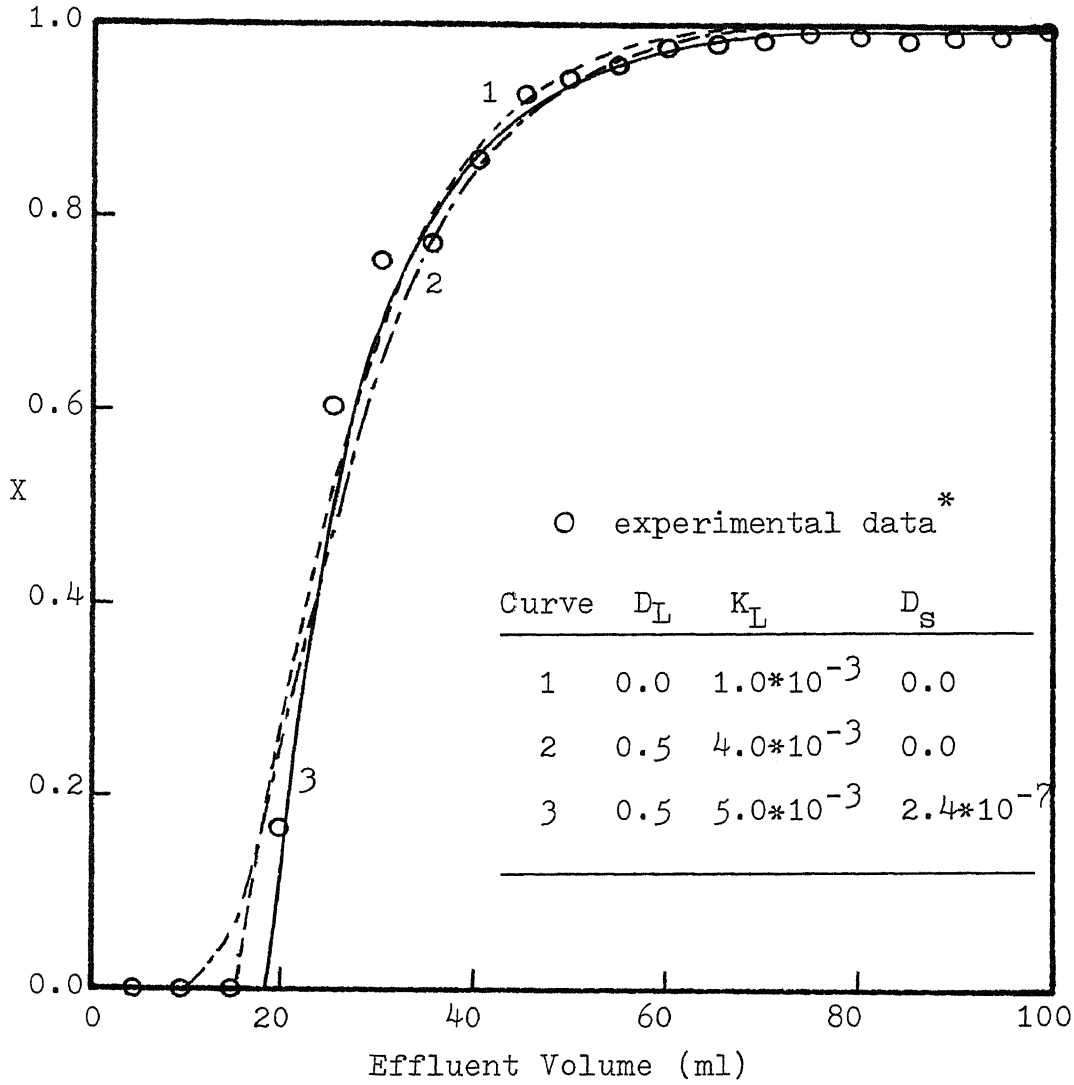

Figure 46. The verification of experimental breakthrough data with pore diffusion model(curve 3)
(Hemoglobin on CM-Sepharose at pH= 6.5)

Condition: Q=1.0, S=2.0, L=8.0, ϵ=0.75

λ=1.0(or mϵ/a=1.0), r_o= 50 μm.

*Ref.(36)

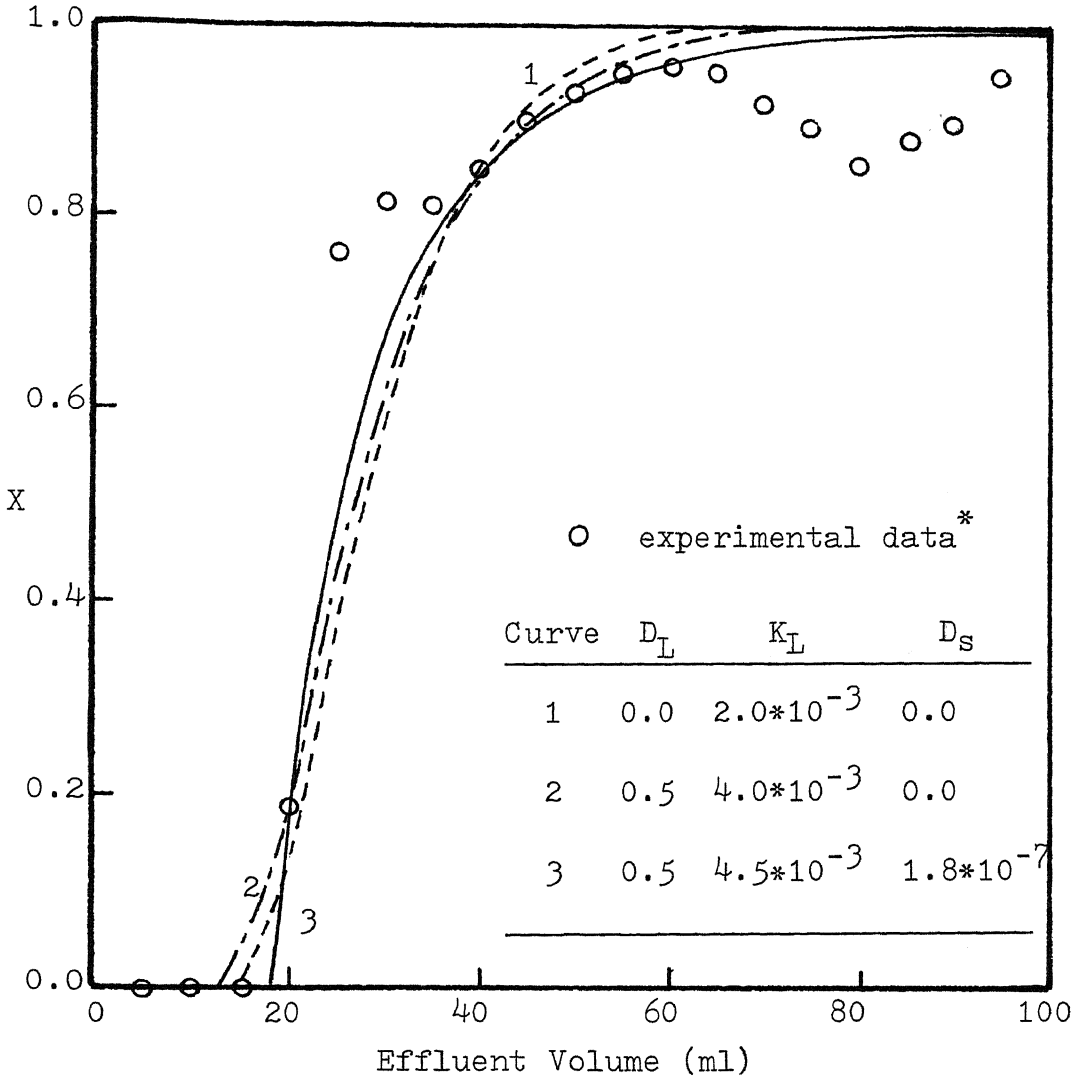

Figure 47. The verification of experimental breakthrough data with pore diffusion model(curve 3) (Albumin on DEAE-Sepharose at pH= 6.5)

Condition: Q=1.0, S=2.0, L=8.0, =0.75
λ=1.0(or mϵ/a=1.0), r_o= 50 μm.

*Ref.(36)

CHAPTER V

CONCLUSIONS AND RECOMMENDATIONS

Two adsorption models have been developed to simulate the unsteady state mass transfer behavior in a packed bed. One is called the surface adsorption model in which the significance of internal diffusion is neglected, and the adsorption process is assumed to be determined by external diffusion and surface adsorption. The other is called pore diffusion model in which the resistance of internal diffusion is considered as significant as that of external diffusion. In both models, the effect of axial dispersion in fluid phase was studied. A total of four cases have been solved analytically. The correlations developed for each case are summarized in Table 3.

A novel and rigorous approach by use of the conservation law was employed to set up the proper boundary conditions for adsorption models. Two different sets of boundary conditions were used in dispersion models; one set is specified by the continuity equation of adsorbate at the entrance of column (z=0), and the other set is characterized by the total material balance of adsorbate over the

Table 3

Summary of Adsorption Models

MODEL / EQUATION		SURFACE ADSORPTION MODEL		PORE DIFFUSION MODEL	
		SIMPLE MODEL (D_L=0)	DISPERSION MODEL	SIMPLE MODEL (D_L=0)	DISPERSION MODEL
Governing Equations	Fluid Phase	$\frac{\partial C_A}{\partial t} = -(\frac{v}{\epsilon})\frac{\partial C_A}{\partial z} - (\frac{K_L a}{\epsilon})(C_A - C_A^*)$	$+D_L \frac{\partial^2 C_A}{\partial z^2}$	$\frac{\partial C_A}{\partial t} = -(\frac{v}{\epsilon})\frac{\partial C_A}{\partial z} - (\frac{K_L a}{\epsilon})(C_A - C_A^*)$	$+D_L \frac{\partial^2 C_A}{\partial z^2}$
	Solid Phase	$\frac{\partial C_{As}}{\partial t} = K_L(C_A - C_A^*)$		$\frac{\partial C_s}{\partial t} = D_s(\frac{\partial^2 C_s}{\partial r^2} + \frac{2}{r}\frac{\partial C_s}{\partial r})$	
Equilibrium Relationship		$C_A^* = m\, C_{As}$		$C_A^* = \lambda\, C_s$	
Analytical Solution		EQ.(2A-22)	EQ.(2B-52)	EQ.(3A-52)	EQ.(3B-47)

entire column. The analytic solutions are presented in the form of breakthrough curves in terms of the variations of system parameters. Referring to the simulated results, it is concluded that:

(1) The adsorption capability can be enhanced by increasing the bed length, L or the cross-sectional area of column, S.

(2) The efficiency of adsorption column can be improved by decreasing the flow rate, Q or increasing the effective contact area, a.

(3) The progress of adsorption is sensitive to the mass transfer coefficient, K_L and the internal diffusivity, D_s. It is found that adsorption rate increases with increasing the mass transfer rate, $K_L a$ or the internal diffusion rate, D_s/r_o^2.

(4) The axial dispersivity does have an effect on the adsorption process; its effect is more significant at lower flow rate and is less noticeable as the flow rate is increased.

The proposed adsorption models were verified experimentally with the system of hemoglobin- albumin- CM sepharose and DEAE sepharose. It was shown that the theoretical predictions are in good agreement with the experimental data. Through the experimental verifications, the following recommendations are drawn:

(1) In this study, it is assumed that the pressure is constant and there is plug flow across the column. However, the pressure may not be constant and there exists some velocity gradient in most practical cases. Therefore, it is suggested that the parabolic type velocity profile should be used in further study.

(2) The equilibrium isotherm is assumed to be a linear relationship between the fluid phase and the solid phase in this study. The equilibrium isotherm is usually sensitive to the thermodynamic control variables such as pressure, temperature, ionic strength, electric field, pH, or affinity. It is found that the equilibrium isotherm may not be linear in some situations even at low concentration of adsorbate (17). Therefore, it is recommended to investigate the nonlinearity of equilibrium isotherm in further study.

APPENDICES

APPENDIX A

COMPUTER PROGRAM IN SEARCH OF EIGENVALUES OF FUNCTION: TAN $(X/2) = -2AX/(A^2 - X^2)$

APPENDIX A

COMPUTER PROGRAM IN SEARCH OF EIGENVALUES
OF FUNCTION: TAN (X/2) = -2AX/(A^2- X^2)

```
C     ****************************************
C     **                                    **
C     ** MATHEMATICAL SIMULATION OF PROTEINS **
C     **    SEPARATION IN A PACKED BED      **
C     **                                    **
C     ** THIS PROGRAM IS USING THE SECANT   **
C     ** METHOD TO SEARCH THE EIGENVALUES OF **
C     ** FUNCTION:                          **
C     **           TAN(X/2)= -2AX/(A*A-X*X)  **
C     **                                    **
C     ****************************************
      IMPLICIT REAL*8(A-H,O-Z)
      DATA A,MAX,ERROR/.1333333D2,60,1.D-10/
      PI=3.1415926D0
      EX=1.D-1
      STEP=PI*2.D0
      I=(A-STEP/2.D0)/STEP+1.D0
      I2=I+1
      I3=I2+1
      IN=1
C     *** THE FIRST ROOT IS X=0.D0 ***
      XO=PI+EX
      XS=(I-1)*STEP+XO
      IF(I.EQ.0)GO TO 19
      IF(I.GT.MAX) I=MAX
   90 DO 10 L=IN,I
      IF(L.GE.I3)XO=XS
      LL=L-IN
      DN=DFLOAT(LL)
      X1=DN*STEP+XO
      XF=X1+EX
      AO=F(X1)
      J=1
   93 BO=F(XF)
      N=1
      S=XF
      T=BO
    8 IF(AO*BO)2,2,4
    2 U=XF-BO*(XF-X1)/(BO-AO)
      N=N+1
      IF(DABS(U-XF)-ERROR)5,5,6
```

```
    6 X1=XF
      A0=B0
      XF=U
      B0=F(U)
      IF(N-400)2,2,5
    4 A0=T
      X1=S
      XF=X1+EX
      J=J+1
      GO TO 93
    5 WRITE(6,50)L,L,U
   50 FORMAT(5X,I3,5X,'BETA(',I3,')=',3X,D16.9)
   10 CONTINUE
      IF(I.GE.MAX)GO TO 30
   19 X0=A+EX
      IN=I2
      I=MAX
      GO TO 90
   30 STOP
      END
C
C     ---------------------------
C     THE EIGENFUNCTION :
C       TAN X = -2AX/(A*A-X*X)
C     ---------------------------
C
      FUNCTION F(X)
      IMPLICIT REAL*8(A-H,O-Z)
      DATA A/.1333333D2/
      F=DTAN(X/2.D0)+2.D0*A*X/(A*A-X*X)
      RETURN
      END
```

APPENDIX B

EXPERIMENTAL STUDY OF PROTEINS SEPARATION IN A PACKED COLUMN

APPENDIX B

EXPERIMENTAL STUDY OF PROTEINS SEPARATION IN A PACKED COLUMN

Preparation of Buffer Solutions

Two kinds of buffer solutions were used in the experiment and for preparing the feed solutions. One buffer employed is a mixture of acetic acid and sodium acetate; the other buffer is a mixture of tris(hydroxylmethyl)aminomethane ($C_4H_{11}NO_3$) and maleic acid (cis-HOOCCH=CHCOOH). The summarized procedures of buffers preparation are listed in Tables 4 and 5 for acetate buffer and Tris-maleate buffer respectively.

In the preparation, the selected amounts of each salt solution were combined to provide a buffer mixture at required pH level, and the NaCl solution was used to provide the needed ionic strength. For the acetate buffer at pH=4.0, the 0.10 M NaCl solution was used, and the 0.05 M NaCl solution was used for the Tris-maleate buffer at pH=6.5.

Preparation of Feed Solutions

Worthington human serum albumin and hemoglobin were selected for the experiment, some of their properties are shown in Table 6.

The feed solutions were prepared by mixing 0.02 wt% of

Table 4*

Preparation of Acetate Buffer

Stock Solutions:

A. 0.15 M solution of acetic acid.

B. 0.15 M solution of sodium acetate.

x ml. of A + y ml. of B, diluted to a total of 100 ml.

x	y	pH
46.3	3.7	3.6
44.0	6.0	3.8
41.0	9.0	4.0
36.8	13.2	4.2
30.5	19.5	4.4
25.5	24.5	4.6
20.0	30.0	4.8
14.8	35.2	5.0
10.5	39.5	5.2
8.8	41.2	5.4
4.8	45.2	5.6

*Reference: Colowick, S.P. and N.O. Kaplan, Methods in Enzymology, NY, Academic Press, p138 (1955).

Table 5*

Preparation of Tris-maleate Buffer

Stock Solutions:

A. 0.10 M solution of Tris acid maleate (12.1 g of tris(hydroxymethyl)aminomethane + 16.6 g of maleic acid).

B. 0.10 M NaOH.

50 ml. of A + x ml. of B, diluted to a total of 200 ml.

x	pH	x	pH
7.0	5.2	48.0	7.0
10.8	5.4	51.0	7.2
15.5	5.6	54.0	7.4
20.5	5.8	58.0	7.6
26.0	6.0	63.5	7.8
31.5	6.2	69.0	8.0
37.0	6.4	75.0	8.2
42.5	6.6	81.0	8.4
45.0	6.8	86.5	8.6

* Reference: Colowick, S.P. and N.O. Kaplan, Methods in Enzymology, NY, Academic Press (1955)

Table 6 (10)

Properties of Protein

Protein	M.W.	Isoelectric Point(pI)	Diffusivity in free solution (21)
Hemoglobin	63000	6.7	$7.6*10^{-7}$ cm^2/sec
Albumin	67000	4.7	$7.0*10^{-7}$ cm^2/sec

protein (hemoglobin or albumin) with the prepared buffer solutions, the corresponding concentration of protein in the feed solutions is almost equal to $1.0*10^{-5}$ M.

System Description

The experimental apparatus is shown in Figure 48. The column (1.6 cm ID and 40 cm length) was packed with CM-sepharose cation exchanger or DEAE- sepharose anion exchanger and ajusted the bed length to 8 cm. The system was maintained at a constant temperature of 288 °K by circulating the cooling water through the jacket of the packed column and the jacket of reservoir. The feed solution was introduced into the system from the bottom of column by a P-3 peristaltic pump (manufactured by Pharmacia Fine Chemicals). The effluent from the top of column was taken as samples. Throughout the experiment, the flow rate was set at 1.0 ml/min.

Samples were analyzed by the spectrophotometer (Bausch & Lomb spectronic 400-3). The concentration of hemoglobin was determined directly from the absorbance at a wavelength of 403 nm. The Bio-Rad protein assay was used to determine the total concentration of proteins from the absorbance at a wavelength of 595 nm. The concentration of albumin was then calculated as the difference between the total concentration of proteins and that of hemoglobin.

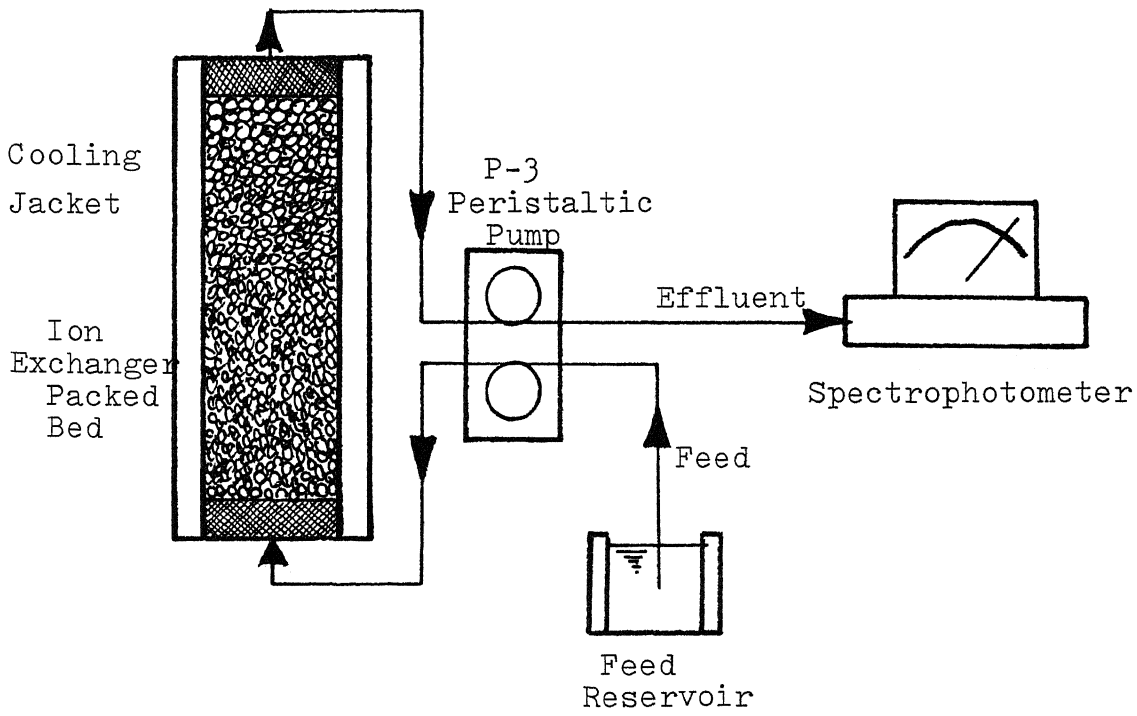

Figure 48. The Experimental Apparatus of Proteins Separations in A Packed Bed

APPENDIX C

COMPUTER PROGRAM FOR THE CALCULATION OF BREAKTHROUGH CURVES BASED ON EQ. (2A-22)

APPENDIX C

COMPUTER GROGRAM FOR THE CALCULATION OF
BREAKTHROUGH CURVES BASED ON EQ.(2A-22)

```
C     ****************************************
C     **                                    **
C     ** MATHEMATICAL SIMULATION OF PROTEINS **
C     **    SEPARATION IN A PACKED BED      **
C     **                                    **
C     **          SURFACE ADSORPTION        **
C     **      SIMPLE MODEL: STEP INPUT      **
C     **                                    **
C     ****************************************
C
      IMPLICIT REAL*8(A-H,O-Z)
      DIMENSION H(25),X(501),TAP(501),TH(501),F1(501)
      DIMENSION F2(501),F3(501),HF(501),SUM(501)
      DIMENSION TSUM(501),VOL(501)
C
C     INPUT THE DATA, MASS TRANSFER COEFFICIENT KL,
C     INTERFACIAL CONTACT AREA A, VOID FRACTION E, AREA
C     BASED EQUILIBRIUM CONSTANT M,BED LENGTH L, VOLU-
C     METRIC FLOW RATE Q, CROSS-SECTIONAL AREA S,
C     ELAPSED TIME T
C
      DATA FK,SA,EPS,SM,Z/2.D-3,2.D2,.75D0,3.D2,.8D1/
      DATA Q,S,T/1.D0,2.D0,1.8D2/
C
C     DEFINE THE DIMENSIONLESS TIME TAU, DISTANCE
C     ZETA AND EVALUATE EFFECTIVE TIME TP,
C     DISTRIBUTION RATIO GAMMA
C
      TP=T-(Z*EPS*S)/Q
      TAU=TP*FK*SM
      ZETA=(Z*S*FK*SA)/Q
      GAMA=SM*EPS/SA
      WRITE(6,79)
   79 FORMAT(10X,'***  SURFACE ADSORPTION ***',/10X,
     $'THE SOLUTION IS FOR SIMPLE MODEL: STEP INPUT')
      WRITE(6,80)TP,TAU,ZETA,GAMA
   80 FORMAT(/,10X,'   TP=',D13.6,/10X,'  TAU=',D13.6,
     $/10X,' ZETA=',D13.6,/7X,'*** GAMA=',D13.6,/)
```

```
      WRITE(6,100)
  100 FORMAT(1H,8X,'EFFL VOL',6X,'TIME,MIN',3X,
     $'STEP CHANGE X(T)',5X,'SOLID CONCN')
C
C     DIVIDE THE DIMENSIONLESS TIME INTO 50 INTERVALS
C
      H(1)=1.D0
      DO 10 I=2,15
   10 H(I)=H(I-1)*I
      DT=TAU/5.D2
      DO 20 J=1,501
      X(J)=(J-1)*DT
      TAP(J)=X(J)/SM/FK
      TH(J)=TAP(J)+(Z*EPS*S)/Q
      VOL(J)=Q*TH(J)
      E1=X(J)+ZETA
      F1(J)=DEXP(-E1)
      E2=X(J)*ZETA*4.D0
      F2(J)=DSQRT(E2)
C
C     EVALUATE THE MODIFIED BESSEL FUNCTION IO(X)
C
      SUM1=1.D0
      K=1
   30 KK=K*2
      SUM1=SUM1+((F2(J)/2.D0)**KK)/(H(K)**2.D0)
      K=K+1
      IF(K-15)30,30,40
   40 F3(J)=SUM1
      HF(J)=F1(J)*F3(J)
   20 CONTINUE
C
C     EVALUATE THE INTEGRAL TERM FOR CONCENTRATION
C     PROFILE
C
      SUM(1)=0.D0
      TSUM(1)=HF(1)+SUM(1)
      DO 60 L=2,501
      SUM(L)=SUM(L-1)+DT*((HF(L)+HF(L-1))/2.D0)
      TSUM(L)=HF(L)+SUM(L)
   60 CONTINUE
C
C     PRINT OUT THE LIQUID CONCENTRATION TSUM AND
C     SOLID CONCENTRATION SUM
C
      WRITE(6,200)(J,VOL(J),TH(J),TSUM(J),SUM(J),
     $J=1,501,25)
  200 FORMAT(I4,2X,D12.5,2X,D12.5,2X,D15.8,3X,D15.8)
      STOP
      END
```

APPENDIX D

COMPUTER PROGRAM FOR THE CALCULATION OF BREAKTHROUGH CURVES BASED ON EQ.(2B-52)

APPENDIX D

COMPUTER PROGRAM FOR THE CALCULATION OF
BREAKTHROUGH CURVES BASED ON EQ.(2B-52)

```
C     ****************************************
C     **                                    **
C     ** MATHEMATICAL SIMULATION OF PROTEINS **
C     **    SEPARATION IN A PACKED BED      **
C     **                                    **
C     **          SURFACE ADSORPTION        **
C     **       DISPERSION MODEL: STEP INPUT **
C     **                                    **
C     ****************************************
      IMPLICIT REAL*8(A-H,O-Z)
      DIMENSION SN1(200),SN2(200),VA(200),VB(200),
     $TM(500),VOL(500),TAU(500),X(500),XSTEP(500)
C
C     INPUT THE DATA: VOLUMETRIC FLOW RATE Q,
C     CROSS-SECTIONAL AREA OF COLUMN S, VOID
C     FRACTION E, AXIAL DISPERSIVITY DL, BED
C     LENGTH L, AREA BASED EQUILIBRIUM CONSTANT
C     M, CONTACT AREA A, MASS TRANSFER COEFF. KL
C
      DATA Q,R,EPS,ED/.25D0,2.D0,.75D0,1.D0/
      DATA H,SM,SA,FK/1.D1,3.D2,4.D2,3.D-4/
      DATA PI,EX,ERROR/3.1415926D0,1.D-1,1.D-10/
      DATA MAX,MT,DT/180,200,2.D0/
C
C     DEFINE THE DIMENSIONLESS PARAMETERS, A,
C     PELECT NUMBER PEL, ALPHA, AND GAMA
C
      A=Q*H/(R*EPS*ED)
      PEL=Q*H/(R*ED)
      ALPHA=FK*SA*H*H/(EPS*ED)
      GAMA=SM*EPS/SA
      WRITE(6,49)FK,ED,H,PEL,ALPHA,GAMA
   49 FORMAT(/,10X,'FK=',D13.6,/10X,'ED=',D13.6,/
     $10X,'H=',D13.6,/10X,'** PELECT NUMBER=',D13.6,
     $/10X,'ALPHA=',DD13.6,/10X,'GAMA=',D13.6)
      ET=A/2.D0
      STEP=PI*2.D0
      I=(A-STEP/2.D0)/STEP+1.D0
      I2=I+1
      I3=I2+1
      IN=1
```

```
      WRITE(6,55)I,A,SM,SA,R
   55 FORMAT(/,10X,'I=',I5,/10X,'A=',D15.7,/10X,'SM=',
     $D15.7,/10X,'SA=',D15.7,/10X,'R=',D15.7)
      WRITE(6,60)
   60 FORMAT(3X,'L=',2X,'N=',4X,'J=',4X,'BETA(L)=',
     $8X,'SN1(L)=',9X,'SN2(L)=',/35X,'VA(L)=',10X,
     $'VB(L)=')
C
C     ------------------------------------------
C     BY USING THE SECANT METHOD TO SEARCH THE
C     EIGENVALUES OF FUNCTION:
C              TAN(X/2)= -2AX/(A*A-X*X)
C     AND THEN CALCULATE THE VALUES PK OR SN
C     ------------------------------------------
C
C     *** THE FIRST ROOT IS X=0.D0 ***
      X0=PI+EX
      XS=(I-1)*STEP+X0
      IF(I.EQ.0)GO TO 19
      IF(I.GT.MAX) I=MAX
   90 DO 10 L=IN,I
      IF(L.GE.I3)X0=XS
      LL=L-IN
      DN=DFLOAT(LL)
      X1=DN*STEP+X0
      XF=X1+EX
      A0=F(X1)
      J=1
   93 B0=F(XF)
      N=1
      S=XF
      T=B0
    8 IF(A0*B0)2,2,4
    2 U=XF-B0*(XF-X1)/(B0-A0)
      N=N+1
      IF(DABS(U-XF)-ERROR)5,5,6
    6 X1=XF
      A0=B0
      XF=U
      B0=F(U)
      IF(N-400)2,2,5
    4 A0=T
      X1=S
      XF=X1+EX
      J=J+1
      GO TO 93
    5 PHI=(A*A+U*U)/4.D0
```

```
C
C     ----------------------------------------
C     BY USING THE EIGENVALUES U`S TO
C     EVALUATE THE VALUES AT POLES SN`S
C     AND THE CORRESPONDING FUNCTION VA&VB
C     ----------------------------------------
C
      P=ALPHA*(GAMA+1.D0)+PHI
      QC=PHI*ALPHA*GAMA
      SN1(L)=(-P+DSQRT(P*P-4.D0*QC))/2.D0
      SN2(L)=(-P-DSQRT(P*P-4.D0*QC))/2.D0
      AG=ALPHA*GAMA
      DEL11=1.D0+(ALPHA*AG)/((SN1(L)+AG)**2.D0)
      DEL21=1.D0+(ALPHA*AG)/((SN2(L)+AG)**2.D0)
      COFF1=(A*A-U*U)/(2.D0*A*U)
      COFF2=(A*A+U*U+A*U*U)/(A*U*U)
      DEL2=COFF1*DCOS(U/2.D0)-COFF2*DSIN(U/2.D0)
      VA(L)=U/(SN1(L)*DEL11*DEL2)
      VB(L)=U/(SN2(L)*DEL21*DEL2)
      WRITE(6,50)L,N,J,U,SN1(L),SN2(L),VA(L),VB(L)
   50 FORMAT(1X,2(1X,I3),3X,I3,3(3X,D13.6)/31X,
     $2(3X,D13.6))
   10 CONTINUE
      IF(I.GE.MAX)GO TO 30
   19 X0=A+EX
      IN=I2
      I=MAX
      GO TO 90
C
C     ----------------------------------------
C     THE CALCULATION OF BREAKTHROUGH CURVE
C     ----------------------------------------
C
   30 WRITE(6,31)
   31 FORMAT(//,9X,'EFFL VOL',7X,'TIME,MIN',8X,
     $'TIME,TAU',6X,'STEP CHANGE X(T)')
      DO 20 L1=1,MT
      DL=DFLOAT(L1)
      TM(L1)=DL*DT
      VOL(L1)=Q*TM(L1)
      TAU(L1)=TM(L1)*ED/H/H
      SUMA=0.D0
      SUMB=0.D0
      DO 40 K=1,MAX
      SNT1=SN1(K)*TAU(L1)+ET
      IF(SNT1.LE.-1.7D2)GO TO 35
      SUMA=SUMA+VA(K)*DEXP(SNT1)
   35 SNT2=SN2(K)*TAU(L1)+ET
      IF(SNT2.LE.-1.7D2)GO TO 45
      SUMB=SUMB+VB(K)*DEXP(SNT2)
   40 CONTINUE
   45 SUM=SUMA+SUMB
      X(L1)=1.D0-SUM
```

```
      IF(X(L1).LE. 0.D0) X(L1)=0.D0
      WRITE(6,70)L1,VOL(L1),TM(L1),TAU(L1),X(L1)
   70 FORMAT(1X,I4,2(3X,D12.5),2(3X,D15.8))
   20 CONTINUE
      STOP
      END
C
C     ----------------------------------------
C     THE EIGENFUCTION:
C               TAN(X/2)= -2AX/(A*A-X*X)
C     ----------------------------------------
C
      FUNCTION F(X)
      IMPLICIT REAL*8(A-H,O-Z)
      DATA Q,R,EPS,ED/.25D0,2.D0,.75D0,1.D0/
      DATA H/1.D1/
      A=Q*H/(R*EPS*ED)
      F=DTAN(X/2.D0)+2.D0*A*X/(A*A-X*X)
      RETURN
      END
```

APPENDIX E

COMPUTER PROGRAM FOR THE CALCULATION OF BREAKTHROUGH CURVES BASED ON EQ. (3B-47)

APPENDIX E

COMPUTER PROGRAM FOR THE CALCULATION OF BREAKTHROUGH CURVES BASED ON EQ.(3B-47)

```
C     ****************************************
C     **                                    **
C     ** MATHEMATICAL SIMULATION OF PROTEINS **
C     **    SEPARATION IN A PACKED BED      **
C     **                                    **
C     **          DIFFUSION IN PORES        **
C     **     DISPERSION MODEL: STEP INPUT   **
C     **                                    **
C     ****************************************
      IMPLICIT REAL*8(A-H,O-Z)
      DIMENSION BETA(180),SUMA(180),SN(180,20)
      DIMENSION RT(180,20),VA(180,20),VB(180,20)
      DIMENSION TM(500),TAU(500),VOL(500),X(500)
C
C     INPUT THE DATA: VOLUMETRIC FLOW RATE Q, CROSS
C     SECTIONAL AREA OF COLUMN S, VOID FRACTION
C     E, AXIAL DISPERSIVITY DL, BED LENGTH L,
C     VOLUME BASED EQUILIBRIUM CONSTANT LAMDA,
C     MASS TRANSFER COEFFICIENT KL, RADIUS OF
C     RESIN PARTICLE RO, INTERNAL DIFFUSIVITY DS
C
      DATA Q,R,EPS,ED/1.D0,2.D0,.75D0,.5D0/
      DATA H,SM,FK/8.D0,1.D0,5.D-3/
      DATA PI,EXX,ERROR/3.1416D0,1.D-2,1.D-10/
      DATA MAX,MIN,MT,EX,DT/80,20,100,1.D-1,2.D0/
      DATA RP,SD/5.D-3,2.4D-7/
C
C     DEFINE THE DIMENSIONLESS PARAMETER: A,
C     PELECT NUMBER, CONTACT AREA SA, THETA,
C     PSI, BIOT NUMBER BI
C
      A=Q*H/(R*EPS*ED)
      PEL=Q*H/(R*ED)
      SA=3.D0*(1.D0-EPS)/RP
      THETA=(Q*RP*RP)/(EPS*R*H*SD)
      PSI=(FK*SA*RP*RP)/(EPS*SD)
      BI=FK*RP/SD
      WRITE(6,49)FK,SA,H,SD,RP,PEL,THETA,SM,BI,PSI
   49 FORMAT(/,10X,'FK=',D13.6,/10X,'SA=',D13.6,/10X,
     $' H=',D13.6,/10X,'SD=',D13.6,/10X,'RP=',D13.6,
     $/10X,'*** PELECT NUMBER=',D13.6,/10X,'THETA=',
     $D13.6,/10X,'SM=',D13.6,/10X,'*** BIOT NUMBER=',
     $D13.6,/10X,'*** COMPETITION PARAMETER=',D13.6)
```

```
      ET=A/2.D0
      STEP=PI*2.D0
      I=(A-STEP/2.D0)/STEP+1.D0
      I2=I+1
      I3=I2+1
      IN=1
      WRITE(6,55)I,A
   55 FORMAT(/,10X,'I=',I5,/10X,'A=',D15.7,////)
C
C     ----------------------------------------
C     BY USING THE SECANT TO SEARCH THE
C     EIGENVALUES OF FIRST EIGENFUNCTION:
C            TAN(X/2)= -2AX(A*A-X*X)
C     ----------------------------------------
C
      XO=PI+EX
      XS=(I-1)*STEP+XO
      IF(I.EQ.0) GO TO 19
      IF(I.GT.MAX) I=MAX
   90 DO 10 L=IN,I
      IF(L.EQ.I3) XO=XS
      LL=L-IN
      DN=DFLOAT(LL)
      X1=DN*STEP+XO
      XF=X1+EX
      AO=F(X1)
      J=1
   93 BO=F(XF)
      N=1
      S=XF
      T=BO
    8 IF(AO*BO)2,2,4
    2 U=XF-BO*(XF-X1)/(BO-AO)
      N=N+1
      IF(DABS(U-XF)-ERROR)5,5,6
    6 X1=XF
      AO=BO
      XF=U
      BO=F(U)
      IF(N-400)2,2,5
    4 AO=T
      X1=S
      XF=X1+EX
      J=J+1
      GO TO 93
    5 BETA(L)=U
      COEF1=(A*U*U+A*A+U*U)/(A*U)
      COEF2=(A*A-U*U)/(2.D0*A)
      DEL=COEF1*DSIN(U/2.D0)-COEF2*DCOS(U/2.D0)
      PHI=(A*A+U*U)/4.D0
```

```
C
C     ----------------------------------------
C     BY USING THE EIGENVALUES OBTAINED FROM
C     FIRST EIGENFUNCTION TO EVALUATE THE
C     EIGENVALUES OF SECOND EIGENFUNCTION:
C
C                       - S(S*S-PHI-PSI)
C       TAN (S) = -------------------------
C                 (S*S-PHI)(SM*BI-1)+PSI
C     ----------------------------------------
C
      WC=(PHI*THETA/A)-(PSI/(SM*BI-1.D0))
      IF(WC.EQ.0.D0) GO TO 299
      WC=DABS(WC)
      WH=DSQRT(WC)
      IH=(WH-PI/2.D0)/PI+1.D0
      IH1=IH+1
      IH2=IH+2
      IHN=1
      XH0=PI/2.D0+EXX
      XHS=(IH-1)*PI+XH0
      IF(IH.EQ.0) GO TO 69
      IF(IH.GT.MIN) IH=MIN
  140 DO 110 M=IHN,IH
      IF(M.GE.IH2) XH0=XHS
      MH=M-IHN
      DM=DFLOAT(MH)
      XH1=DM*PI+XH0
      XHF=XH1+EX
      AH0=RF(XH1,U)
      JH=1
  143 BH0=RF(XHF,U)
      NH=1
      SH=XHF
      TH=BH0
   58 IF(AH0*BH0)52,52,54
   52 RU=XHF-BH0*(XHF-XH1)/(BH0-AH0)
      NH=NH+1
      IF(DABS(RU-XHF)-ERROR)65,65,66
   66 XH1=XHF
      AH0=BH0
      XHF=RU
      BH0=RF(RU,U)
      IF(NH-400)52,52,65
   54 AH0=TH
      XH1=SH
      XHF=XH1+EX
      JH=JH+1
      GO TO 143
```

```
   65 RT(L,M)=RU
      SN(L,M)=RU*RU
      VA(L,M)=DF(RU)
      VB(L,M)=(U*U)/(RU*RU*DEL*DF(RU))
  110 CONTINUE
      IF(IH.GE.MIN) GO TO 120
   69 XH0=WH+EXX
      IHN=IH1
      IH=MIN
      GO TO 140
  120 WRITE(6,50)L,L,BETA(L),(SN(L,M),M=1,5),
     $(VA(L,M),M=1,5),(VB(L,M),M=1,5)
   50 FORMAT(1X,I3,2X,'EIGENVALUE (',I3,') =',2X,D13.6,
     $/19X,'*****     ROOTS... 5 TERMS     *****'/1X,
     $5(1X,D13.6),/1X,5(1X,D13.6),/1X,5(1X,D13.6))
   10 CONTINUE
      IF(I.GE.MAX) GO TO 30
   19 X0=A+EX
      IN=I2
      I=MAX
      GO TO 90
  299 WRITE(6,300)
  300 FORMAT(//,5X,' **** THE SYSTEM IS WRONG *** ',//)
C
C     ----------------------------------------
C     THE CALCULATION OF BREAKTHROUGH CURVE
C     ----------------------------------------
C
   30 WRITE(6,35)
   35 FORMAT(//10X,'EFFL VOL',7X,'TIME MIN',8X,'TIME,TAU',
     $7X,'STEP CHANGE X(T)')
      DO 20 L1=1,MT
      DL=DFLOAT(L1)
      TM(L1)=DL*DT
      TAU(L1)=TM(L1)*SD/(RP*RP)
      VOL(L1)=Q*TM(L1)
      SUM=0.D0
      DO 40 K=1,MAX
      SUMB=0.D0
      DO 41 KK=1,MIN
      SNT=ET-(SN(K,KK)*TAU(L1))
      IF(SNT.LT.-1.D2) GO TO 45
      IF(DABS(VB(K,KK)).LE.ERROR) GO TO 45
      SUMB=SUMB+VB(K,KK)*DEXP(SNT)
   41 CONTINUE
   45 SUMA(K)=SUMB
      IF(SUMB-ERROR) 47,47,46
   46 SUM=SUM+SUMA(K)
   40 CONTINUE
   47 X(L1)=1.D0-SUM
```

```
      IF(X(L1).LE. 0.D0) X(L1)=0.D0
      WRITE(6,70)L1,VOL(L1),TM(L1),TAU(L1),X(L1)
   70 FORMAT(1X,I4,2(3X,D12.5),2(3X,D15.8))
   20 CONTINUE
      STOP
      END
C
C     ----------------------------------------
C     THE FIRST EIGENFUNCTION:
C          TAN(X/2)= -2AX(A*A-X*X)
C     ----------------------------------------
C
      FUNCTION F(X)
      IMPLICIT REAL*8(A-H,O-Z)
      DATA Q,R,EPS,ED/1.D0,2.D0,.75D0,.5D0/
      DATA H/8.D0/
      A=Q*H/(R*EPS*ED)
      F=DTAN(X/2.D0)+2.D0*A*X/(A*A-X*X)
      RETURN
      END



C
C     ----------------------------------------
C     THE SECOND EIGENFUNCTION:
C
C                    - S(S*S-PHI-PSI)
C       TAN (S) = ---------------------------
C                 (S*S-PHI)(SM*BI-1)+PSI
C     ----------------------------------------
C
      FUNCTION RF(YO,XU)
      IMPLICIT REAL*8(A-H,O-Z)
      DATA Q,R,EPS,ED/1.D0,2.D0,.75D0,.5D0/
      DATA H,SM,FK/8.D0,1.D0,5.D-3/
      DATA RP,SD/5.D-3,2.4D-7/
      A=Q*H/(R*EPS*ED)
      SA=(1.D0-EPS)*3.D0/RP
      THETA=(Q*RP*RP)/(EPS*R*H*SD)
      PSI=(FK*SA*RP*RP)/(EPS*SD)
      BI=FK*RP/SD
      PHIN=(A*A+XU*XU)/4.D0
      CH1=YO*(YO*YO-(PHIN*THETA/A)-PSI)
      CH2=(YO*YO-(PHIN*THETA/A))*(SM*BI-1.D0)+PSI
      RF=CH2*DTAN(YO)+CH1
      RETURN
      END
```

```
C
C     ----------------------------------------
C     THE DIFFERENTIATION OF CHARACTERISTIC
C     EQUATION:
C                  F(P)= (A*A+U*U)/4
C     ----------------------------------------
C
      FUNCTION DF(YO)
      IMPLICIT REAL*8(A-H,O-Z)
      DATA Q,R,EPS,ED/1.D0,2.D0,.75D0,.5D0/
      DATA H,SM,FK/8.D0,1.D0,5.D-3/
      DATA RP,SD/5.D-3,2.4D-7/
      SA=(1.D0-EPS)*3.D0/RP
      A=Q*H/(R*EPS*ED)
      THETA=(Q*RP*RP)/(EPS*R*H*SD)
      PSI=(FK*SA*RP*RP)/(EPS*SD)
      BI=FK*RP/SD
      Y2=YO*DCOS(YO)+(SM*BI-1.D0)*DSIN(YO)
      YB=DCOS(YO)
      YD=PSI*SM*BI/2.D0
      YF=DSIN(YO)
      TERM=((YF*YF+YB*YB)-(YF*YB/YO))*YD/Y2/Y2
      DF=A*(1.D0+TERM)/THETA
      RETURN
      END
```

NOMENCLATURE

A = dimensionless parameter = $vL/\epsilon D_L$

a = effective contact area = $3(1-\epsilon)/r_o$, cm^2/cm^3

B = dimensionless parameter = $K_L aL/v$

B_i = Biot number = $K_L r_o/D_s$, dimensionless

C_A = local concentration of adsorbate in fluid phase, g-mole/ cc

C_{Ao} = step input in concentration of adsorbate, g-mole/ cc,min

C_A^* = equilibrium concentration of adsorbate in fluid phase, g-mole/ cc

C_{As} = local concentration of adsorbate on solid phase, g-mole/ cm^2

C_s = local concentration of adsorbate in solid phase, g-mole/ cm^3

d_p = diameter of solid particle, cm

D_L = effective axial dispersivity of adsorbate in fluid phase, $cm^2/$ min

D_s = effective internal diffusivity of adsorbate in solid phase, $cm^2/$ min

F = a function of p

K_L = effective mass transfer coefficient of adsorbate in fluid phase, cm/ min

L = bed length, cm

m = area based equilibrium constant, cm^2/cm^3

N_{Ar} = mass flux of adsorbate A in r-direction within solid particle, g-mole/ cm^2,min

p = image of Laplace transformation, dimensionless

Q = superfacial flow rate, cc/ min

r = radial distance from the center of solid particle, cm

r_o = radius of solid particle, cm

R = dimensionless radial distance from the center of the solid particle

S = cross-sectional area of column, cm^2

t = elapsed time, min

$U(t)$ = step function in time, min

v = superfacial fluid velocity, cm/ min

X = dimensionless local concentration of adsorbate in fluid phase

X^* = dimensionless equilibrium concentration of adsorbate in fluid phase

Y = dimensionless local concentration of adsorbate in solid phase

Y_s = dimensionless local concentration of adsorbate on solid phase

z = distance in the flow direction, cm

Greek Letters

ϵ = void fraction of the packed bed, dimensionless

η = dimensionless distance in flow direction

α = dimensionless parameter = $K_L a L^2/\epsilon D_L$

β_n = eigenvalues of function $\tan(x/2)=-2Ax/(A^2- x^2)$

γ = distribution ratio = $m\epsilon/a$, dimensionless

$_n$ = eigenvalues of function $\tanh(x/2)=-2Ax/(A^2- x^2)$

τ = dimensionless time

ω = film resistance parameter = $K_L a r_o^2/\epsilon D_s$, dimensionless

θ = bed length parameter = $v r_o^2/\epsilon L D_s$, dimensionless

λ = volume based equilibrium constant, dimensionless

Φ, Φ_n = dimensionless parameter = $(A^2 + \beta_n^2)/4$

REFERENCES

REFERENCES

1. Bird, R.B., W.E. Stewart, and E.N. Lightfoot, Transport Phenomena, John Wiley & Sons Inc., NY, 702 (1960).

2. Broughton, D.B., "Molex: Case History of a Process," Chem. Eng. Prog., 64(8), 60 (1968).

3. Broughton, D.B., J.M. Neuzil, J.M. Pharis, and C.S. Brearley, "The Parex Process for Recovering Paraxylene," Chem. Eng. Prog., 66(9), 70 (1970).

4. Brown, P.R. High Pressure Liquid Chromatography, Academic Press, NY (1973).

5. Chao, J.F., J.J. Huang, and C.R. Huang, "Continuous Multiaffinity Separation of Proteins: Cyclic Processes," AIChE Symp. Ser., 78(219), 39 (1982).

6. Chao, R. and H.E. Hoelscher, "Simultaneous Axial Dispersion and Adsorption in A Packed Bed," AIChE J., 12 (2), 271 (1966).

7. Chen, H.T., T.K. Hsieh, H.C. Lee, and F.B. Hill, "Separation of Proteins via Semicontinuous pH Parametric Pumping," AIChE J., 23, 695 (1977).

8. Chen, H.T., Y.W. Wong, and S. Wu, "Continuous Fractionation of Protein Mixtures by pH Parametric Pumping," AIChE J., 25(2), 320 (1979).

9. Chen, H.T., U. Panchareon, W.T. Yang, C.O. Kerobo, and R.J. Parisi, "Separation of Proteins via pH Parametric Pumping," Sep. Sci. & Tech., 15(6), 1377 (1980).

10. Chen, H.T., W.T. Yang, U. Panchareon, and R.J. Parisi, "Separation of Proteins via Multicolumn pH Parametric Pumping," AIChE J., 26(5), 839 (1980).

11. Chen, H.T., Z.M. Ahmed, and V. Rollan, "Parametric Pumping with pH and Ionic Strength: Enzyme Purification," I&EC Fundamentals, 20, 171 (1981).

12. Chen, H.T., C.O. Kerobo, H.C. Hollein, and C.R. Huang "Research on Parametric Pumping," Chem. Eng. Ed., 15(4), 166 (1981).

13. Colwell, C.J. and J.S. Dranoff, "The Kinetics of Sorption by Ion Exchange Resin Beds," AIChE J., 12, 304 (1966).

14. Colwell, C.J. and J.S. Dranoff, "Nonlinear Equilibrium and Axial Mixing Effects in Intraparticle Diffusion Controlled Sorption by Ion Exchange Resin Bed," I&EC Fundamentals, 8(2), 193 (1969).

15. Deisler Jr. P.F. and R.H. Wilhelm, "Diffusion in Beds of Porous Solids," Ind. Eng. Chem., 45(6), 1219 (1953).

16. Glueckauf, E., K.H. Barker, and G.P. Kitt, "Theory of Chromatography," Discussions of The Faraday Society, 7, 199 (1949).

17. Graham, E.E. and C.F. Fook, "Rate of Protein Absorption and Desorption on Cellulosic Ion Exchanger," AIChE J., 28(2), 245 (1982).

18. Gustafson, K.E., Introduction to Partial Differential Equations, John Wiley & Sons Inc., NY (1980).

19. Hougen, O.A. and W.R. Mashall, "Adsorption from a Fluid Stream Flowing Through a Stationary Branular Bed," Chem. Eng. Prog., 43(4), 197 (1947).

20. Kasten, P.R., L. Lapidus, and N.R. Amundson, "Mathematics of Adsorption in Beds. V. Effect of Intraparticle Diffusion in Flow Systems in Fixed Beds," J. Phy. Chem., 56, 683 (1952).

21. Keller, K.H., E.R. Canales, and S. Yum II., "Tracer and Mutual Diffusion coefficient of Proteins," J. Phy. Chem., 75, 379 (1971).

22. King, C.J., Separation Processes, McGraw-Hill Book Co., NY (1971).

23. Lapidus, L. and N.R. Amundson, "Mathematics of Adsorption in Beds. VI. The Effect of Longitudinal Diffusion in Ion Exchange and Chromatographic Column," J. Phy. Chem., 56, 984 (1952).

24. Masamune, S. and J.M. Smith, "Transient Mass Transfer in a Fixed Bed," I&EC Fundamentals, 3(2), 179 (1964).

25. Masamune, S. and J.M. Smith, "Adsorption Rate Studies-Interaction of Diffusion and Surface Processes," AIChE J., 11(1), 34 (1965).

26. Mickley, H.S., T.K. Sherwood, and C.E. Reed, Applied Mathematics in Chemical Engineering, McGraw-Hill Book Co., NY (1957).

27. Pigford, R.L., B. Baker III., and D.E. Blum, "Cycling Zone Adsorption: A New Separation Process," I&EC Fundamentals, 8, 848 (1969).

28. Raghavan, N.S. and D.M. Ruthven, "Numerical Simulation of a Fixed Bed Adsorption Column by the Method of Orthogonal Collocation," AIChE J., 29(6), 922 (1983).

29. Rasmuson A. and I. Neretnieks, "Exact Solution of a Model for Diffusion in Particles and Longitudinal Dispersion in Packed Beds," AIChE J., 26(4), 686 (1980).

30. Rasmuson, A., "Exact Solution of a Model for Diffusion and Transient Adsorption in Particles and Longitudinal Dispersion in Packed Beds," AIChE J., 27(6), 1032 (1981).

31. Rodrigues, A.E. and D. Tondeur, Percolation Processes, NATO (1978).

32. Rosen, J.B.,"Kinetics of a Fixed Bed System for Solid Diffusion into Spherical Particles," J. Chem. Phy., 20(3), 387 (1952).

33. Rosen, J.B., "General Numerical Solution for Solid Diffusion in Fixed Beds," Ind. Eng. Chem., 48(6), 1590 (1954).

34. Schneider, P. and J.M. Smith," Adsorption Rate Constants from Chromatography," AIChE J., 14(5), 762 (1968).

35. Snyder, L.R. and J.J. Kirkland, Introduction to Modern Liquid Chromatography, John Wiley & Sons Inc., NY (1979).

36. Varuntanya, C., Supplemented Report, M.S. Thesis, NJIT (1982).

37. Wilhelm, R.H., A.W. Rice, and A.R. Bendelius, "Parametric Pumping: A Dynamic Principle for Separating Fluid Mixtures," I&EC Fundamentals, 5(1), 141 (1966).

38. Wilhelm, R.H., A.W. Rice, R.W. Rolk, and N.H. Sweed, " Parametric Pumping: A Dynamic Principle for Separating Fluid Mixtures," I&EC Fundamentals, 7(3), 337 (1968).

39. Tien, C. and G. Thodos, "Ion Exchange Kinetics for Systems of Linear Equilibrium Relationships," AIChE J., 6 (3), 364 (1960).

40. Treybal, R.E., Mass Transfer Operation, McGraw-Hill Book Co., NY (1968).

41. Zwiebel, I. and R.L. Gariepy, "Adsorption of Binary Mixtures in Fixed Beds," AIChE Symp. Series, 67 (117), 17 (1971).

42. Zwiebel, I., R.L. Gariepy, and J.J. Schnitzer, "Fixed Bed Desorption Behavior of Gases with Nonlinear Equilibrium: Part I. Dilute, One Component, Isothermal Systems," AIChE J., 18(6), 1139 (1972).

43. Zwiebel, I., C.M. Kralik, and J.J. Schnitzer, "Fixed Bed Desorption Behavior of Gases with Nonlinear Equilibrium: Part II. Dilute, Multicomponent, Isothermal Systems," AIChE J., 20(5), 915 (1974).